KU LEUVEN

FACULTY OF SCIENCE

Structure based development of *Plasmodium* hypoxanthine-guanine phosphoribosyltransferase inhibitors: a proof of concept study

Manon LAPORTE

Supervisor: Prof. Dr. Lieve Naesens

Co-supervisor: Prof. Dr. Patrick Van Dijck

Thesis presented in
fulfillment of the requirements
for the degree of Master of Science
in Biology

Academic year 2013-2014

DANKWOORD

Deze thesis had niet tot stand kunnen komen zonder de hulp van een aantal belangrijke mensen die ik graag afzonderlijk bedank.

Als eerste wil ik mijn promotor, Prof. Lieve Naesens, van harte bedanken dat zij mij de kans gegeven heeft om bij haar mijn thesis uit te voeren. Haar enthousiasme is erg aanstekelijk en heeft ervoor gezorgd dat ik steeds met heel veel plezier aan deze thesis gewerkt hebt.

Prof. Patrick Van Dijck dank ik voor zijn bereidheid om mijn co-promotor te zijn en voor zijn gastvrijheid om mij mee uit te nodigen op labmeeting in Blankenberge met zijn labo.

Mijn speciale dank gaat ook uit naar Ria Van Berwear voor haar nauwgezette hulp bij de HPLC en radioactieve experimenten. Ook alle andere collega's en mijn bureaugenoten wil ik bedanken voor de aangename werksfeer en voor hun raad waar ik altijd op kon rekenen.

Graag dank ik ook Prof. Philippe Van den Steen en Erwin Swinnen voor hun bereidheid en tijd om dit werk te lezen.

Pieter-Jan, mijn zussen, oma's, vrienden en familie wil ik bedanken voor al de leuke en ontspannende momenten tussendoor.

Mama en papa, bedankt voor het vertrouwen en alle kansen die jullie ons geven.

Manon, 24 mei 2014

TABLE OF CONTENTS

LIST OF ABBREVIATIONS

1306	human skin fibroblasts
2,6-DAP	2,6-diaminopurine
293AD	human embryonic kidney cells
^{3}H	tritium
6-azaU	6-azauridine
6-MP	6-mercaptopurine
6-TG	6-thioguanine
6-TGMP	6-thioguanine monophosphate
A549	human lung carcinoma cells
ACT	artemisinin-based Combination Therapy
Ad	adenovirus
Ad-*Pf*	adenoviral vector expressing codon optimized *P. falciparum* HGPRT
Ad-*Pv*	adenoviral vector expressing codon optimized *P.vivax* HGPRT
Ad-WThu	adenoviral vector expressing wild type human HGPRT
Ad-ΔEx2hu	adenoviral vector expressing mutant exon 2 deleted human HGPRT
ADA	adenosine deaminase
Ade	adenine
AdeI	adenylosuccinate lyase deficient Chinese hamster ovary cells
Ado	adenosine
ADP	adenosine-5'-diphosphate
ADSL	adenylosuccinate lyase
AIDS	acquired immune deficiency syndrome
AIP	acyclic immucillin phosphonate
AK	adenosine kinase
AMP	adenosine 5'- monophosphate
ANP	acyclic nucleoside phosphonate
AP	alkaline phosphatase
APRT	adenine phosphoribosyltransferase
ATCC	American Type Cell Culture Collection
ATP	adenosine-5'-triphosphate
bp	base pair
C32	human melanoma cells
CAR	coxsackie-adenovirus receptor
CC_{50}	50% cytotoxic concentration
cDNA	complementary DNA
CHO	chinese hamster ovary
CMV	cytomegalovirus
Compound 8	{2-[3-(Guanin-9(6H)-yl)-2-(2-bis(hydroxyphosphoryl)ethoxy)-propoxy]ethyl}phosphonic Acid
Compound 10	tetra-(L-Phenylalanine ethyl ester) Prodrug of compound 8
Compound 16	{[(2-[(Hypoxanthin-9H-yl)methyl]propane-1,3-diyl)bis(oxy)]bis-(methylene)}diphosphonic Acid
Compound 17	{[(2-[(Guanin-9H-yl)methyl]propane-1,3-diyl)bis(oxy)]bis-(methylene)}diphosphonic Acid

Compound 18	tetra-(L-Phenylalanine ethyl ester) Prodrug of compound 16
Compound 19	tetra-(L-Phenylalanine ethyl ester) Prodrug compound 17
Compound 23	mono(hexadecyloxypropyl) Ester prodrug of PEEG
CPE	cytopathogenic effect
CS	circumsporozoite
CTP	cytidine-5'-triphospate
dADP	2'-deoxyadenosine-5'-diphosphate
dATP	2'-deoxyadenosine-5'-triphosphate
dCTP	2'-deoxy-5'- cytidinetriphosphate
dGDP	2'-deoxyguanosine-5'-diphosphate
dGTP	2'-deoxyguanosine-5'-triphosphate
DMEM	Dulbecco's modified Eagle's medium
DNA	2'-deoxyribonucleic acid
DPM	desintegrations per minute
E	early
EDTA	ethylenediaminetetraacetic acid
EtBr	ethidiumbromide
FACS	fluorescence activated cell sorter
FCS	fetal calf serum
GDP	guanosine-5′-diphosphate
GFP	green fluorescent protein
GMP	guanosine-5′-monophosphate
GSK	GlaxoSmithKline
GTP	guanosine-5′-triphosphate
HeLa	Henrietta Lacks
HGPRT	hypoxanthine-guanine phosphoribosyltransferase
HIV	human immunodeficiency virus
HPLC	high-performance liquid chromatography
hu	human
Hx	hypoxanthine
IC_{50}	50% inhibitory concentration
ImmH	immucillin H
IMP	inosine-5'-monophosphate
IMPDH	inosine-5'-monophosphate dehydrogenase
IOCB	Institute of Organic Chemistry and Biochemistry
IRES	internal ribosome entry site
ITR	inverted terminal repeats
k_{cat}	turnover number (catalytic constant)
kDa	kilo Dalton
K_i	inhibitor constant
K_M	Michaelis-Menten constant
LB	Luria broth
MDCK	Madin-Darby canine kidney
MEM	minimal essential medium
MOI	multiplicity of infection

MPA	mycophenolic acid
MSDS	Material Safety Data Sheet
NSDS	Nuclide Safety Data Sheet
mRNA	messenger ribonucleic acid
MTA	methylthioadenosine
NT1	nucleoside transporter 1
NTD	neglected tropical disease
PCR	polymerase chain reaction
PDB	Protein Data Bank
PEEG	9-[2-(2-phosphonoethoxy) ethyl]guanine
PEEHx	9-[2-(2-phosphonoethoxy)ethyl] hypoxanthine
Pf	*Plasmodium falciparum*
PFU	plaque forming unit
PNP	purine nucleoside phosphorylase
PP_i	pyrophospate
PRPP	5-phosphoribosyl-1-pyrophosphate
PSP	purine salvage pathway
Pv	*Plasmodium vivax*
PV	parasitophorous vacuole
RBC	red blood cell
RBV	ribavirin
RNA	ribonucleic acid
RPMI	Roswell Park Memorial Institute medium
RR	ribonucleotide reductase
S/N	signal to noise
S-AMP	succinyl-adenosine 5'-monophosphate
SDS-PAGE	sodium dodecyl sulphate polyacrylamide gel electrophoresis
S-HPMPG	(S)-9-(3-hydroxy-2-phosphonomethoxypropyl)guanine
UTP	uridine-5'-triphosphate
WHO	World Health Organization
WT	wild type
XMP	xanthosine-5'-monophosphate
XPRT	xanthine phosphoribosyltransferase

SUMMARY

The malarial parasites *Plasmodium falciparum* (*Pf*) and *Plasmodium vivax* (*Pv*), are purine auxotrophs that rely on the salvage of host purines for their survival and growth. A critical enzyme in this salvage pathway, hypoxanthine guanine phosphoribosyltransferase (HGPRT), is recognized as a promising antimalarial drug target.

A collaboration between the universities of Queensland, Prague and Leuven led to the development of unique acyclic nucleoside phosphonates (ANPs) that are structural analogues of the HGPRT nucleotide reaction products, IMP and GMP. These ANPs are potent inhibitors of human, *Pf* and *Pv* HGPRT in enzymatic assays and have antimalarial activity in *Pf*-infected erythrocytes. However, since the protozoan parasite has many possible target proteins, it remains to be established that the antiparasitic effect is indeed linked to inhibition of the HGPRT enzyme. We developed a cellular assay to complement the enzymatic assays (in which purified HGPRT enzymes are studied in a cell-free environment), and the *Plasmodium* cell culture assay (that involves replication of the whole *Pf* parasite). We first created adenoviral (Ad) vectors containing the cDNA sequences encoding human, *Pf* and *Pv* HGPRT. These Ad vectors were used to transduce HGPRT-deficient human 1306 cells to obtain high HGPRT expression levels. After two days, HGPRT activity was determined by measuring ^{3}H release from [2,8-^{3}H]Hypoxantine in the presence or absence of ANP prodrugs. With this new test, we already identified three rationally designed ANP compounds that indeed act as HGPRT inhibitors in a cellular context and are thus relevant antimalarial drug leads for further optimization.

SAMENVATTING

De malaria parasieten, *Plasmodium falciparum* (*Pf*) en *Plasmodium vivax* (*Pv*), zijn purine auxotrofen en afhankelijk van de salvage van gastheer purines voor hun overleving en groei. Een essentieel enzym in deze salvage pathway, hypoxanthine guanine phosphoribosyltransferase (HGPRT), wordt algemeen beschouwd als een beloftevol anti-malaria doelwit.

Een samenwerking tussen de universiteiten van Queensland, Praag en Leuven heeft geleid tot de ontwikkeling van acyclische nucleoside fosfonaten (ANP's), die structuuranalogen zijn van de HGPRT nucleotide reactieproducten, IMP en GMP. Deze ANP's zijn in enzymstudies krachtige inhibitoren van de menselijke, *Pf* en *Pv* HGPRT enzymen. Bovendien onderdrukken ze de groei van *Pf* in *in vitro* geïnfecteerde rode bloedcellen. Echter, aangezien de protozoaire parasiet beschikt over meerdere proteïnen die het doelwit kunnen zijn van deze inhibitoren, is bijkomende evidentie nodig om te bewijzen dat het groei inhiberende effect inderdaad het gevolg is van HGPRT inhibitie. Wij ontwikkelden een cellulaire assay die complementair is aan de enzym assay (waarbij opgezuiverd HGPRT onderzocht wordt in een celvrije omgeving) en de *Plasmodium* celcultuur assay (die replicatie van de gehele parasiet bestudeert). We creëerden adenovirus (Ad) vectoren die de cDNA sequenties bevatten voor de humane, *Pf* en *Pv*HGPRT enzymen. Na Ad- transductie van HGPRT-deficiënte 1306 cellen werden zo hoge expressieniveaus van HGPRT verkregen. HGPRT enzymactiviteit werd gemeten door bepaling van de ^{3}H release vanuit [2,8-^{3}H]Hypoxanthine in aan- of afwezigheid van ANP prodrugs. Met deze test konden we reeds aantonen dat drie rationeel ontworpen moleculen inderdaad HGPRT inhiberen. Deze ANP's zijn dus interessante lead compounds voor verdere onwikkeling tot antimalaria geneesmiddelen.

1 INTRODUCTION

1.1 General Introduction on Malaria

Malaria is still one of the most important infectious diseases in developing countries. Around 3 billion people, half of the world's population, live in areas at risk. In 2012, malaria was responsible for more than 200 million clinical cases, resulting in the death of about 627,000 people (WHO, 2012). Malaria is caused by protozoan parasites of the *Plasmodium* genus and is transmitted through the bite of an infected female *Anopheles* mosquito. Five species of *Plasmodium* infect humans: *P. falciparum, P. vivax, P. malariae*, *P. ovale* and *P. knowlesi. P. falciparum* is the deadliest of the five species, causing 90% of the malaria-linked deaths in sub-Saharan Africa, mostly among children under the age of five (WHO). *P. vivax* is geographically the most widespread species. It occurs mainly in Central and Southeast Asia, but is also present in South and Central America (Guerra et al. 2010), making it the main cause of malaria outside Africa. *P. vivax* malaria is often called a neglected disease since it has not received as much attention as *P. falciparum* malaria because it causes fewer deaths. However, it can remain in a dormant stage in the liver for up to 2 years that can evade several of the standard antimalarial drugs. Therefore, a single infection can result in several clinical relapses. *P. malariae* (present in Africa, Asia and South America) and *P. ovale* (West-Africa and Central Asia), cause fewer cases and are substantially less dangerous than *P. falciparum* and *P. vivax* (WHO Fact sheet N°94, 2014). *P. knowlesi* (South-East Asia) primarily infects macaques but is becoming more prevalent in humans (Kantele and Jokiranta 2011).
In September 2000, the United Nations set up "The Millennium Development Goals". These are eight international development goals to eliminate extreme hunger, poverty and disease by 2015. The sixth goal "To combat HIV/AIDS, malaria, and other diseases" has led to the foundation of several initiatives, including the U.S. President's Malaria Initiative and the Global Fund to Fight AIDS, Tuberculosis, and Malaria (Hotez et al. 2007). The latter is supported by the Bill and Melinda Gates Foundation. These initiatives have led to a considerable increase in financial support and concerted efforts have led to a reduction in malaria mortality rate of 42% globally and 49% in the African region, as compared to the situation in 2000 (WHO Fact sheet N°94, 2014). This has been achieved by a multifaceted approach that includes insecticide and larvicide spraying, the use of insecticide-impregnated bed nets and antimalarial chemotherapy. The latter is the only tool available for treatment of the disease and is threatened by emerging parasite drug resistance. Therefore, the discovery of new drugs with novel mechanisms of action is essential for the world's future ability to treat and control malaria (Ridley 2002).

1.1.1 Scientific classification of the genus *Plasmodium*

Plasmodium is a genus that belongs to the apicomplexan parasites. The Apicomplexa are a phylum of diverse obligate intracellular parasites including *Plasmodium* spp., *Toxoplasma gondii* (the cause of toxoplasmosis) and *Eimeria spp* (the cause of coccidiosis). Apicomplexan parasites share a variety of morphological traits that are characteristic for this phylum. These protists are highly polarized cells with an elongated shape (Figure 1.1). The apex is a specialized region with a collection of unique organelles (rhoptries, micronemes, apical polar ring, and conoid) required for motility, adhesion and invasion of host cells, and establishment of the parasitophorous vacuole (Morrissette and Sibley 2002). In addition to the apical complex, the apicomplexans have another unique structural feature, from which the name of the phylum is derived: the apicoplast, an essential chloroplast-like organelle, acquired via secondary endosymbiosis (Köhler et al. 1997). This organelle contains its own genome and carries out isoprenoid, fatty acid, and heme biosynthesis (Ramakrishnan et al. 2012).

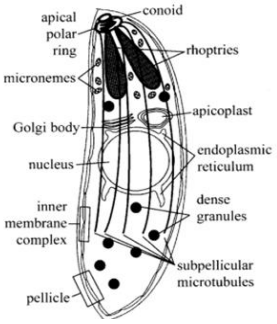

FIGURE 1.1 | **Typical morphology of apicomplexan parasites**
(Morrissette and Sibley 2002).

1.1.2 Life cycle of the malaria parasite

The complex life cycle of the malaria is shown in Figure 1.2. First, during a blood meal of a female *Anopheles* mosquito, the human host becomes infected by sporozoites, that are produced in the salivary glands of the mosquito vector. The sporozoites travel through the bloodstream to the liver and infect the hepatocytes (Stage 1, Figure 1.2). *P. vivax* parasites settle in the hepatocytes in a dormant form, called hypnozoites, which can remain dormant for a few weeks up to 2 years. In the liver cells, schizonts are formed, which segment into several thousand merozoites which are released into the bloodstream when the hepatocyte ruptures. The merozoites invade the red blood cells where the parasites multiply rapidly by asexual replication (Stage 2, Figure 1.2), leading to the first clinical symptoms: fever, headache, chills and vomiting. *P.vivax* is restricted to reticulocytes (immature red blood cells). At synchronized intervals of 48 hours, the merozoites destruct the host red blood cells and infect new red blood cells. This causes severe anemia and splenomegaly. Malaria mortality is primarily due to organ dysfunction, in particular of the brain (cerebral malaria), due to sequestration of infected erythrocytes in the micro-vasculature. A fraction of merozoites infecting red blood cells develop into male and female gametocytes in a process called gametocytogenesis. Gametocytes are ingested when another *Anopheles* mosquito takes a blood meal from an infected person. The gametocytes mature into macro (female) and micro (male) gametes which, after fertilization and zygote formation in the mosquito's midgut, produce a motile ookinete. The ookinete penetrates the wall of the midgut and forms oocysts (Stage 3, Figure 1.2). When the oocyst ruptures, it releases sporozoites that migrate through

the mosquito's body to the salivary glands, ready to infect a new human host (Bousema and Drakeley 2011; Pasvol 2010; Sauerwein et al. 2011; Wells et al. 2009).

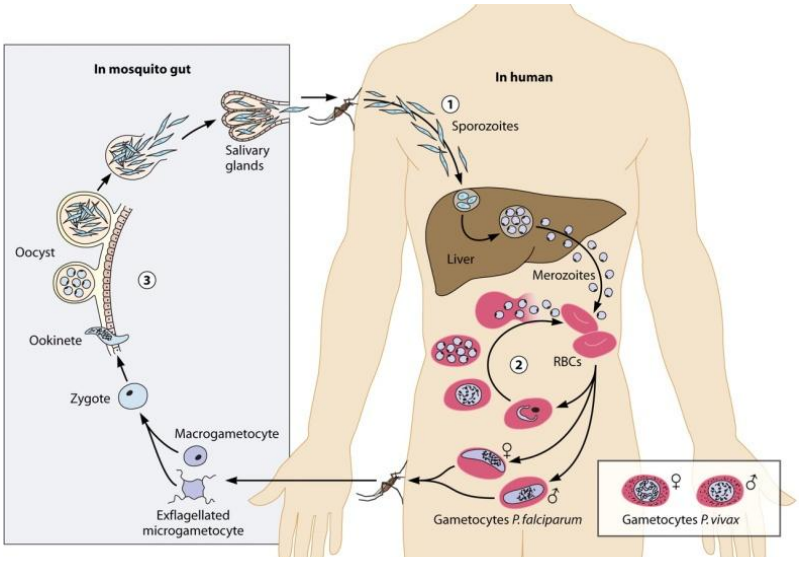

FIGURE 1.2 | **Life cycle of *Plasmodium*.** See text for a detailed description of the consecutive stages 1, 2 and 3 (Bousema and Drakeley 2011).

1.1.3 Current status of antimalarial chemotherapy and vaccine development

The frontline defense against malaria is the use of chemotherapeutic drugs which were discovered many years ago but have not been efficient in disease eradication (Table 1.1). The most widely used antimalarials are chloroquine and sulfadoxine-pyrimethamine (Fansidar®), both blood-stage schizonticides. They interrupt mitotic division in the red blood cells, preventing (prophylaxis) or terminating clinical attacks of malaria (Baird 2005). Primaquine is the only licensed tissue-stage schizonticide, acting on liver schizonts and the dormant hypnozoites of *P. vivax*, preventing primary or secondary attacks of clinical malaria. Furthermore, it also acts as a gametocytocide, thus preventing infection of mosquitoes and transmission of the disease (Baird 2005). An important drawback of primaquine is that it causes haemolysis in patients with glucose-6-phosphate dehydrogenase deficiency, which is widespread in malaria-endemic regions (Horn and Duraisingh 2014). The drug combination atovaquone/proguanil, known under the trade name Malarone®, is an antimalarial medication that is primarly used as a prophylactic agent by travelers. Many travelers prefer Malarone® for malaria chemoprophylaxis because it causes fewer side effects than Lariam® (mefloquine), notorious for causing neuropsychiatric side-effects and vivid nightmares (Overbosch et al. 2001). Although very effective, its price is too high for use in developing countries. Many strains of *P. falciparum* and *P. vivax* have acquired resistance to the widely used antimalarial agents. Decreased susceptibility is associated with mutations in transporters, leading to decreased drug access, and mutations in target enzymes, leading to a decreased affinity of the inhibitors (Table 1.1) (Baird 2005).

TABLE 1.1 | **Cost, mechanism of action, cause of resistance and primary clinical application of frequently used antimalarial therapies** (Baird 2005; Ridley 2002).

Therapy	Cost[a]	Mechanism of action	Mutations associated with *Pf* drug resistance[b]	Application
Chloroquine	0.11	Most likely by inhibition of haemozoin biocrystallization, resulting in the accumulation of cytotoxic haem.	Pfcrt1 transporter	Blood-stage schizonticide
Mefloquine (Lariam®)	2.55	*Idem*	Pfmdr1 transporter	Blood-stage schizonticide
Sulfadoxine-pyrimethamine (Fansidar®)	0.14	Inhibition of folate synthesis by inhibition of two enzymes: dihydrofolate reductase (pyrimethamine) and dihydroopteroate synthase (sulfadoxine).	Dihydroopteroate synthase Dihydrofolate reductase	Blood-stage schizonticide
Primaquine	1.68	Not well understood. Possibly, it acts by generating ROS or by interfering with oxidative metabolism.	Pfmdr1 transporter	Tissue stage schizonticide, gametocytocide
Atovaquone-Proguanil (Malarone®)	48	Atovaquone selectively inhibits the parasitic electron transport chain via inhibition of cutochroom c reductase. Proguanil functions as a dihydrofolate reductase inhibitor.	Cytochroom c reductase	Blood-stage schizonticide (prophylaxis)
Artemisinin combination therapy (ACT)	> 1	Generation of free radicals and alkylation of *Plasmodium* proteins.	?	Blood-stage schizonticide, gametocytocide

[a]The cost shown is the cost in U.S. dollars for one adult treatment regimen (Baird 2005)
[b]Pfcrt1= *P. falciparum* chloroquine resistance transporter, Pfmdr1= *P. falciparum* multi drug resistance transporter.

Given the assumption that monotherapy stimulates the development of drug resistance, combination therapy is now the state-of-the-art strategy to treat malaria. At present, the WHO recommends artemisinin based -combination therapy (ACT) as the first-line treatment against *P.falciparum* malaria. Artemisinin is an endoperoxide containing natural product isolated from the leaves of *Artemisia annua* (sweet wormwood), a plant used by Chinese herbalists since 168 B.C. In the presence of intraparasitic iron, the drug is converted into free radicals and other electrophilic intermediates which then alkylate specific malaria target proteins (Meshnick, Taylor, and Kamchonwongpaisan 1996). Unfortunately, artemisinin resistant *P. falciparum* strains have already been detected in four Southeast Asian countries: Cambodia, Myanmar, Thailand, and Vietnam (Dondorp et al. 2009). Whole-genome sequencing revealed that mutations in the so-called K13-propeller domain are associated with artemisinin resistance (Ariey et al. 2014). It is proposed that mutations in the K13 propeller region may be associated with an enhanced anti-oxidant response, however the exact mechanism is currently unknown (Ariey et al. 2014). Blood-stage infections with *P. vivax* are generally still treatable with chloroquine, which remains the WHO's recommendation for first-line treatment. In areas where chloroquine-resistant strains are present, the use of ACT's is recommended (Wells et al. 2009).

Currently, no malaria vaccine is commercially available, despite many efforts and intensive research for decades. The complexity of the parasite's life cycle, with many mechanisms to avoid the host immune system, makes vaccine development a very challenging task. The most promising malaria vaccine candidate, RTS,S/AS01 of GlaxoSmithKline (GSK), targets the sporozoites and intra-hepatic stages of the most deadliest form of malaria, *P. falciparum* (Moorthy and Ballou 2009). The RTS,S/AS01 vaccine contains a recombinant antigen expressed in *S. cerevisiae*. RTS,S is a hybrid polypeptide consisting of a portion of the malarial circumsporozoite (CS) protein fused to the surface antigen S of the hepatitis B virus. CS is a sporozoite surface antigen and is released at the apex during invasion of hepatocytes (Stewart and Vanderberg 1988). The vaccine also contains the GSK Adjuvant System, AS01, which consists of a liquid suspension of liposomes with two immunostimulant components: 3'-O-desacyl-4'-monophosphoryl lipid A and Quillaja saponaria 21 (QS21). This adjuvant has been developed to induce a strong T-cell mediated immune response and improves protection after vaccination (Garçon et al. 2007). Currently, this vaccine is in phase III clinical trials in seven countries in sub-Saharan Africa (WHO). The latest results from a 18-months follow-up showed that children aged 5-17 months at first vaccination with RTS,S/AS01 experienced 46% fewer cases of clinical malaria. For children aged 6-12 weeks at first vaccination, the efficacy was only 27% (malaria vaccine initiative, press release 2013). These efficacy data are somewhat lower than the results from a one-year follow-up Phase III trial, in which the efficacy of RTS,S/AS01 was 56% against clinical malaria for the 5-17 month-old age group (Agnandji et al. 2011) and 31% in the 6-12 week-old age group (Agnandji et al. 2012). This indicates that the duration of protection is limited.

Until a good vaccine becomes available, chemotherapy will remain the mainstay for both prevention and treatment of malaria. Since drug resistance to older antimalarials is widespread, and resistance to artemisinin is emerging with the potential to spread to other regions, new effective drugs are required with novel mechanisms of action. One approach is to exploit metabolic differences between the human host and the parasite. All the protozoan parasites studied to date are unable to synthesize purine nucleotides de novo and hence rely entirely on salvage strategies to meet their purine demands for nucleic acid synthesis, required for their survival and replication. For more than 40 years, enzymes involved in the purine salvage pathway (PSP) of parasitic protozoa have been considered as promising targets for drug development (Walsh and Sherman, 1968). In particular, the hypoxanthine-guanine phosphoribosyltransferase (HGPRT) enzyme is widely considered as a promising antimalarial drug target, based on its central, if not indispensable role in the PSP (Berg et al. 2010; Cassera et al. 2011; Downie et al. 2008; de Jersey et al. 2011; Ullman and Carter 1995).

1.2 The Role of HGPRT in Purine Synthesis

Purines are essential molecules for all living organisms. Purine containing nucleotides are the building blocks of nucleic acids (DNA and RNA), and purine bases are constituents of enzyme cofactors (e.g. NAD^+, FAD), sources of chemical energy (e.g. ATP, GTP) or signaling molecules (e.g. cAMP).

In general, purine nucleotides can be synthesized via two metabolic pathways (Figure 1.3). First, purines can be synthesized de novo starting from phosphoribosyl pyrophosphate (PRPP), which is produced from ribose-5-phosphate and ATP by PRPP synthetase. The purine ring is subsequently built upon this structure in a multi-step process which requires the contribution of four amino acids, two folates, CO_2 and four ATP molecules. The central purine nucleotide inosine-5'-monophosphate (IMP) is then converted to either adenine (AMP, ADP, and ATP) or guanine nucleotides (GMP, GDP, and GTP). The adenine nucleotides are formed via the intermediate succinyl-AMP. The guanine nucleotides are synthesized via xanthosine-5'-monophosphate (XMP). After further conversion to ATP and GTP, these purine ribonucleotides are used in RNA synthesis. Ribonucleotide reductase (RR) catalyzes the formation of 2'-deoxynucleotides dADP and dGDP, which after conversion into dATP and dGTP, provide the substrates for DNA synthesis (Hatse et al. 1999).

Alternatively, AMP, IMP and GMP can also be salvaged in the purine salvage pathway. Two highly active purine phosphoribosyltransferases with different specificities recover purine nucleobases in the presence of PRPP to their respective nucleosides. Adenine phosphoribosyltransferase (APRT) catalyzes the formation of AMP from adenine, whereas hypoxanthine-guanine phosphoribosyltransferase (HGPRT) catalyzes the salvage synthesis of IMP and GMP from the purine bases hypoxanthine and guanine, respectively (Hatse et al. 1999).

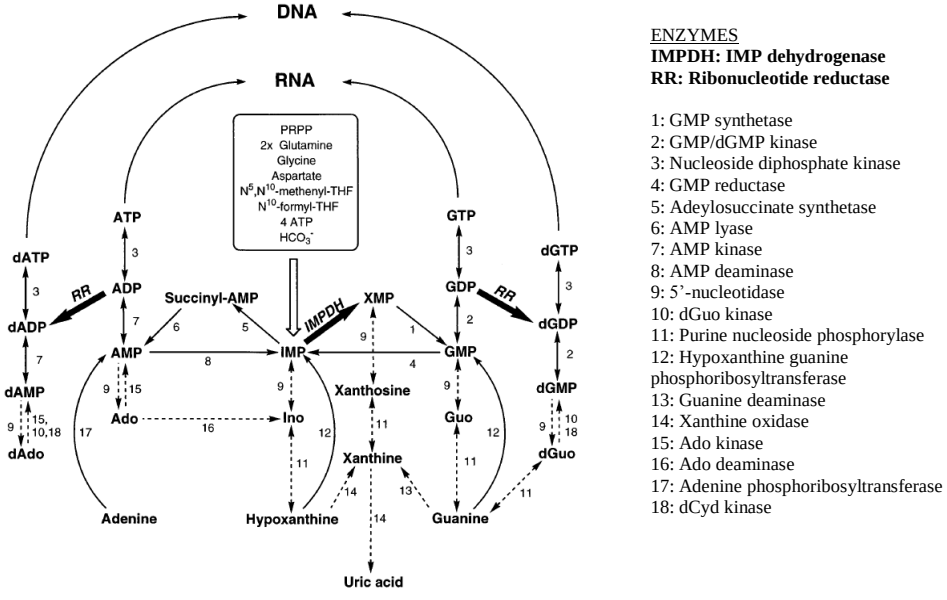

FIGURE 1.3 | **De novo and salvage synthesis of purine nucleotides in mammalian cells** (Hatse et al. 1999)**.**

The reaction catalyzed by HGPRT is shown in more detail in Figure 1.4. Human (huHGPRT) and *P. vivax* (*Pv*HGPRT) only use hypoxanthine and guanine as substrates. *P. falciparum* (*Pf*HGPRT) can also use xanthine as a substrate. HGPRT transfers the 5-phosphoribosyl group from 5-phosphoribosyl 1-pyrophosphate (PRPP) to a 6-oxopurine base (guanine, hypoxanthine or xanthine), generating the corresponding nucleoside-5'-monophosphates (GMP, IMP or XMP) and inorganic pyrophosphate (PP_i). A divalent cation, usually magnesium, is essential for catalysis (Keough et al. 1999). The reaction mechanism for huHGPRT is ordered: first, PRPP.Mg^{2+} binds, followed by the purine base. After the reaction, PP_i dissociates from the complex and the nucleoside monophosphate is released in the rate-limiting step. The reaction mechanism of *Pf*HGPRT and *Pv*HGPRT has not yet been fully established but is expected to be similar (Keough et al. 2009).

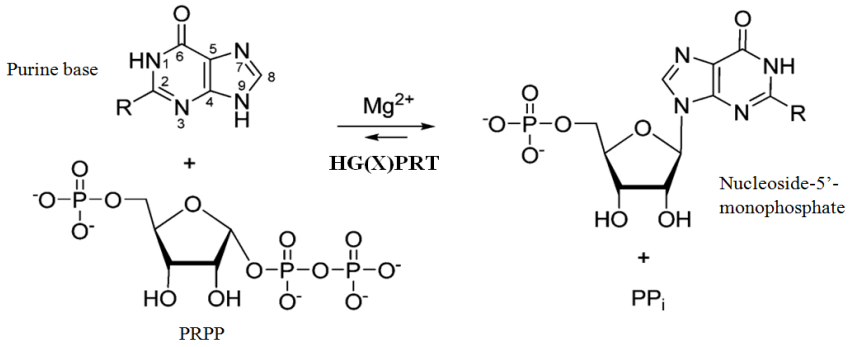

FIGURE 1.4 | **The reaction catalyzed by HGPRT.** The naturally occurring purine bases are guanine (R is -NH_2), hypoxanthine (R is -H), and xanthine (R is =O). The corresponding nucleoside-5'-phosphates are GMP (R is -NH_2), IMP (R is -H) and XMP (R is =O) (Figure adapted from de Jersey et al. 2011).

The HGPRT enzyme is intensively investigated for at least two reasons: (i) mutations in the gene encoding huHGPRT lead to the Kelley-Seegmiller syndrome (Seegmiller et al. 1967) and Lesch-Nyhan syndrome (lesch and Nyhan, 1964). This is explained in more detail in Paragraph 1.2.1. (ii) *Plasmodium spp.* and other protozoan parasites are unable to synthesize purine rings de novo and completely rely on salvage of purines from the host. Therefore, parasitic purine salvage enzymes are considered as promising drug targets to combat infections with parasitic protozoa (see paragraphs 1.2.2 and 1.2.3).

1.2.1 Disorders in the purine salvage pathway in humans

Mutations in the HPRT1 gene, located on the X-chromosome, cause a variety of clinical symptoms. Because inheritance of HGPRT deficiency is X-linked recessive, mostly males are affected and heterozygous female are carriers. Nowadays, more than 300 mutations in the HPRT1 gene have been identified that are associated with HGPRT deficiency. Depending on the degree of enzymatic deficiency the clinical symptoms are different (Torres and Puig 2007). Partial deficiency of HGPRT, known as the Kelley-Seegmiller syndrome, leads to

accumulation of uric acid. When HGPRT is deficient, purines are broken down but not recycled, producing abnormally high levels of uric acid. High uric acid levels lead to gouty arthritis and the formation of uric acid stones in the urinary tract (Seegmiller et al. 1967). This uric acid overproduction can be treated with allopurinol, a xanthine oxidase inhibitor (Torres and Puig 2007) (Nyhan et al., 2010).

The most severe form of HGPRT deficiency is known as the Lesch-Nyhan syndrome, described by M. Lesch and W. Nyhan in 1964. This corresponds to virtually complete HGPRT deficiency. Besides having severe gout and kidney problems, these patients suffer from serious neurological problems. These symptoms include severe action dystonia, choreoathetosis, ballismus, cognitive and attention deficit, and self-injurious behavior. The prevalence of Lesch-Nyhan syndrome is approximately 1:380,000. The mechanisms leading to the neurobehavioral abnormalities are unclear. Various studies suggest that the neurological symptoms could be related to low levels of the neurotransmitter dopamine in the basal ganglia, but the relationship between the dopamine deficit and the purine metabolic disorder is still unknown. Because the exact cause of the neurological dysfunction is poorly understood, no effective therapies exist (Torres and Puig 2007) (Nyhan et al., 2014).

1.2.2 The purine salvage pathway in *Plasmodium spp.*

The completion of the *P. falciparum* and *P. vivax* genome sequencing project (Gardner et al., 2002; Carlton, 2003) confirmed that, in these parasites, the salvage pathway is the only metabolic route for synthesis of the 6-oxopurine nucleoside monophosphates IMP, XMP and GMP. Although older studies have reported APRT activity (Pollack et al. 1985; Queen et al. 1989), no gene encoding APRT has been identified in *Plasmodium*, nor in other Apicomplexan parasites (Berg et al. 2010; Downie et al. 2008; Hyde 2007). The reported APRT activity was shown to be 1,500 lower than that present for HGPRT (Queen et al. 1989). Thus, whether or not *Plasmodium* has APRT activity, purine salvage in the parasite is mainly dependent on the activity of HGPRT.

Figure 1.5 shows the interactions between the human host and parasite purine pathways in erythrocytes that are infected with *P. falciparum*. The *Plasmodium* parasite is surrounded by a parasitophorous vacuolar (PV) membrane, formed during invasion. This membrane separates the cytosol of the host erythrocyte and the intracellular parasite. Host purine bases and nucleosides are transported via the parasite encoded nucleoside transporter *Pf*NT1. Other transporters may also be present on the plasma membrane, but the identities and properties of these have not yet been determined (Berg et al. 2010). Within the parasite, the metabolism of purines appears to be funneled through hypoxanthine to IMP. Hypoxanthine is stated to be the major purine source in human serum (concentration ~ 8 µM) (Berg et al. 2010; Downie et al. 2008; Traut 1994) and is the key precursor for the synthesis of all other purines within the

parasite. The central role of hypoxanthine in purine metabolism is demonstrated by the strict dependence on hypoxanthine supplementation in *Pf* cell culture media (Cassera et al. 2011; de Jersey et al. 2011). Hypoxanthine is both transported into the cytoplasm and produced from adenosine and methylthioadenosine (MTA), by the sequential action of *Pf* adenosine deaminase (ADA) and *Pf*PNP in the parasite cytosol (Figure 1.5). Subsequently, hypoxanthine is converted to IMP by *Pf*HGPRT. IMP can then be converted to adenylate or guanylate nucleotides. *Pf*HGPRT also converts xanthine and guanine to XMP and GMP, respectively, and these are further converted into G nucleotides. An intact polyamine and purine salvage pathway is crucial for parasite survival since erythrocytes also lack the de novo polyamine and purine synthesis pathways (Berg et al. 2010). Furthermore, during the intra-erythrocyte growth phase (Stage 2, Figure 1.2), the synthesis of RNA and DNA molecules is heavily upregulated, making it vulnerable to disruption of the purine supply (Kicska et al. 2002).

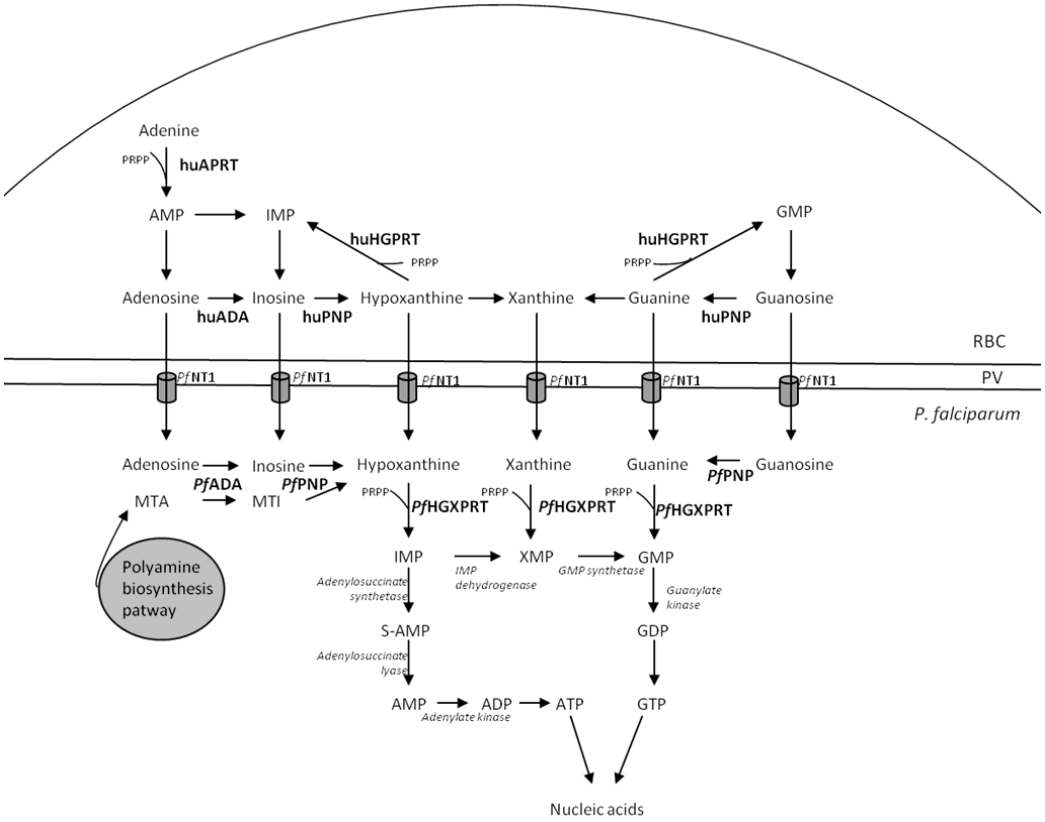

FIGURE 1.5 | **Purine salvage pathway of *P. falciparum* within the infected erythrocyte.**
The central metabolite, hypoxanthine is produced from adenosine by the sequential action of huADA/ *Pf*ADA and huPNP/*Pf*PNP present in the red blood cell cytoplasm and parasite cytosol respectively. *Pf*ADA and *Pf*PNP have a dual role and are also capable of acting on MTA and MTI, respectively, salvaging purines from the polyamine biosynthesis pathway. Adenosine, inosine, hypoxanthine, xanthine, guanine and guanosine are transported across the parasite plasma membrane by *Pf*NT1. *Pf*HGXPRT converts hypoxanthine to IMP, guanine to GMP, and xanthine to XMP. IMP, GMP, and XMP are then converted to guanylate and adenylate nucleotides, used in nucleic acid synthesis. Abbreviations: RBC: red blood cell; *PV:* parasitophorous vacuole; MTA: methylthioadenosine; MTI: methylthioinosine; ADA: adenosine deaminase; PNP: purine nucleoside phosphorylase; *Pf*NT1: *Pf* nucleoside transporter 1 (Figure adapted from Downie et al. 2008).

Since *Pf*PNP is essential for formation of hypoxanthine, blocking of *Pf*PNP has the potential to block purine salvage. Hypoxanthine depletion through inhibition of erythrocyte PNP and *Pf*PNP kills parasites in erythrocyte cell culture (Kicska et al. 2002). However, parasite killing by inhibition of PNP can be rescued with the addition of hypoxanthine (Kicska et al. 2002). Thus, since hypoxanthine is the major purine source in human serum, *Pf*ADA and *Pf*PNP are unlikely to play an essential function under physiological conditions. Blocking of the PSP at the *Pf*ADA or *Pf*PNP step alone will be circumvented by the salvage of host hypoxanthine, xanthine and guanine by HGPRT. The apparent dependence of the malarial parasite on HGPRT for nucleotide synthesis makes this enzyme a more promising drug target (Berg et al. 2010; Downie et al. 2008).

1.2.3 The purine salvage pathway in other parasitic protozoa

Plasmodium is the best known protozan species that causes disease, but other protozoan purine auxotrophs exist that cause a range of Neglected Tropical Diseases (NTD's) (Table 1.2). The three NTD's with the highest death rates are Chagas' disease, sleeping sickness, and visceral leishmaniasis (Hotez et al.2007) which are caused by the protozoan parasites *Trypanosoma cruzi*, *Trypanosoma brucei* and *Leishmania donovani*, respectively. All these species are transmitted via insect vectors. In contrast to malaria, these three protozoan infections do not receive sufficient international attention, and little research and treatment funding for these diseases are available (Bell et al. 2012). The drugs available for treating these infections are expensive, ineffective in disease eradication and often show unacceptable levels of toxicity (Bell et al. 2012; Ullman and Carter 1995). Therefore, new and improved antiparasitic agents are needed.

TABLE 1.2 | **Neglected Tropical Diseases caused by parasitic protozoa.**

Disease	**Etiologic agent**	**Insect vector**	**Affected regions**	**Estimated number of annual cases[a]**	**Estimated number of annual deaths[a]**
Leishmaniasis	*Leishmania spp.*	Phlebotomine sandflies	Tropics and substropics	1.3 million	20 000 – 30 000
Chagas' disease (American trypanosomiasis)	*Trypanosoma cruzi*	Reduviid bugs (triatomines)	Latin America	7 to 8 million	?
Sleeping sickness (African trypanosomiasis)	*Trypanosoma brucei gambiense, T.b. rhodesiense*	Tsetse flies (*Glossina spp.*)	Sub-Saharan Africa	20 000	?

[a]WHO, most recent data

The PSPs of *P. falciparum*, *T. brucei*, *T. cruzi* and *L. donovani* have been reviewed by Berg *et al.* (2010) and the potential role of the different salvage enzymes as drug targets was critically evaluated. There are considerable differences in the salvage pathways and preferred substrates among these parasites. The parasites all have evolved a unique PSP with different compositions of purine salvage enzymes with different substrate affinities. This diversity in

PSPs among parasitic protozoa could be due to the fact that they inhabit distinct environmental milieus leading to different selective pressures (Ullman and Carter 1995).

L. donovani possesses four enzymes that are capable of converting host purines to the nucleotide level: HGPRT, APRT, xanthine phosphoribosyltransferase (XPRT) and adenosine kinase (AK). None of these four enzymes is, by itself, absolutely essential for purine salvage, since mutant *Leishmania* parasites deficient in any one of the four enzymes are perfectly viable (Berg et al. 2010; Boitz and Ullman 2010). Furthermore, triple mutants (Δhgprt/Δaprt/ak$^-$ and Δxprt/Δaprt/ak$^-$) are also viable, showing that a functional HGPRT or XPRT is sufficient to generate all required purines for survival. Indeed, a Δhgprt/Δxprt double mutant is absolutely reliant on the presence of adenine or adenosine as purine source (Boitz and Ullman 2006). Due to the elaborate and versatile purine salvage machinery of *L. donovani*, inhibition of a single enzyme will not be sufficient to kill this parasite. Inhibition of multiple salvage enzymes by combination therapy is a reasonable alternative, e.g. combination therapy that targets both HGPRT and XPRT might be a rational therapeutic strategy (Berg et al. 2010).

The PSP of *T. brucei* is also highly versatile. This parasite can grow on a single purine source (with adenosine being the preferred substrate) and converts it to the IMP branchpoint. From this branchpoint, all other nucleotides can be made (Lüscher et al. 2007). This means that, like in the case of *L. donovani*, no single salvage enzyme is essential for survival. Again, inhibition of multiple enzymes could provide a good therapeutic alternative. Another strategy is to exploit differences in parasite and host PSPs to specifically activate subversive substrates to toxic antimetabolites. *T. brucei* adenosine kinase has the potential of activating (i.e. phosphorylating) adenosine analogues to adenosine antimetabolites (Lüscher et al. 2007).

The PSP of *T. cruzi* is not well explored but bisphosphonate inhibitors were shown to inhibit *T. cruzi* HGPRT with K_i values ranging from 23 to 189 µM (Fernández et al. 2004).

In comparison with the protozoan parasites mentioned above, *P. falciparum* has a very simple salvage synthesis pathway maintained by only three key enzymes: PNP, ADA and HGPRT (Figure 1.5). Therefore, single enzyme inhibition seems enough to inhibit parasite growth *in vitro* (Cassera et al. 2011; Clinch et al. 2013; Keough et al. 2009; Keough, Špaček, et al. 2013).

1.2.4 Comparison of amino acid sequence, enzyme structure and kinetic properties of human, *Pf* and *Pv*HGPRT

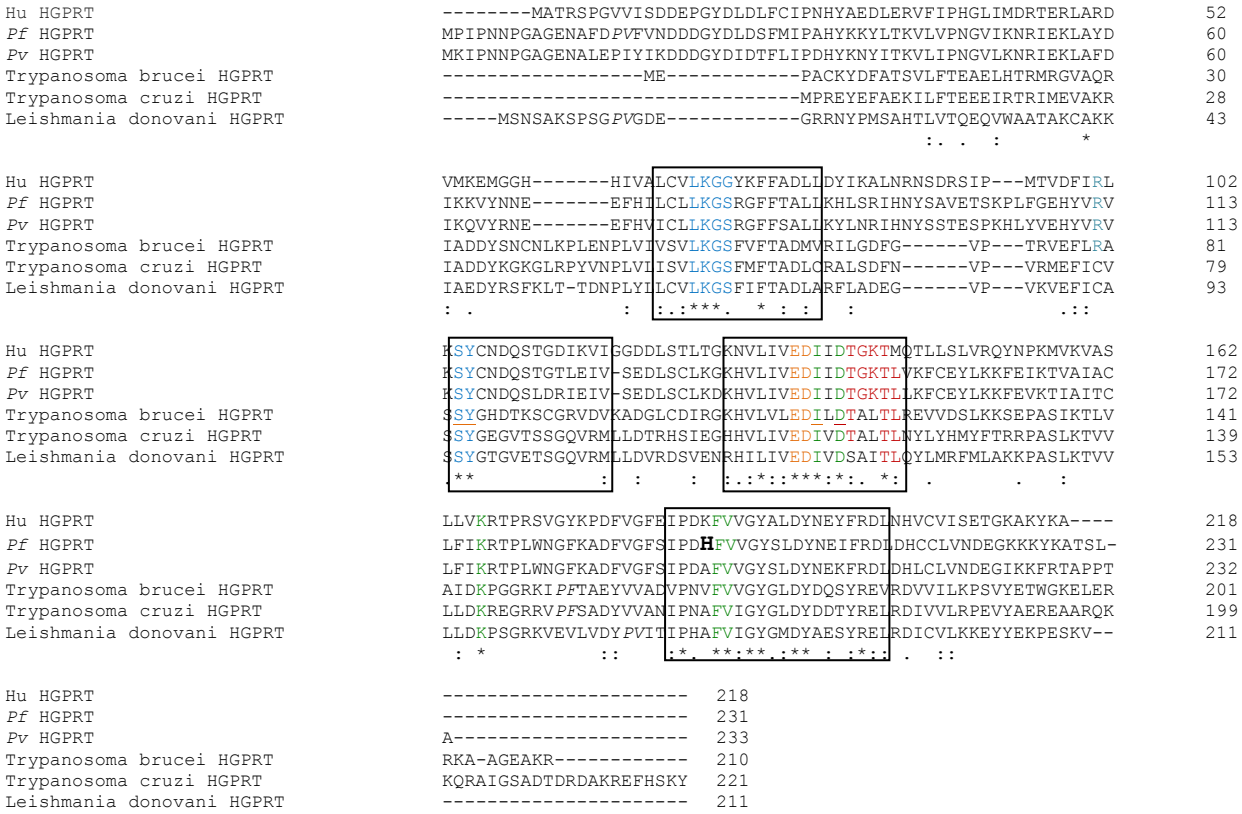

FIGURE 1.6 | **Multiple sequence alignment of HGPRT amino acid sequences of indicated species.** The amino acid sequences of human (UniProt number: P00492.2), *Plasmodium faciparum (P20035.1*) , *Plasmodium vivax (A5K7E9), Trypanosoma brucei (Q07010.1) , Trypanosoma cruzi* (AAB46391.1) and *Leishmania donovani* (P43152.1) HGPRT were aligned using Clustal Omega. "*" indicates identical residues, ":" indicates conserved substitutions and "." indicates semi-conserved substitution (similar shapes). Conserved regions are indicated with square boxes. The large mobile loop is underlined in huHGPRT. The residues involved in purine binding are colored green. Residues involved in pyrophosphate binding are colored blue. The 5'-phosphate binding loop is colored red. The ribose binding residues are colored orange. Residues that have multiple binding functions are colored and underlined in the corresponding colors; e.g. D148 is involved in both purine and 5'-phosphate binding. His196, responsible for xanthine selectivity of *Pf*HGPRT, is shown in bold.

The amino acid sequences of the five protozoan parasites discussed were aligned with human HGPRT (Figure 1.6). The length of the proteins varies from 211 to 221 amino acids. Despite the distant phylogenetic relationship between humans and parasites, they share significant HGPRT sequence homology. Pairwise alignments of human HGPRT with parasite HGPRT sequences indicate an amino acid sequence identity ranging from 32-48%. The two *Plasmodium* enzymes have 77% sequence identity. Despite significant overall sequence differences, the residues that make up the active site (indicated by square boxes) are largely conserved across the different species. Therefore, it is proposed that drugs directed towards *Plasmodium* HGPRT could also serve as lead compounds for inhibition of other protozoan parasites (de Jersey et al. 2011).

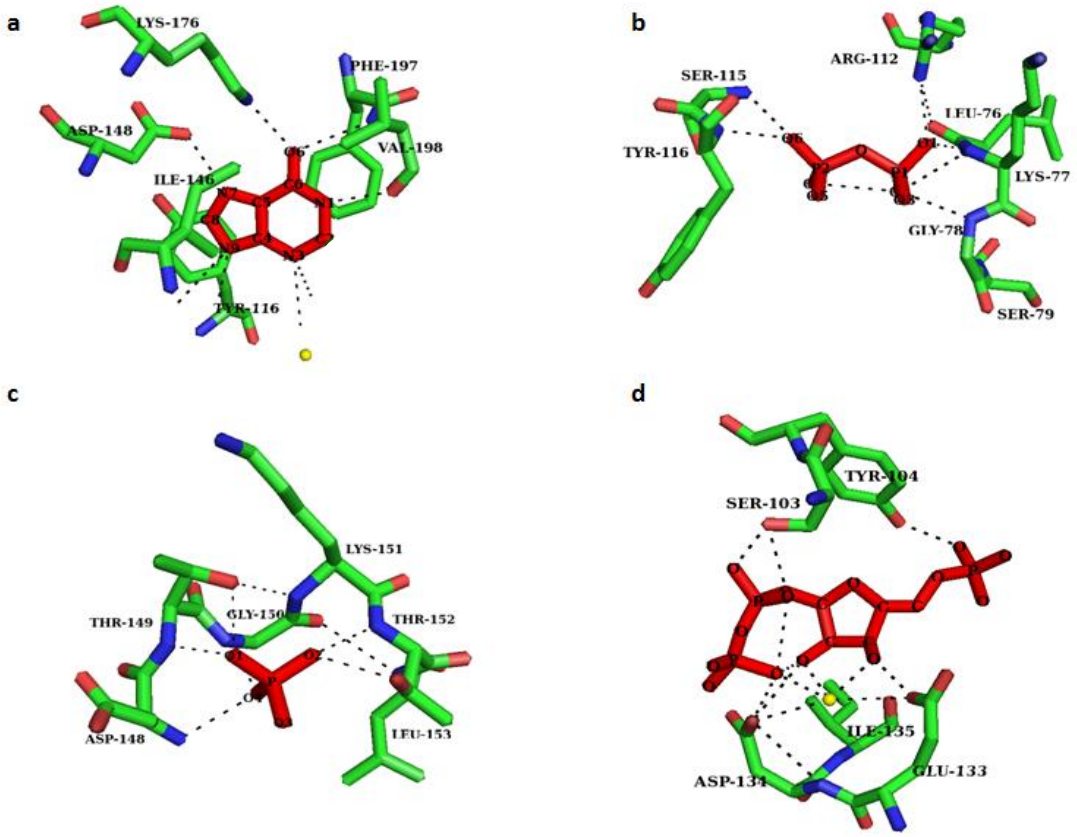

FIGURE 1.7 | **The active site of the HGPRT enzyme**. (a) The purine binding site of *Pf*HGPRT with bound hypoxanthine (Pdb code: 3OZF). (b) The pyrophosphate binding site of *Pf*HGPRT (Pdb code: 3OZF). (c) The 5'-phosphate binding of *Pf*HGPRT (Pdb code: 3OZF). (d) The PRPP binding pocket of huHGPRT (Pdb code:1D6N). Substrates are colored red and presented as stick models. Important active site residues are shown in stick model and colored by element (C is green, N is blue, O is red). The yellow sphere represents Mg^{2+}. Figures were made with the graphic computer program PyMol (http://www.pymol.org/).

The active site contains four critical regions required for catalysis: the purine binding site, the pyrophosphate binding site, the 5′-phosphate binding site and the PRPP binding site. The residues involved in binding the purine substrate are Asp148, Lys176, Phe197 and Val198 (Figure 1.7a) (*Pf*HGPRT numbering), and these are completely conserved across the different species (Figure 1.6, indicated in green). The carboxyl group of Asp148 forms a hydrogen bond to N_7 of the purine substrate. The side chain amide group of Lys176 and backbone amide of Val198 form hydrogen bonds to the exocyclic oxygen O_6 of the purine substrate. Therefore, Lys176 and Val198 play a critical role in 6-oxopurine substrate specificity. Because adenine has an NH_2 group at the 6-carbon position, these hydrogen bonds cannot be formed, precluding adenine from binding within the active site of HGPRT (Craig and Eakin, 2000). Val198 also interacts with N_1 of the purine ring via its carbonyl oxygen. Furthermore, the N_3 nitrogen of the purine ring forms hydrogen bonds with a water molecule, coordinated by Mg^{2+}. Phe197 forms a π-stacking interaction with the purine ring. Pyrophosphate is coordinated by the amide nitrogens of Leu 76, Lys77, Gly78, Ser 79, Arg112, Ser115, and Tyr116 (Figure 1.7b) (Hazleton et al. 2012). The 5'-phosphate group is held in place by hydrogen bonds with the main chain nitrogen atoms of Asp148, Thr149, Gly150 and Thr152

and with the side-chain hydroxyl groups of Thr152 and Thr149 (Figure 1.7c). The PRPP binding motif of huHGPRT is shown in Figure 1.7d. The acidic Glu-Asp dipeptide (Glu133-Asp134) in the center of the PRPP binding motif forms hydrogen bridges with the 2'- and 3'-hydroxyl groups of the ribose ring. The Ser-Tyr dipeptide belongs to a flexible loop region (100-117, human numbering, underlined in Figure 1.6) that closes over the active site during catalysis (Keough et al. 2005).

Despite the significant conservation of residues making up the active site, there are marked differences in catalytic efficiencies for the naturally occurring purine bases between the human and malarial enzymes (Table 1.3).

TABLE 1.3 | **Comparison of kinetic constants of human and *Plasmodium* HGPRT** (de Jersey et al. 2011)**.**

	Substrate	**k_{cat} (s^{-1})**	**K_M (µM)**	**k_{cat}/K_M (μM^{-1} s^{-1})**
huHGPRT	Hypoxanthine	5.2 ± 0.4	3.4 ± 1.0	1.5
	Guanine	8.2 ± 0.6	1.9 ± 0.4	4.3
	Xanthine	/	/	
***Pf*HGXPRT**	Hypoxanthine	0.33 ± 0.08	0.07 ± 0.03	4.7
	Guanine	0.66 ± 0.07	0.83 ± 0.5	0.8
	Xanthine	3.3 ± 0.2	189 ± 18	0.02
***Pv*HGPRT**	Hypoxanthine	0.74 ± 0.01	0.93 ± 0.12	0.8
	Guanine	1.7 ± 0.03	1.9 ± 0.4	0.9
	Xanthine	/	/	

A first important difference lies in their different substrate affinity. As mentioned above, the human enzyme and *Pv*HGPRT only use hypoxanthine and guanine as a substrate (Keough et al. 2010), while *Pf*HGPRT can also use xanthine (Keough et al. 1999). It has been shown that His196 (Figure 1.6), located in the active site of *Pf*HGPRT is responsible for xanthine selectivity. Site-directed mutagenesis to lysine, the corresponding residue of huHGPRT, resulted in loss of xanthine converting activity (Sarkar et al. 2004).The preferred substrate of huHGPRT is guanine; this is evident from the higher turnover rate and the higher affinity for guanine compared to hypoxanthine. *Pf* and *Pv*HGPRT bind hypoxanthine more tightly than guanine. This is logical since hypoxanthine is the major purine source in erythrocytes. In terms of catalytic efficiency (k_{cat}/K_M), *Pv*HGPRT has no preferred substrate while *Pf*HGPRT prefers hypoxanthine as its substrate. Besides the difference in substrate use, there are marked differences in catalytic efficiencies for the naturally occurring bases between the three enzymes. The k_{cat} values of huHGPRT for hypoxanthine and guanine are 16- and 12-fold higher than for *Pf*HGPRT, and 7- and 5-fold higher compared to *Pv*HGPRT. Thus, the human enzyme converts the naturally occurring bases more efficiently than the parasite enzymes. This is very surprising when considering the indispensable role of *Plasmodium* HGPRT in the purine salvage pathway of the parasite. An explanation could be that the HGPRT protein

expression levels are much higher in the *Plasmodium* parasite, compared to the huHGPRT levels in the human erythrocyte in which the parasite resides. Thus, turnover rates do not have to be as high for the *Plasmodium* enzymes compared to the human enzyme (de Jersey et al. 2011; Keough et al. 2010).
The differences in base affinity and specificity also indicate that the three enzymes have differences in their active site, a factor that can be exploited for drug design (de Jersey et al. 2011). Most likely, the regions surrounding the active site (e.g. the mobile loop) harbor subtle differences that may influence substrate (and inhibitor) binding. Unfortunately, the exact reason for these differences in substrate affinity is still not understood, which is mainly due to the fact that relevant crystal structures of *Pv* and *Pf*HGPRT are not yet available (de Jersey et al. 2011).

1.3 HGPRT as Drug Target

During the last decade, two classes of HGPRT inhibitors have been developed. Immucillin-5'-phosphates were the starting point for the development of Acyclic Immucillin Phosphonates (AIPs) and AIP prodrugs by Vern Schramm and coworkers. Acyclic Nucleoside Phosphonates (ANPs) that contain a 6-oxopurine base were described as a new class of antimalarial therapeutics by Dianne Keough and collaborators in 2009. Recently, this group described new ANP compounds with a second phosphonate group attached that are called bisphosphonates.

1.3.1 Immucillin-5'-phosphates and derivatives

Immucillins were originally developed as transition state analogue inhibitors of purine nucleoside phosphorylase (PNP) (Miles et al. 1998). ImmucillinH is a potent inhibitor of human and *Pf*PNPs (Kicska et al. 2002). Li et al. (1999) identified immucillin-5'-phosphates as transition-state analogue inhibitors for human and *Pf*HGPRT. ImmucillinHP (transition-state analogue of IMP) and ImmucillinGP (transition-state analogue of GMP) are thus far the most powerful HGPRT inhibitors ever described (Figure 1.8). These compounds bind with K_i values as low as 1 nM. Their binding constants are more than 1,000-fold tighter than the binding of the nucleotide substrate (Li et al. 1999). Although immucillin-5'-phosphates are potent inhibitors, they cannot be used as antimalarial therapeutics as they are not selective, expensive to synthesize and cell impermeable due to the negative phosphate charge. Also, the 5'-phosphate group is susceptible to cleavage by intracellular phosphohydrolases (Clinch et al. 2013; Hazleton et al. 2012). In the following years, ImmHP and ImmGP were used as lead compounds for the design of related inhibitors that could circumvent these problems.
Inspired by the work of Keough et al. a new class of HGPRT inhibitors, the Acyclic Immucillin Phosphonates (AIPs) was developed (Clinch et al. 2013; Hazleton et al. 2012). Keough et al. developed 6-oxopurine ANPs that were shown to be potent and selective inhibitors of human and *Pf*HGPRT (see below) (Keough et al. 2009). A major advantage of

the ANPs is that they contain a stable carbon-phosphorus bond instead of a labile phosphate-ester bond, so they cannot be hydrolyzed to inactive derivatives inside the cell (see paragraph 1.3.2). Unlike the ANPs of Keough et al., the AIPs created by Schramm and coworkers contain a cationic reaction center to develop transition state mimics with high binding affinities (Figure 1.8). Compound 2, a potent AIP inhibitor with an affinity comparable to ImmHP, is highly selective for the parasite enzyme (Clinch et al. 2013). However, due to the negatively charged phosphonate group, the AIPs lack membrane permeability. Therefore, no activity against cultured parasites is demonstrated (Hazleton et al. 2012). The next step was the development of AIP prodrugs that can cross the erythrocyte membrane, the parasitophorous vacuole and the parasite plasma membrane. AIP prodrug 3 appeared to be able to cross the erythrocyte membrane, but HPLC data suggested that 3 is rapidly converted to 2 by intracellular enzymes, resulting in inhibition of erythrocyte PNP (Hazleton et al. 2012). At higher concentrations, 3 also crosses the parasite membrane and inhibits *Pf*HGPRT activity (Hazleton et al. 2012). Lysophospholipid AIP prodrugs (compound 4 in Figure 1.8) are expected to reach the parasite's cytoplasm were they are activated by phospholipase C, creating 2 which inhibits *Pf*HGPRT. These lysophospholipid AIP prodrugs demonstrate antimalarial activity against cultured *P. falciparum* strains with IC_{50} (50% Inhibitory Concentration) values ~ 3 µM and inhibit the incorporation of [2,8-^{3}H]hypoxanthine into the parasite nucleotide pool (Hazleton et al. 2012). This is consistent with their role as HGPRT inhibitors. Unfortunately, cytotoxicity values towards human cells were not provided.

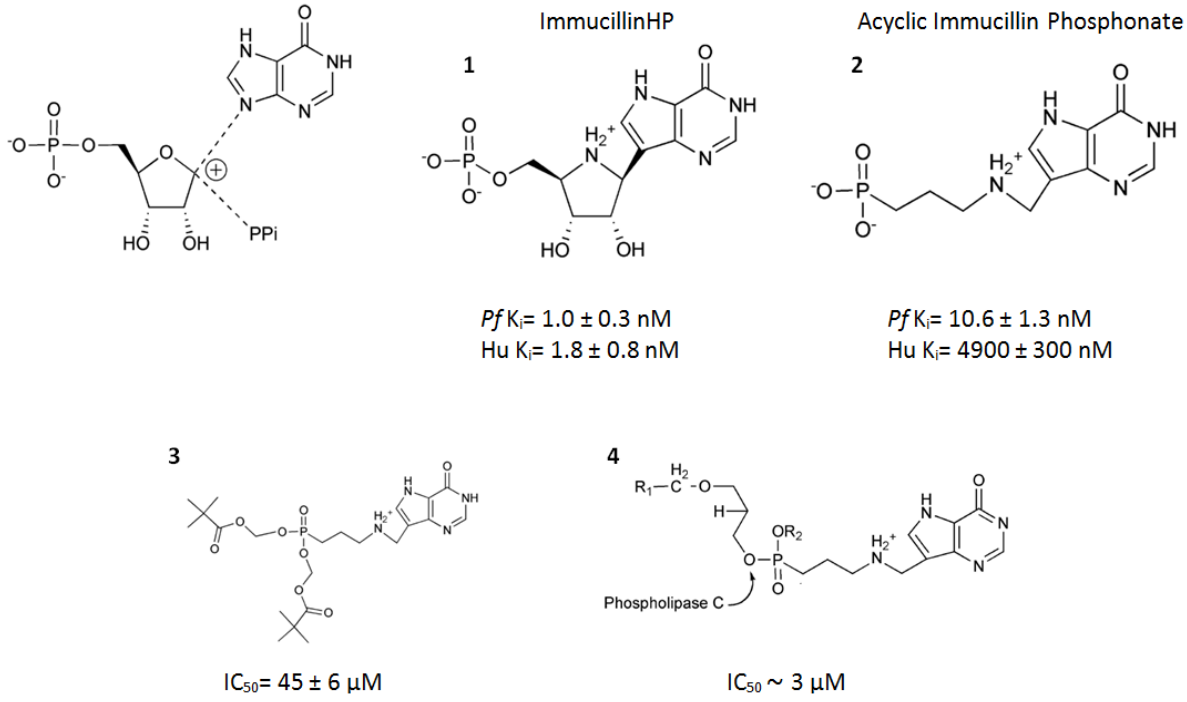

FIGURE 1.8 | **Immucillin-5'-phosphates and analogues as HGPRT inhibitors.** Left corner: proposed transition state for HGPRT with a protonated N_7 and oxocarbenium ion at C_1. ImmucillinHP mimics the ribooxacarbenium ion positive charge. The AIPs contain a phosphonate group instead of a phosphate group but maintain key features of ImmucillinHP. AIP prodrug 3, the bis-pivalate of 2, is converted in the erythrocyte to 2 and inhibits human PNP. Compound 4 is a schematic representation of a lysophospholipid AIP prodrug (Clinch et al. 2013; Hazleton et al. 2012).

1.3.2 Acyclic Nucleoside Phosphonates (ANPs)

A highly successful collaboration between the laboratories of Erik De Clercq (Rega Institute, KU Leuven) and Antonín Holý [Institute of Organic Chemistry and Biochemistry (IOCB), Czech Republic] led to the discovery of the antiviral activity of acyclic nucleoside phosphonates in the late 1980s (De Clercq et al., 1986; De Clercq et al., 1987). Twenty years after the broad antiviral activity spectrum of the acyclic nucleoside phosphonates was first described, ANPs have become important antiviral drugs for infections with the human immunodeficiency virus (HIV), hepatitis B virus (HBV), or DNA viruses. Cidofovir is clinically approved for the treatment of cytomegalovirus retinitis in AIDS patients and has off-label use for the treatment of herpes-, papilloma-, polyoma-, adeno- and poxvirus infections. Adefovir is used in the treatment of HBV infections and tenofovir is widely used in the treatment of HIV and HBV infections (De Clercq and Holý 2005; De Clercq 2007). 'Classical' antiviral nucleoside analogues such as acyclovir and ganciclovir require intracellular phosphorylation to their monophosphate forms to become active. Viruses can become resistant to these compounds by altering or lacking the activating phosphorylating enzyme (Naesens et al. 1996). The ANP compounds were originally designed to circumvent this first phosphorylation step. The antiviral ANPs (tenofovir, adefovir, and cidofovir) containing an adenine or cytosine base are structural analogues of adenosine 5'-monophospate and cytidine- 5'-monophosphate, respectively. The three drugs act in a similar fashion: first they are converted to triphosphate analogues (ANPpp) in two intracellular phosphorylation steps carried out by cellular kinases. These ANPpp metabolites then interact as competitive inhibitors/alternative substrates with respect to the normal substrates (dATP and dCTP). Whereas cidofovir acts on viral DNA-dependent DNA polymerases, tenofovir and adefovir target the reverse transcriptases of HIV and HBV. Incorporation of the active diphosphorylated forms at the 3'-end of the growing DNA chain leads to termination of chain elongation (De Clercq and Holý 2005; De Clercq 2007).

In 2009, a new collaboration between the University of Queensland (Australia), the IOCB and the Rega Institute led to the discovery that ANPs could also serve as potent and direct inhibitors of *Pf*HGPRT (Keough et al. 2009). ANPs containing a guanine or hypoxanthine base show structural similarity to the purine nucleoside 5'-monophosphates, GMP and IMP, the products of the HGPRT-catalyzed reaction (Figure 1.9). There are three major differences between the ANPs and the mononucleotides they resemble. First, the ANPs possess a stable P-C-O bond (group B, Figure 1.9) instead of the phosphoric ester group (=P-O-C-) in the natural nucleotide. This P-C-O- linkage is resistant to enzymatic dephosphorylation and the action of hydrolases (i.e. esterases and exonucleases), making ANPs stable *in vivo* (De Clercq and Holý 2005). The absence of a glycosidic bond in the structure of ANPs further decreases their susceptibility to chemical and biological degradation (Keough et al. 2009). Second, the position of the oxygen atom in the acyclic chain is altered compared with the position it

would normally occupy in the ribose ring of the mononucleotide product. Third, the flexibility of the linker (group C, Figure 1.9) allows the compounds to adopt a conformation suitable for interaction with the active site of the target enzyme (Keough et al. 2009).

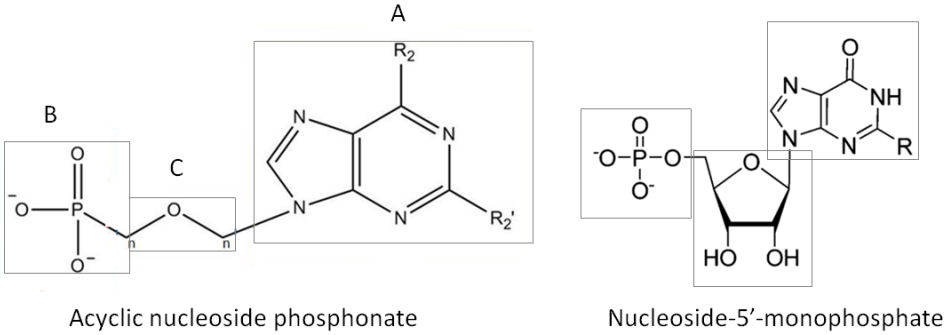

FIGURE 1.9 | **General structure of the Acyclic Nucleoside Phosphonates (left) mimicking purine nucleoside-5'-monophosphates (right).** The ANPs consist of a purine base (group A) joined by a linker (group C) to a phosphonate moiety (group B). In contrast to the AIPs, ANPs have neutral reaction centers.

The ANPs with a 6-oxopurine base were the first compounds showing that selective inhibition of *Pf*HGPRT over huHGPRT is possible, with K_i values as low as 0.1 µM (Table 1.4) (Keough et al. 2009). This is favorable as inhibition of huHGPRT could potentially have serious side-effects (paragraph 1.2.1). However, slight inhibition of the human enzyme during malaria treatment is not expected to be deleterious. Patients with a HGPRT enzyme that has only 3% of the activity of normal HGPRT lead normal lives (Dawson et al. 2005). The only result is uric acid overproduction, and this can easily be managed by allopurinol (a xanthine oxidase inhibitor) treatment (Keough et al. 2009). Inhibition studies showed that besides *Pf*HGPRT and huHGPRT, also *Pv*HGPRT (Keough et al. 2010) and *E. coli* HGPRT (Keough, Hocková, et al. 2013) are inhibited by these ANPs. Furthermore, three ANP compounds were able of arresting the growth of *P. falciparum* in erythrocyte cultures (Table 1.4) (Keough et al. 2009). At present, *P. vivax* cannot be maintained in *in vitro* cell culture, so *P. falciparum* is the only cell culture model available to test antimalarial compounds.

TABLE 1.4 | **K_i values, antimalarial activity *in vitro* and cytotoxicity for eight ANPs (**Keough et al. 2009**).**

ANP	K_i (µM)		Ratio (K_i(Hu) /K_i(*Pf*))	IC_{50} (µM)[a]	CC_{50} (µM)		
	HuHGPRT	*Pf*HGPRT			A549[b]	C32[c]	C32TG[d]
PEEG	1 ± 0.50	0.1 ± 0.02	10		>300	>300	>300
PEEHx	3.6 ± 0.2	0.3 ± 0.04	12				
S-HPMPG	5.9 ± 0.4	0.6 ± 0.2	10				
PMEG	29 ± 4	1.6 ± 0.2	18	14	17		
Cyclic (S)-HPMPG	90 ± 10	8 ± 1	11	1	489		
Cyclic (R)-HPMPG	19 ± 5	1 ± 0.2	19	46	>1000		

[a]Inhibition of parasite growth was determined for the Dd2 *Pf* strain, a chloroquine resistant *Pf* strain. [b] Human lung carcinoma cells. [c] Human melanoma cells. [d] Thioguanine-resistant and HGPRT-deficient mutant of C32 cell line.

The crystal structures of huHGPRT in complex with PEEG, PEEHx and (S)-HPMPG provided important insights into how the inhibitors bind to the active site. To date, no crystal structure of *Pf*HGPRT or *Pv*HGPRT in complex with an ANP is available. In order to increase inhibitor affinity, molecular modeling led to the design of new compounds containing a second phosphonate group that occupies the PP_i binding pocket of the HGPRT enzyme (Figure 1.10).

A promising bisphosphonate lead compound is compound **17**, {[(2-[(Guanine-9Hyl)methyl]propane-1,3-diyl)bis(oxy)]bis(methylene)} diphosphonic acid, a guanine bisphosphonate and nanomolar inhibitor of huHGPRT, *Pf*HGPRT and *Pv*HGPRT (Table 1.5).

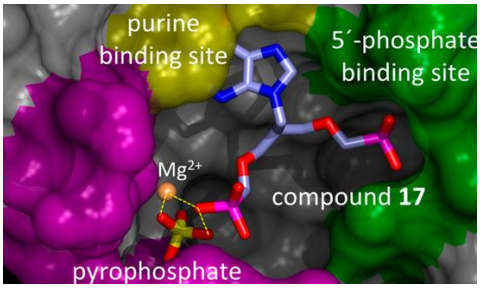

FIGURE 1.10 | **Compound 17 in complex with huHGPRT.** Compound **17** fills three critical locations within the active site of huHGPRT: the purine binding site, the 5'-phosphate binding site and the PP_i binding pocket. The second phosphonate group is held in position by interactions with the magnesium ion (Dianne T Keough, Špaček, et al., 2013).

TABLE 1.5 | **K_i values of ANP bisphosphonates and antimalarial activity and cytotoxicity of lipophilic ANP prodrugs.** The chemical structures of the lipophilic prodrugs and the active bisphosponates are shown below (Keough, Špaček, et al. 2013).

			K_i (µM)[a]			IC_{50} (µM)[b]		CC_{50} (µM)[b]		
Compd	**Purine base**	**Prodrug of**	**huHGPRT**	***Pf*HGXPRT**	***Pv*HGPRT**	**D6[c]**	**W2[d]**	**A549[e]**	**C32[f]**	**C32TG[g]**
10 (PP-P364)	G	**8**	0.6 ± 0.02	0.5 ± 0.01	0.7 ± 0.02	6.6 ± 2.3	7.7 ± 2.1	107 ± 55	48 ± 2	46 ± 4
18 (PP-P343)	Hx	**16**	1 ± 0.1	5 ± 1	2 ± 0.3	3.8 ± 0.5	4.0 ± 0.9	101 ± 17	41 ± 6	55 ± 4
19 (PP-P351)	G	**17**	0.03 ± 0.002	0.07 ± 0.01	0.6 ± 0.07	9.7 ± 1.6	7.1 ± 2.1	>300	130 ± 15	109 ± 8

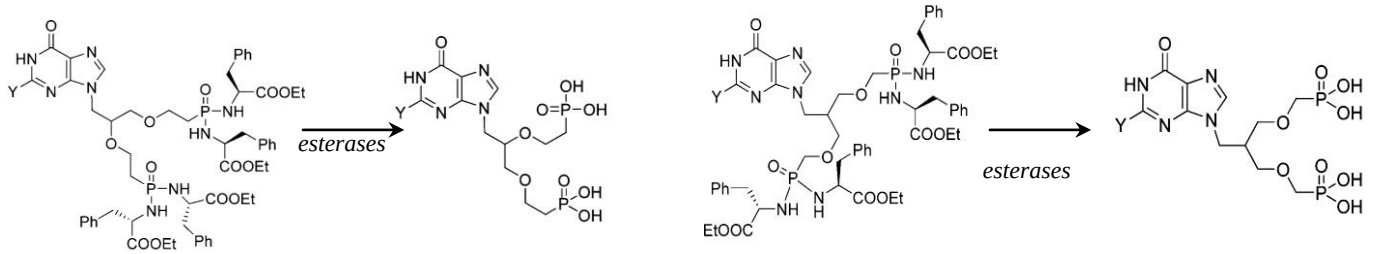

10 (Y= NH_2) **8** (Y= NH_2) **18** (Y= H) **19** (Y= NH_2) **16** (Y= H) **17** (Y= NH_2)

[a] Inhibitor constants for the bisphosphonate inhibitors **8**, **16** and **17**.
[b] *In vitro* antimalarial activity and cytotoxicity of bisphosphonate prodrugs **10**, **18** and **19**.
[c] *Pf* strain sensitive to most drugs. [d]Chloroquine-and pyrimethamine-resistant *Pf* strain. [e] Human lung carcinoma cells.
[f] Human melanoma cells. [g] Thioguanine-resistant and HGPRT-deficient mutant of C32 cell line.

The bisphosphonate compounds (**8**, **16** and **17** Table 1.5) are negatively charged under physhiological pH and are thus not able to cross the cell membrane. Therefore, no antimalarial activity is observed *in vitro* (Keough, Špaček, et al. 2013). To allow cell membrane passage, the highly polar bisphosphonate groups are masked by lipophilic phosporamidate groups. This prodrug technology has proved effective for several compounds with antiviral or anticancer activity (Mehellou et al. 2009). The bisphoshonate prodrugs (**10**, **18** and **19**) are not active themselves and first need to be hydrolyzed to the active compounds by esterases inside the cell (Table 1.5). At present it is not known if the prodrug is hydrolyzed within the red blood cell and the ANP enters the parasite, or whether the prodrug is transported via the parasitophorous vacuole and the parasite plasma membrane to the parasite's cytosol were it is hydrolyzed to the active compound (Keough, Špaček, et al. 2013). These prodrugs are effective in inhibiting parasite growth with IC_{50} values as low as 3.8 µM while having no or low cytotoxicity in human cell lines (Table 1.5).

The data provided in Tables 1.4 and 1.5 support the hypothesis that inhibition of HGPRT is responsible for the growth inhibitory effect of the malaria parasite but further evidence is needed to fully establish this mechanism. Thus far, HGPRT inhibition has only been proven in cell-free enzymatic studies. However, the observed antiparasitic activity *in vitro* might arise from cytototoxic effects in which other *Plasmodium* targets are involved (Berg et al. 2010). For example, it is not unlikely that certain ANPs are converted to toxic metabolites by cellular kinases within the protozoal cell, thereby inhibiting other cellular enzymes, e.g. DNA polymerases (see antiviral activity), resulting in cessation of parasite replication. To validate HGPRT as the target of the ANP prodrugs, a complementary cell assay is needed that allows us to directly investigate the inhibition of human, *Pf* and *Pv*HGPRT in a cellular context.

2 RESEARCH OBJECTIVES

Resistance of *Plasmodium* species towards current antimalarial medicines is a prevailing problem. New therapeutics with novel mechanisms of action are required to support combination therapy approaches promoted by the World Health Organization. The HGPRT enzyme of *Plasmodium* is a well established antimalarial drug target. Acyclic nucleoside phosphonates (ANPs) containing a guanine or hypoxanthine base were the first compounds known to selectively inhibit *Pf*HGPRT and *Pv*HGPRT over huHGPRT in enzymatic assays (Keough et al. 2009, 2010). Furthermore, they arrest parasitaemia in erythrocyte cultures of *P. falciparum* and have low cytotoxicity towards human cell lines (Keough et al. 2009; Keough Špaček et al. 2013). Our goal was to develop a novel cell culture assay that provides a link between the enzymatic assays and the *Pf*-infected erythrocyte assay. This complementary method would help to investigate whether the antiparasitic effect of the ANPs is indeed the result of inhibition of the HGPRT enzyme of *Plasmodium*.

I. The first aim of this thesis was the construction of recombinant adenoviral (Ad) vectors that contain the cDNA encoding human, *Pf* or *Pv*HGPRT. With these Ad vectors, we aimed at obtaining high levels of enzyme activity after the transduction of HGPRT-deficient human cell lines (HeLaTG, C32TG and 1306) (Figure 2.1, step 1 and 2). To determine which target cell type to chose, the transduction efficiency of the different cell lines with the Ad vectors was evaluated by fluorescence microscopy, Western blot analysis, flow cytometry and measurement of obtained HGPRT enzymatic activity by measuring ^{3}H release from [2,8-^{3}H]Hx (Figure 2.1, step 3) .

II. To validate the strength of our new assay, we first wanted to investigate the inhibitory effect of several known inhibitors and purine base analogues on HGPRT activity, and compare the results obtained in Ad-transduced cells with results in A549 cells (containing endogenous HGPRT activity). The final goal of this thesis was to verify whether the logically designed ANP bisphophonates indeed possess HGPRT inhibitory activity in a cellular context (Figure 2.1, Step 4). Furthermore, we wanted to compare the ANP structure-activity relationship obtained in our new cell culture assay with that obtained in the enzymatic studies performed by our collaborator D. Keough.

III. In a small side project, we examined the purine metabolism in wild type Chinese hamster ovary (CHO-K1) and an adenylosuccinate lyase (ADSL)-deficient mutant cell line derived thereof (AdeI). This comparative study was aimed at understanding the differences in purine salvage metabolism between AdeI and CHOK1 cells, and at investigating whether these cells could be useful in cytotoxicity assays with the ANPs. We hypothesized that cells with an aberrant purine synthesis pathway would be more sensitive to HGPRT inhibition.

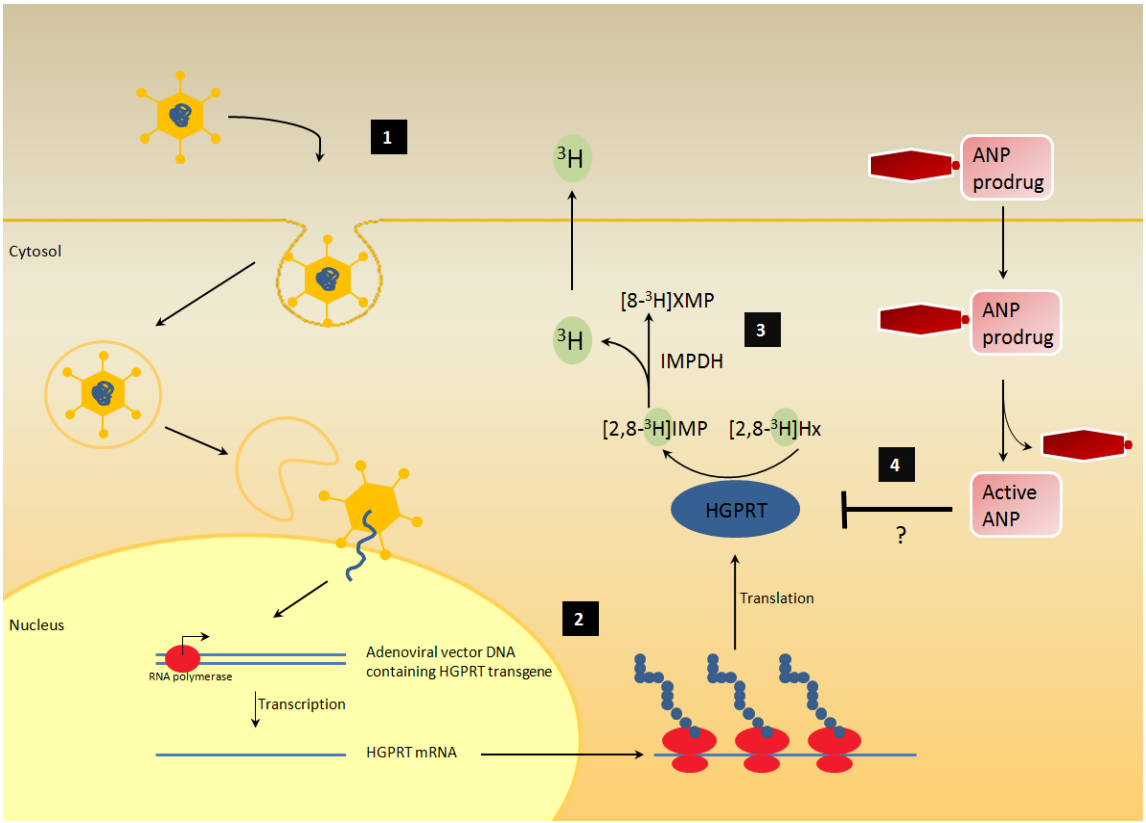

FIGURE 2.1 | **Schematic representation of the cellular assay that we aimed to construct.** (1) A recombinant adenoviral vector, containing the cDNA of human, *Pv* or *Pf*HGPRT, infects an HGPRT-deficient cell line. (2) The adenoviral DNA is transcribed and translated by the host transcriptional machinery, resulting in high HGPRT protein expression levels. (3) HGPRT enzymatic activity is measured with the tritium release assay. Adenoviral infected cells are exposed to radiolabeled [2,8-^{3}H]hypoxanthine which is converted to [8-^{3}H]XMP by the sequential action of HGPRT and IMPDH. In the latter reaction, one ^{3}H label is released, that diffuses out of the cell in the culture medium. The amount of released ^{3}H, measured by liquid scintillation, gives a measure of HGPRT activity. (4) The central question in this project is whether lipophilic prodrugs of bisphosphonate ANPs have an inhibitory effect on HGPRT in a cellular context. This will be quantified by determining the inhibitor concentration needed to reduce enzymatic conversion of [2,8-^{3}H]Hx (assessed by the ^{3}H release assay) by 50%.

3 MATERIALS AND METHODS[1]

3.1 Chemical Compounds

Cytostatic nucleoside analogues were purchased from Sigma-Aldrich (St-Louis, MO). Experimental phosphonate and bisphosphonate inhibitors were synthesized by Dr. D. Hocková and colleagues (IOCB, Prague, Czech Republic).
Radiolabeled nucleobases [2,8-^{3}H]Hx (specific radioactivity: 15 Ci/mmol) and [8-^{3}H]Ade (specific radioactivity: 26 Ci/mmol) were obtained from Moravek Biochemicals Inc. (Brea, CA). Prior to its use in ^{3}H release experiments, the [2,8-^{3}H]Hx stock was purified to reduce the presence of ^{3}H contaminants within the stock. One hundred microliter, i.e. 100 µCi of the [2,8-^{3}H]Hx stock (1mCi/ ml) was injected onto a Superspher 100RP-18 endcapped column (Merck) and separated with two buffers: buffer A: 0.05 M NH_4-formate, pH 5 and buffer B: 50% 0.05 M NH_4-formate pH 5, 50% acetonitrile. The following gradient was used (flow: 1 ml/min): 0 min: 100% A, 0-10 min: 0 - 100% B, 10-15 min: 0 - 100% A, 15-20 min: 100% A. Half-minute eluate fractions were collected and 1 µl of each fraction was counted for radio-activity in a scintillation counter. The fractions containing purified [2,8-^{3}H]Hx with high radioactive counts, were first combined, then distributed over five eppendorf tubes (~ 20 µCi per tube) and submitted to solvent evaporation in a SpeedVAC apparatus. Dry samples were stored at -20°C and reconstituted in 500 µl DMEM as such (final activity in tube: 0.04 µCi/µl) prior to use in experiments.

3.2 Cell Cultures and Media

Cell lines were purchased from the following sources: A549 human lung carcinoma cells and C32TG human melanoma cells: from the American Type Culture Collection (ATCC) (Rockville, MD); 1306 human skin fibroblasts: from the European Collection of Cell Cultures; 293AD human embryonic kidney cells: from Cell BioLabs (Cat. No. AD-100) and HeLa TG human cervical cancer cells: from the Japan Riken Cell Bank. Madin-Darby canine kidney (MDCK) cells were a kind gift from Dr. M. Matrosovich (Philipps-Universität, Marburg, Germany). Wild-type Chinese Hamster Ovary cells (CHOK1) and AdeI cells, which are CHO cells deficient in adenylosuccinate lyase (ADSL), were kindly provided by Dr. D. Patterson (Eleanor Roosevelt Institute, Denver, US). Both cell lines were maintained in RPMI 1640 medium (Invitrogen, Carlsbad,CA), supplemented with 10% fetal calf serum, 2 mM L-glutamine and 0.075% sodium bicarbonate. The culture medium of AdeI cells was supplemented with 30 µM adenine. MDCK, A549, C32TG, 1306, HeLa TG and 293AD cells were maintained in Dulbecco's modified Eagle's medium (DMEM) (Invitrogen, Carlsbad, CA) supplemented with 10% fetal calf serum (FCS), 1 mM sodium pyruvate and 0.075%

[1] A risk assessment that examines the risks and control measures related to the used chemical compounds, biological agents and equipment is enclosed in the Addendum page 74.

sodium bicarbonate. 1306, C32TG and HeLa TG cells are cell lines obtained by selection for 6-thioguanine (6-TG) resistance. To maintain selection pressure, their medium was supplemented with 50 µM 6-TG. Prior to their use in experiments, the cells were grown for one passage in the absence of 6-TG.

For cotransfection experiments and Ad vector amplification, 293AD cells were maintained in OptiMEM-I reduced serum medium (Invitrogen, Carlsbad, CA) with 2% FCS and antibiotics (20 µg/ml gentamycine and 0.5 µg/ml amphotericin B). When used in experiments, 1306 cells were seeded onto 0.5% gelatin (Porcine skin Type A, Sigma)-coated plates in minimal essential medium (MEM) (Invitrogen, Carlsbad, CA) with 10% FCS, 2 mM L-glutamine and non-essential amino acids. When cells were infected with the Ad vectors, the concentration of FCS was reduced to 2% and 20 µg/ml gentamycine and 0.5 µg/ml amphotericin B was added. All cells were grown in a humidified incubator at 37°C with a constant gas phase of 5% CO_2.

3.3 Generation of Recombinant Adenoviral Vectors

3.3.1 Cloning of *Pv, Pf* and huHGPRT genes in pacAd5 CMV-IRES GFP shuttle vector

Plasmid purification. Glycerol stocks of competent JM109 *E. coli* cells that were transformed with the plasmids shown in Table 3.1 were stored at -80°C. An aliquot of each glycerol stock was grown overnight in 5 ml LB medium plus 100 µg per ml kanamycin or ampicillin at 37°C, 200 rpm. The next day, plasmids were purified using the centrifugation procedure of Wizard Plus SV Miniprep DNA purification System (Promega). DNA concentration was determined using the Thermo Scientific NanoDrop™ 1000 Spectrophotometer.

TABLE 3.1 | **Description of starting plasmid materials.**

Plasmid[a]	Antibiotic resistance gene	MCS contains
pIDTSmart (2.7 kb)	kanamycine	*Pv*HGPRT (714 bp; codon-optimized)
pIDTSmart (2.7 kb)	kanamycine	*Pf*HGPRT (708 bp; codon-optimized)
pCAGEN (4.7 kb)	ampicillin	WThuHGPRT (673 bp, obtained from C32)
pCAGEN (4.7 kb)	ampicillin	ΔEx2huHGPRT (566 bp, obtained from C32TG)
PacAd5 CMV-IRES GFP shuttle vector (7.5 kb)	ampicillin	
PacAd5 9.2-100 backbone vector (34.9 kb)	ampicillin	

[a]See also Supplemental Figures 1, 2 and 3.

Introduction of *EcoRI* and *BamHI* restriction sites in huHGPRT inserts. The pIDTSmart plasmids contain the codon optimized genes for the HGPRT enzyme of *P. vivax and P. falciparum,* respectively (Supplemental Figure 1). These HGPRT DNA sequences are flanked by an *Eco*RI (5') en *Bam*HI (3') restriction site, necessary for sticky end ligation in the PacAd5 CMV-IRES GFP shuttle vector (Supplemental Figure 2). Since the WThuHGPRT and ΔEx2huHGPRT DNA sequences in the pCAGEN vector were not flanked by these two restriction sites, the sites were introduced by an Expand High Fidelity (HF) PCR reaction

(Roche) using primer 26 and 30 (Table 3.2). The PCR fragments were separated on a 2% agarose gel and stained with ethidium bromide. The ~700 bp (WT huHGPRT HF PCR product) and ~600 bp (ΔEx2huHGPRT HF PCR product) bands were excised with a scalpel and purified using the Wizard SV gel & PCR Clean-up System (Promega). DNA concentration was determined using the Thermo Scientific NanoDrop™ 1000 Spectrophotometer.

Restriction enzyme digestion with *EcoRI* and *BamHI*. The pIDTSmart-KAN-*Pv* HGPRT and pIDTSmart-KAN-*Pf* HGPRT plasmids (donor plasmids), the HF huHGPRT PCR fragments and the PacAd5 CMV-IRES GFP shuttle vector (recipient plasmid) were digested with *Eco*RI en *Bam*HI for 5 hours at 37°C. The *Pv* and *Pf* HGPRT *Eco*RI-*Bam*HI digests were separated from the pIDTSmart-KAN plasmid by gel electrophoresis (2% agarose, EtBr visualization), excised from the gel and purified using the Wizard SV gel & PCR Clean-up System (Promega). The huHGPRT *Eco*RI-*Bam*HI digests were not submitted to electrophoresis but directly purified with the same Promega purification kit. The digested shuttle vector was treated with alkaline phosphatase (AP). AP removes the 5'-phosphate groups, thereby preventing self-ligation of the vector. First, the restriction enzymes were inactivated by placing the mixture 10 min at 65°C, followed by 3 min on ice. One microliter AP (1U/µl, Roche) was added to 5 µg digested vector DNA and incubated for 1 hour at 37°C. AP was inactivated by placing the mixture 10 min at 65°C. Then, the digested vector was separated from undigested vector on a 0.7% agarose gel. Positive bands were cut out off the gel and purified using the Wizard SV gel & PCR Clean-up System (Promega). DNA concentrations of the digested shuttle vector and the *EcoRI/BamHI* digested HGPRT fragments were obtained using the Thermo ScientificNanoDrop™ 1000 Spectrophotometer.

Cohesive end ligation of HGPRT inserts into shuttle vector. The ligation was performed according to the Promega T4 DNA Ligase protocol. One hundred nanogram vector was used with varying ratios of insert to vector: 2:1, 4:1 and 6:1. For optimal ligation efficiency the reaction mixture was incubated overnight at three different temperatures: 3 h at 22°C, 8 h at 16°C and 6 h at 4°C. In this way, the optimal T4 DNA ligase temperature (37°C) was balanced with the melting temperature of the sticky ends being ligated. T4 DNA ligase was inactivated by heating the mixture 10 min at 65°C.

Transformation of HGPRT-shuttle vectors in JM109 competent *E.coli* cells. Five microliter of the ligation reaction mixture was added to 45 µl competent JM109 cells and placed on ice for 20 min. Then a heat shock was performed by placing the tubes 45 sec at 42°C, followed by 2 min on ice. 250 µl Super Optimal Broth (SOC) medium (Invitrogen) was added and transformed cells were grown in a shaking incubator for 1 h at 37°C. Then, transformed *E. coli* cells were plated (50 µl and 250 µl) onto LB agar plates (35g/l) containing 100 µg/ml ampicillin and incubated overnight at 37°C. The next day, six colonies were picked per insert. To verify the presence of the cloned HGPRT fragment, the colonies were screened by Go Taq

PCR (Promega), using primers 39 and 40 (Table 3.2). The HGPRT PCR products were subsequently separated on a 2% agarose gel with EtBr detection. From those transformed *E. coli* colonies for which a positive band appeared, glycerolstocks were frozen at -80°C. Two colonies of each HGPRT insert were grown overnight in 50 ml LB medium plus 100 µg/ml ampicillin at 37°C, 200 rpm. The next day, HGPRT-shuttle vectors were purified using the centrifugation procedure of PureYield Midiprep System (Promega). DNA concentrations were obtained using the Thermo Scientific NanoDrop™ 1000 Spectrophotometer.

Sequencing of HGPRT-shuttle vectors. To verify that no accidental mutations in the HGPRT inserts had appeared during HF-PCR or subcloning, the HGPRT-shuttle vectors were sequenced using Big Dye Terminator Cycle sequencing. First, the vectors were purified with the Wizard Plus SV Miniprep DNA purification System (Promega). Then, they were amplified by PCR, using two outer primers (No. 39 and 40) and four (*Pf*HGPRT and PvHGPRT) or two (huHGPRT) inner primers (Table 3.2). After ethanol precipitation and reconstitution in formamide, the samples were sent for sequence analysis.

TABLE 3.2 | **Primers used for cloning and sequencing.**

Name	No.	Primer sequence	Application
WT-huHGPRT FOR *EcoRI*	26	5'GAGAGAGAATTCGCTCCGTTATGGCGACC 3'	Introduction of *EcoRI* and *BamHI* restriction sites by HF-PCR.
WT-huHGPRT REV *BamHI*	30	5' CTCTCGGATCCTGAACTCTCA 3'	
WT-huHGPRT SEQ FOR	28	5'GACCAGTCAACAGGGGACAT 3'	Sequencing of huHGPRT
WT-huHGPRT SEQ REV	29	5'CCTGACCAAGGAAAGCAAAG 3'	
Pv HGPRT SEQ FOR1	31	5' AGAGTTCCATGTGATCTGCCTGCT 3'	Sequencing of *Pv*HGPRT (codon optimized)
Pv HGPRT SEQ FOR2	32	5' TCCATTGTGGAACGGGTTCAAAGC 3'	
Pv HGPRT SEQ REV1	33	5' ATCGAAGGCCAGCTTCTCGATTCT 3'	
Pv HGPRT SEQ REV2	34	5' AGCTTTGAACCCGTTCCACAATGG 3'	
Pf HGPRT SEQ FOR1	35	5' TCGGATCGAGAAACTGGCTTACGA 3'	Sequencing of *Pf*HGPRT (codon optimized)
Pf HGPRT SEQ FOR2	36	5'AATGGCTTCAAAGCCGACTTCGTG 3'	
Pf HGPRT SEQ REV1	37	5'TATGCGGGACAAATGTTTCA 3'	
Pf HGPRT SEQ REV2	38	5'AAGTCGGCTTTGAAGCCATTCCAGAGA 3'	
Shuttle outer FOR (CMVp forward)	39	5' GTGGGAGGTCTATATAAGCAGAGCTCG 3'	Outer FOR and REV primer for shuttle vector and Ad-vector sequencing (~ 100bp/ 150bp before/ after MCS) and screening of transformed JM109 *E. coli* colonies.
Shuttle outer REV (IRES reverse)	40	5' CTCACATTGCCAAAAGACG 3'	

3.3.2 Generation of recombinant Ad vectors by co- transfection of 293AD cells

Shuttle and backbone vector linearization with *PacI*. Midipreps of PadAd5 CMV-IRES GFP shuttle vectors containing the cloned HGPRT cDNA sequences and the PacAd5 9.2-100 backbone vector (Supplemental Figure 3) were digested with *PacI* (Biolabs, 10U/µl) for 2 h at 37°C. Digested and undigested plasmid DNA (0.5 µg of each) were run on a 0.8% agarose gel to confirm the completion of *PacI* digestion (for the shuttle vectors one band of ~ 8kb appeared. For the backbone vector two bands were seen: one band of ~33 kb and a second

band of 2.0 kb). *PacI* digested vectors were purified with Promega Wizard SV Gel and PCR Clean-Up System (Promega) followed by ethanol precipitation.

Transfection of 293AD cells. The day before transfection, 293AD cells were trypsinized with 0.05% trypsine-EDTA (Invitrogen) and seeded at 215,000 cells/ well in a 12-well plate. On the day of transfection, around 70-80% confluency was reached. Growth medium was removed and replaced with 2 ml OptiMEM-I Reduced Serum Medium (Invitrogen) supplemented with 2% FCS, but containing no antibiotics since this could lead to cell toxicity during transfection. The plates returned to the incubator for 1 h before transfection. Linearized shuttle and backbone vector were diluted in 25 µl OptiMEM-I as such and subsequently 1:1 mixed. To maximize transfection success, four different combinations of total DNA quantities were prepared: 0.7 µg shuttle-0.18µg backbone, 0.5 µg shuttle-0.125µg backbone, 0.35µg shuttle-0.0875 µg backbone and 0.25µg shuttle-0.0625 µg backbone (shuttle:backbone ratio was in all cases 4:1). Lipofectamine-2000 (Invitrogen) was diluted in OptiMEM-I as such (for 1 well of a 12-well plate: 3.5 µl Lipofectamine was diluted in 50 µl OptiMEM-I as such), vortexed and incubated for 10 minutes at room temperature. After this incubation period, shuttle-backbone mixes and diluted Lipofectamine-2000 were combined (total volume of 100 µl), gently mixed (not vortexed since this could lead to DNA shearing of the backbone plasmid) and incubated for 30 minutes at room temperature. Then, the 100 µl DNA-Lipofectamine complexes were added to each well, while gently rocking the plate back and forth. After 24 h incubation at 37°C, the medium containing the transfection mix was changed by OptiMEM-I, supplemented with 2% FCS and antibiotics. Cells were incubated for 10-20 days at 37°C. Each day, cells were checked for the presence of plaques using a light microscope, and GFP expression was monitored using a fluorescence microscope.

Harvesting of crude adenoviral lysate and Ad vector amplification. After approximately 10-17 days, when half of the cells were detached from the bottom of the well, adenovirus containing cells were collected (~2 ml) by scraping the cells off the plate with a sterile pipette, and the mixtures of cells plus medium were transferred to sterile 15 ml tubes. Viruses were released from cells by three freeze/thaw cycles (10 minutes on dry ice/ 10 minutes in a water bath of 37°C). Then, the cell lysate was centrifuged at 3000 rpm for 20 minutes at 4°C to pellet cell debris. One ml of the supernatant (in total 1.5 ml) was stored as initial viral stock (S_0 stock) at -80°C; the remaining 500 µl was diluted 3 fold in 1 ml OptiMEM-I as such and was used for adenovirus amplification. Therefore, 600,000 293AD cells were seeded in a 6-well plate the day before infection. On the day of infection, medium was removed and cells were washed once with OptiMEM-I as such. Then, the diluted initial virus stock was added in triplo to the dry wells (500 µl to each well) and incubated for 1 h at 37°C, allowing adenovirus adherence. After 1 h, 1.5 ml OptiMEM-I supplemented with 2.5% FCS and antibiotics was added without virus removal (final 2% FCS). Three days later, complete cytopathic effect (CPE) was seen with more than 95% of the cells detached. Adenoviral vectors were harvested as

described above and stored at -80°C (S_1 stock). In the second round of amplification, 293AD cells were cultured in 75-cm^2 culture flasks. When 70% confluency was reached, medium was changed to OptiMEM-I with 2% FCS and antibiotics, and either 400 or 100 µl of 1/10 diluted S_1 stock was added to the medium. After completion of CPE (3 days), cells and culture medium were collected into 50 ml falcon tubes. Adenoviral particles were released by three freeze-thaw cycli, cell debris was pelleted by centrifugation and supernatants were divided in aliquots (S_2 stock) and stored at -80°C.

Sequencing of recombinant Ad vectors. To verify that no accidental mutations in the HGPRT inserts had occurred during homologous recombination after co-transfection, recombinant Ad vectors were sequenced. A549 cells (375,000 cells per well in OptiMEM-I with 2% FCS and antibiotics) were infected with the Ad S_2 stock. Three days after infection, DNA was purified using the E.Z.N.A. blood DNA kit (Omega). HGPRT sequences were then amplified by HF-PCR, using the two outer primers (No. 39 and 40, Table 3.2). Five µl of each PCR sample was separated on a 2% agarose gel. The remaining PCR sample was used for sequencing by Big Dye Terminator Cycle sequencing.

Titration of Ad vector S_2 stocks. A viral plaque assay was performed to determine virus concentration as plaque-forming units per ml (PFU/ml). The day before viral infection, 293AD cells were seeded in a 12-well plate at 330,000 cells/well. Starting from a 1/50 dilution of the adenoviral S_2 stocks, 5-fold dilutions were prepared in DMEM as such. Cells were washed once with DMEM as such, then 400 µl of each virus dilution was added to each well. The infected cells were incubated one hour at 37°C allowing virus adsorption, and every 10 minutes plates were gently rocked back and forth to evenly distribute the virus. A 1.6% agar (Sigma Cat. No. A-9915) stock solution (i.e. 0.8 g in 50 ml sterile water) was heated in the microwave and 1:1 mixed with DMEM 2x (supplemented with 4% FCS and 0.75% bicarbonate). After 1 h incubation, medium containing viral dilutions was aspirated and 1 ml agar overlay solution was added to each well (final agar concentration: 0.8%). After agar solidification (approximately 10 minutes) plates were incubated for 6 days at 37°C. To facilitate visualization of plaques, 1 ml of a second agar overlay containing 0.45 % neutral red was added on top of the first overlay. On day 8, wells containing between 5-50 plaques were counted macroscopically. Then, cells were stained with crystal violet to make sure that no plaques were missed. First, cells were fixated with 3.7% formaldehyde for 1 h. Then, the agar plug was removed and 500 µl 0.5% crystal violet (1 gram in 200 ml methanol) solution was added to the wells. After 30 min, the crystal violet solution was removed. The viral titer (in PFU/ml) was calculated using following formula: # plaques/ (D*V), D = dilution factor, V = volume of diluted virus added to the well.

To exclude any potential contaminations of wild-type replication-competent adenovirus within the Ad vector S_2 stocks, the plaque assay was also performed on A549 cells, using the same procedure.

3.3.3 Adenoviral transduction of different target cells

Infection of different cell lines with Ad vectors. In a preliminary set of experiments we assessed Ad transduction efficiency in different cell types (MDCK, A549, HeLa, HeLaTG, C32TG, and 1306) without precise titer assessment of our stocks. Cells were seeded in 12-well plates to reach 80-90% confluency on the day of infection. After aspirating the medium from the plate, cells were infected with 400 µl virus (i.e. viral S_2 stock, 2-fold diluted in culture medium) for one hour at 37°C, while rocking the plate every 20 min. After virus adsorption, 1.6 ml fresh complete culture medium (with 2% FCS) was added, without virus removal. Transduction efficiency was evaluated after 24, 48 and 72 hours by fluorescence microscopy.

Determination of transduction efficiency of HGPRT-deficient target cells using flow cytometry. To quantify the transduction efficiency of the HGPRT-deficient cell lines (C32TG, 1306 and HeLaTG), the cells were submitted to flow cytometric analysis. C32TG, 1306 and HeLaTG were seeded in 12-well plates at 300,000 cells per well the day before infection. After removal of the medium, cells were infected with Ad vector S_2 stocks at a multiplicity of infection (MOI) of 32, 16 or 8 PFU/cell. After a 1-hr incubation period, virus was removed and 2 ml fresh culture medium (with 2% FCS) was added to each well. Two days post infection, cells were trypsinized and resuspended in culture medium. After resting 30 min at 37°C, cells were collected by centrifugation (8 min, 1800 rpm, 4°C). The cell pellet was washed two times with 600 µl PBS containing 2% FCS. In the final step, cells were fixated with 2% formaldehyde in PBS and analyzed on a FACSscan flow cytometer (BD Biosciences).

Assessment of HGPRT protein expression by Western blot analysis. HeLaTG, C32TG and 1306 cells were seeded in 6-well plates at 300,000 cells/ well. One day later, cells were infected with Ad vector S_2 stocks at an MOI of 16 (Ad-WThu and Ad-ΔEx2) or 50 (Ad-*Pv* and Ad-*Pf*) PFU/cell. Total cell lysates of Ad-infected and uninfected 1306, C32TG and HeLaTG were prepared with ice-cold protein extraction buffer containing 0.02 M Tris-HCl (pH 7.4), 0.137 M NaCl, 2 mM Na_2EDTA, 1% Triton X-100, 1 mM Na-vanadate, 2 mM Na-pyrophosphate, 10% glycerol, 144 mM PMSF, 0.01 mg/ml leupeptine and 0.025 M β-glycerophosphate. After determining the protein content of each sample by the Bradford assay, fifteen micrograms of total protein was loaded on 12% Tris-Glycine gels and separated by SDS-PAGE. Separated proteins were then transferred to polyvinylidene fluoride membranes (Amersham Biosciences) by electroblotting (Trans-Blot SD semi-Dry transfer Cell, Bio-Rad). Blocking of membranes was performed overnight by placing the blots in 5% nonfat dry milk in PBS at 4°C. After two wash steps (2 x 5 min) in PBS with 0.1% Tween-20, blots were stained with rabbit anti-HGPRT antibody (Ab10479, Abcam; dilution 1/1000) or mouse anti-β-actin antibody (A5441, Sigma-Aldrich; dilution 1/5000) for 1 h, followed by a horseradish peroxidase-linked secondary antibody: anti-rabbit HRP (P0399, Dako; 1/4000) or anti-mouse HRP (P0447, Dako; 1/1000) for 45 minutes. Antibodies were diluted in 2% nonfat dry milk in PBS with 0.1% Tween-20. Visualization of the protein bands was done with the ECLplus

ragent from GE Healthcare and protein bands were imaged by the V3 Western Workflow™ (Bio-Rad).

Tritium release assay. This assay was originally optimized for suspension cells by Balzarini and De Clercq (1992). To measure HGPRT enzyme activity obtained after Ad transduction a tritium release assay was performed (Figure 3.1). HGPRT-deficient cells, seeded in 12-well plates, were infected with Ad S_2 stocks as above. After 48 h incubation, culture medium was removed and replaced by 600 µl fresh medium with 10% FCS to resume HGPRT activity. After 4 h pre-incubation, 20 µl of reconstituted [2,8-^{3}H]Hx (~0.8 µCi per well) was added to the medium. After the indicated time points, the supernatant was withdrawn and added to an ice-cold suspension of 600 µl activated charcoal (Sigma) (150 mg/ml) in 7.5% trichloroacetic acid (TCA). TCA precipitates proteins, DNA and RNA and the activated charcoal absorbs nucleotides and free [2,8-^{3}H]Hx. After standing 10 min on ice, the suspension was centrifuged at 12000 rpm for 10 min and the supernatant (containing free ^{3}H) was added to 9 ml Optiphase Hisafe 3 (Perkin Elmer). Radioactivity was counted by liquid scintillation counting (on a Tri-Carb 2810 TR, Perkin Elmer). To correct for free ^{3}H present in the [2,8-^{3}H]Hx stock, two cell controls (i.e. non-Ad-infected cells) were measured and the obtained radioactive value was subtracted from the experimental values. Radioactivity incorporated into nucleic acids was determined after 24 h incubation with [2,8-^{3}H]Hx. After removal of the supernatant, cells were lysed with 500 µl methanol 66%. The cell pellet was collected by centrifugation, resuspended in 200 µl PBS, mixed with 9 ml Optiphase HiSafe 3, and counted for radioactivity.

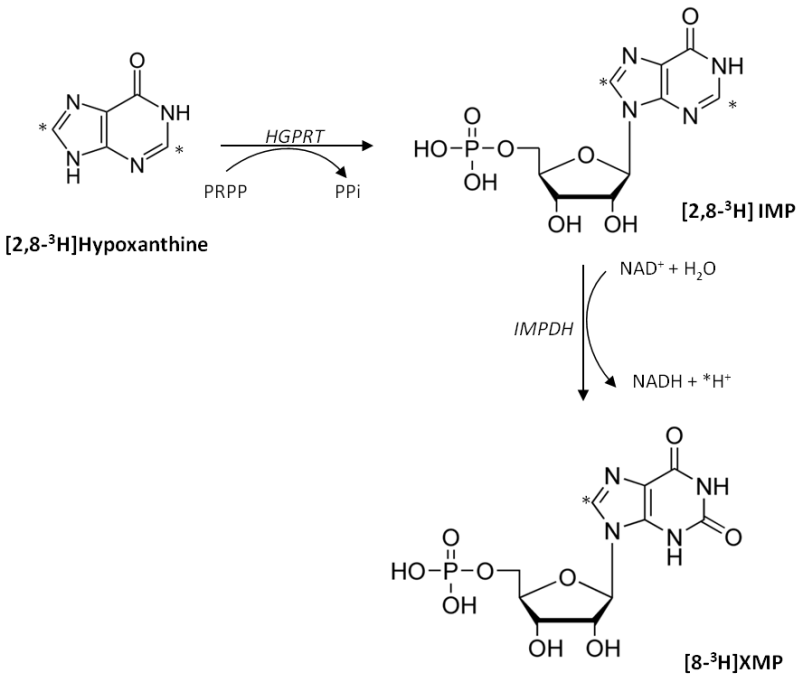

FIGURE 3.1 | **Tritium release assay.** In this assay, cells are exposed to [2,8-^{3}H]Hypoxanthine which is converted to [2,8-^{3}H] IMP by HGPRT. The latter is oxidized to [8-^{3}H]XMP by IMPDH. During the reaction catalyzed by IMPDH, ^{3}H is released. Measuring the amount of released ^{3}H thus gives a measure of HGPRT activity. The asterisk marks the position of the tritium label.

HPLC analysis of purine nucleotides in Ad transduced 1306 cells. Cells were seeded at 1,000,000 cells in 25-cm^2 flasks. One day later, cells were infected as described above at an MOI of 100 (Ad-*Pv*, Ad-*Pf* and Ad-ΔEx2hu) or 25 (Ad-WThu). Two days later, Ad-transduced cell cultures and a non-transduced cell control were exposed for 24 h to 2 µCi [2,8-^{3}H]Hx (specific radioactivity: 15 Ci/mmol) or 3.5 µCi [8-^{3}H]Ade (specific radioactivity: 26 Ci/mmol) (final concentration of radiolabeled compound: 0.0133 µM, concentration of hypoxanthine in medium: 4.4 µM). After 24 h incubation at 37°C, the cultures were washed three times with serum-free DMEM medium, then trypsinized with 0.05% trypsine-EDTA and resuspended in 5 ml DMEM as such. The cells were centrifuged (6 min, 1200 rpm) and the supernatant was discarded. The cell pellet was extracted with 500 µl ice-cold methanol 66%. After standing on ice for 15 minutes, the cell lysates were centrifuged (13000 rpm, 10 minutes, 4°C) and clarified extracts and residual methanol insoluble pellets were frozen at -20°C. The clarified extracts were subjected to high-performance liquid chromatography (HPLC) analysis to separate [2,8-^{3}H]Hx or [8-^{3}H] Ade derived metabolites on a Partisphere strong anion exchange column (Whatman). Extracts were separated with two phosphate buffers (Buffer A: 5 mM $NH_4H_2PO_4$, pH 5 and Buffer B: 0.3 mM $NH_4H_2PO_4$, pH 5) with the following gradient (flow: 2 ml /min): 0 min- 5 min: 100% A, 5 min- 20 min: 0-100% B, 20 min- 40 min: 100% C, 40 min- 45 min: 0-100% B, 45 min- 50 min: 100% B. One-minute eluate fractions were collected, Optiphase HiSafe 3 (Perkin Elmer) was added and radioactivity was counted by liquid scintillation. Incorporation of [2,8-^{3}H]Hx or [8-^{3}H]Ade into nucleic acids was measured by directly measuring the radioactivity in the methanol-insoluble fraction.

3.4 HGPRT Inhibitor Assays

The tritium release test was also used to determine the effect of different inhibitors on human HGPRT in A549 cells and on *Pv*HGPRT or huHGPRT after Ad transduction of 1306 cells. For this purpose, A549 cells (containing endogenous HGPRT activity) and 1306 cells (deficient in HGPRT) were seeded at 300,000 cells per well in 12-well plates. One day later, 1306 cells were infected with 400 µl Ad S_2 stocks as above (Ad-WThu: MOI = 25, Ad-*Pv*: MOI = 100) and incubated for 48 h at 37°C. To perform the HGPRT inhibition tests, the culture medium was removed (i.e. one day after seeding the A549 cells or two days after Ad transduction of 1306 cells), and replaced by 540 µl fresh medium (with 10% FCS) and 60 µl of product solution (i.e. 10x product solutions prepared in DMEM as such). Alternatively, lipophilic prodrugs with low solubility were diluted directly in 600 µl medium with 10% FCS. The cells were pre-incubated for 4 h with the test compounds to allow their cell uptake and intracellular conversion to the active metabolites, and then 20 µl reconstituted [2,8-^{3}H]Hx (~ 0.8 µCi/µl) was added. After incubation with [2,8-^{3}H]Hx during 45 min (A549), 90 min (Ad-

huHGPRT transduced 1306 cells) or 180 min (Ad-*Pv*HGPRT transduced 1306 cells), the amount of released ^{3}H was determined as described above.

3.5 Purine Metabolism and Cytotoxicity studies in CHOK1 and AdeI

HPLC analysis of purine metabolites. To compare the enzymatic activities of HGPRT and APRT in CHOK1 and AdeI cells, confluent cell cultures in 25-cm^2 flasks were exposed for 24 h to 2 µCi [2,8-^{3}H]Hx (specific radioactivity: 15 Ci/mmol) or 3.5 µCi [8-^{3}H]Ade (specific radioactivity: 26 Ci/mmol) (final concentration of radiolabeled compound: 0.0133 µM). After 24 h incubation at 37°C, cell extracts were analyzed by HPLC to determine the radioactivity incorporated into purine nucleotide pools. Incorporation of [2,8-^{3}H]Hx or [8-^{3}H]Ade into nucleic acids was measured by directly measuring the radioactivity in the methanol-insoluble fraction. For a more detailed explanation of cell extract preparation and separation of the nucleotides, see above: HPLC analysis of purine nucleotides in Ad transduced 1306 cells. Also, the effect of four inhibitors (RBV, MPA, PEEG and PEEHx) on purine metabolism was studied. Inhibitors were added to the culture medium at a final concentration of 100 µM (RBV, PEEG and PEEHx) or 20 µM (MPA) and cells were pre-incubated for 4 h at 37°C before the addition of 2 µCi [2,8-^{3}H]Hx. After 24 h incubation at 37 °C, extracts were made as described above.

Cytotoxicity assays. To compare the cytostatic activity of nucleoside analogues in CHOK1 and ADSL-deficient AdeI cells, cells were seeded into 96-well plates at 5,000 (AdeI) or 15,000 (CHOK1) cells per well. After 24 h incubation at 37°C, test compounds (6-TG, PMEG, MPA, 2,6-DAP, RBV, 5-FU) were added at serial dilutions. After three days incubation at 37°C (to ensure multiple rounds of cell division), cells were trypsinized with 0.05% (CHOK1) or 0.25% (AdeI) trypsine-EDTA and counted with a Coulter Counter. The IC_{50}, or compound concentration required to reduce cell proliferation by 50%, was calculated by extrapolation.

AdeI growth curves. AdeI cells were seeded at 5,000 cells/ well in five 96-well plates in RPMI medium supplemented with 10% FCS, sodium bicarbonate and L-glutamine. Cells were supplemented with adenine and hypoxanthine in different combinations of concentration (from 30 µM Ade + 30µM Hx to 0 µM Ade +0 µM Hx). Each day, one plate was removed from the incubator to trypsinize the cells with 100 µl 0.25% trypsine-EDTA followed by cell counting with a Coulter Counter.

4 RESULTS

4.1 Generation of Recombinant Adenoviral Vectors as a tool to transduce HGPRT-deficient cell lines

4.1.1 Construction of Ad vectors expressing WThuHGPRT/ ΔEx2huHGPRT/ *Pf*HGPRT or *Pv*HGPRT

The first goal of this thesis was to construct adenoviral (Ad) vectors (serotype 5), expressing either the human (WT or mutant) or the plasmodial (*Pf* or *Pv*) HGPRT enzyme. These vectors could then be used as a tool to transduce HGPRT-deficient cells. We chose Ad vectors because they have a number of important advantages: their genome can be easily manipulated; they induce high expression levels of the protein of interest; are able of infecting a wide range of host cells (both dividing and non dividing); they grow at high titers; and, finally, their genome remains stable. Furthermore the viral DNA remains epichromosomal (i.e. it does not integrate in the host genome) so it does not interrupt normal gene function of the host cell (Vector Biolabs). These properties make Ad vectors far more efficient gene delivery tools compared to gene delivery by lipid-based transfection approaches. The cell entry and gene transduction pathway of Ad vectors is shown schematically in Figure 4.1.

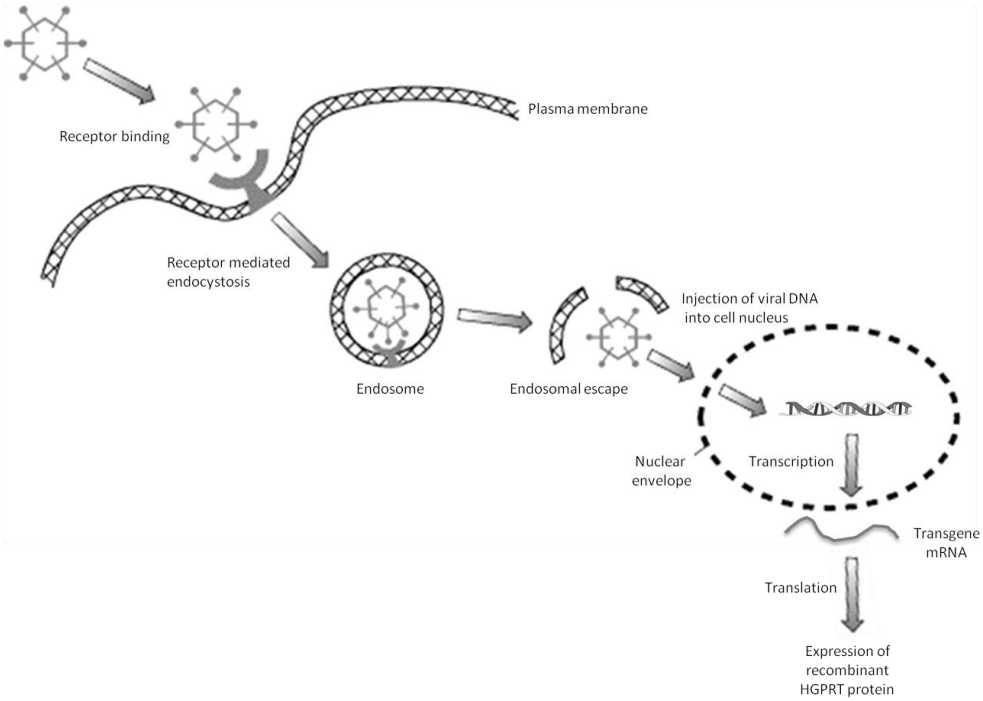

FIGURE 4.1 | **Simplified scheme of the adenoviral transduction mechanism.** The infection starts by binding of the adenovirus fiber knob to the coxsackievirus and adenovirus receptor (CAR) on the host cell membrane, which is followed by a secondary interaction between an Arg-Gly-Asp motif on the penton base protein of the Ad vector and an αv-integrin on the host plasma membrane. This co-receptor interaction allows the vector to enter the cell via receptor-mediated endocytosis through clathrin-coated vesicles. After escape of the virion from the endosome, the capsid is degraded and the double stranded viral DNA enters into the nucleus through the nuclear pore complex. The viral DNA remains epichromosal and is transcribed by the host transcriptional machinery (Pankajakshan et al. 2013). In this way, the recombinant protein, in our case *Pf*HGPRT, *Pv*HGPRT, WThuHGPRT or ΔEx2huHGPRT is expressed in the Ad vector-infected cells. Figure adapted from Classical Gene Therapy, 2012.

We constructed four separate E1/E3 deleted recombinant Ad vectors using the RAPAd® CMV Adenoviral Bicistronic Expression System technology (Cell Biolabs, Cat. No: VPK-254) (Anderson et al. 2000). The RAPAd® system makes use of an adenovirus type 5 backbone vector (pacAd5 9.2-100) and a shuttle (PadAd5 CMV-IRES GFP) vector (Figure 4.2). The shuttle vector contains the left end (353 bp) of the Ad genome which is followed by a cytomegalovirus (CMV) promoter site ahead of a multiple cloning site (MCS). The genes coding for the plasmodial or human HGPRT enzyme (*Pf*HGPRT, *Pv*HGPRT, WThuHGPRT and ΔEx2huHGPRT) were cloned in the MCS of the shuttle vector. ΔEx2huHGPRT (i.e. exon 2-deleted huHGPRT) encodes an HGPRT unrelated protein and served as a negative control. The MCS of the shuttle vector is followed by an internal ribosome entry site (IRES) and a GFP cDNA sequence. Since the transgene and GFP gene are separated by the IRES sequence, both genes are transcribed as separate proteins and not as a fusion protein. In this way, the functional properties of both proteins are ensured. The backbone vector pacAd5 9.2-100 carries the majority of the viral genome but lacks the left-hand inverted terminal repeats (ITR), the packaging signal and E1/ E3 sequences. The deletion of these sequences greatly reduces (or eliminates) the accidental production of replication-competent Ad particles due to homologous recombination with the E1 sequence in the 293 cells (also, see risk assessment) (Anderson et al. 2000). After subcloning our genes of interest in the MCS of the shuttle vector, the shuttle and backbone vector were digested with *PacI* and linear DNA fragments were cotranfected in the E1-expressing 293AD packaging cell line (Step 1, Figure 4.2). After cotransfection, the backbone and shuttle vector recombine through a shared 9.2-16.1 kb adenoviral gene region. Through the process of homologous recombination, a replication-incompetent recombinant Ad vector is obtained that contains the cloned transgene (Step 2, Figure 4.2). The final Ad vector obtained (from left to right) is composed of the 5'end of the Ad genome containing the left hand ITR (which serves as origin for replication) and packaging signal (which mediates viral packaging), followed by the CMV promoter ahead of the cloned transgene which is separated from the GFP gene by IRES. This left part is obtained from the shuttle vector. Thus, the shuttle vector complements the backbone deletion of the packaging signal and left hand ITR. The right part of the Ad vector is obtained from the backbone vector and contains the majority of the Ad genome, except for the E1 and E3 genes. The E1 deletion makes the virus replication-incompetent; in this way a high expression of the transgene can be obtained without killing the target cells. Since 293AD cells constitutively express E1 adenoviral genes, they complement the E1-deletion and allow vector replication. Deletion of E3 reduces the host immune response but does not affect virus production in cell culture (Ginsberg et al. 1989).

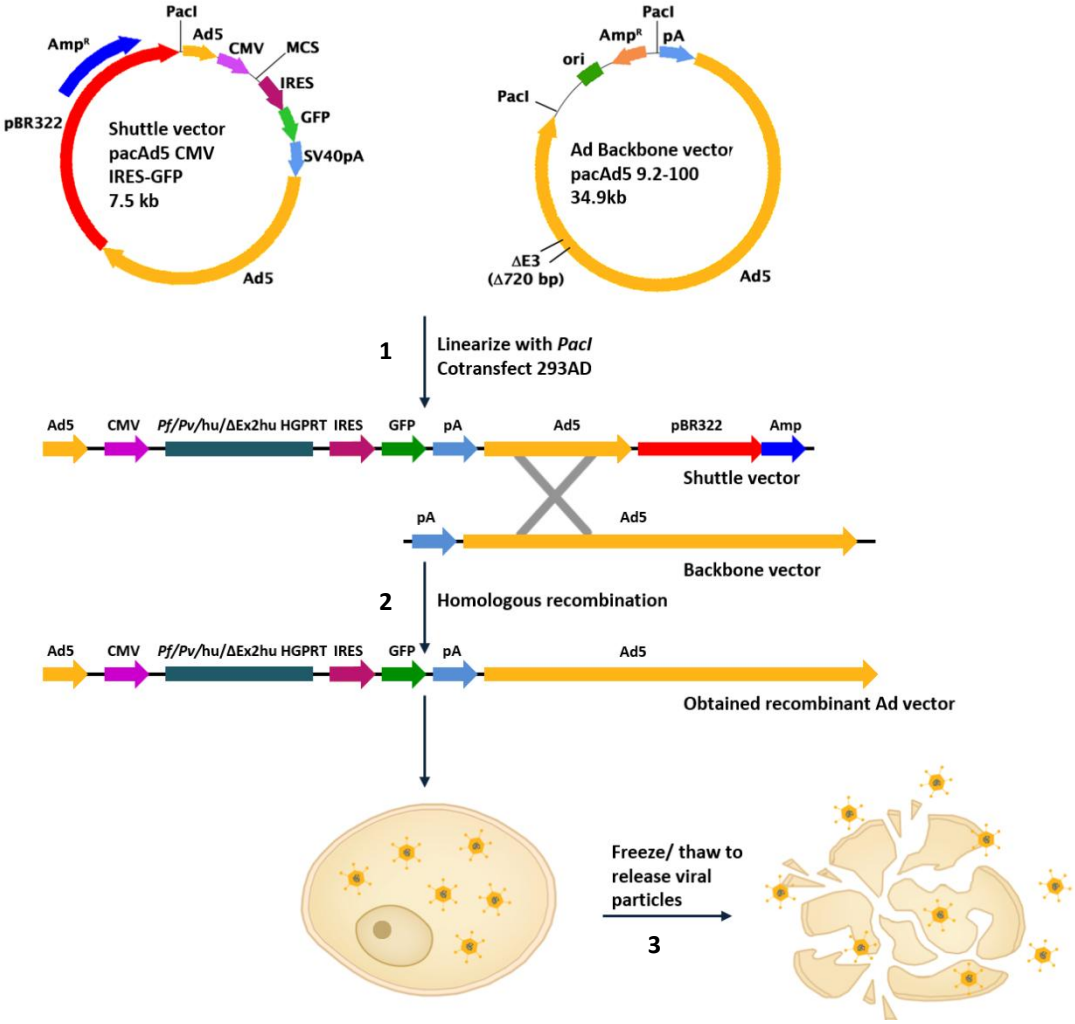

FIGURE 4.2 | **Schematic representation of the procedure to generate recombinant Ad vectors using the RAPAd® system.** The PacAd5 CMV IRES-GFP shuttle vector contains the cloned transgene and the Ad5 9.2-100 backbone contains the majority of the adenoviral genome, except E1 and E3 sequences, the packaging signal and the left hand ITR. Through homologous recombination, recombinant Ad vectors are produced in the E1-expressing packaging cell line 293AD. See text for a detailed description of the consecutive stages 1, 2 and 3.

Figure 4.3 shows images of 293AD cells at an early time point (i.e. at 24 h) after cotransfection (Figure 4.3 A), as well as cells showing manifest cytopathic effect (CPE) at the time when the virus was harvested (Figure 4.3 B). One day after co-transfection, GFP expression was already obvious. This indicated that the shuttle vector was successfully transfected and transcribed. Successful transfection of the backbone vector could not yet be seen at this stage, since it does not carry a fluorescent reporter gene. Each day after cotransfection, cell morphology was checked to detect CPE as the sign that recombinant Ad had formed. After 7 days, the first indications of plaque formation were seen. When approximately half of the cells appeared detached from the bottom of the plate (~10-17 days, Figure 4.3 B), both medium and cells were collected and subjected to three freeze/thaw cycles to release adenoviral particles from the cells (Step 3, Figure 4.2).

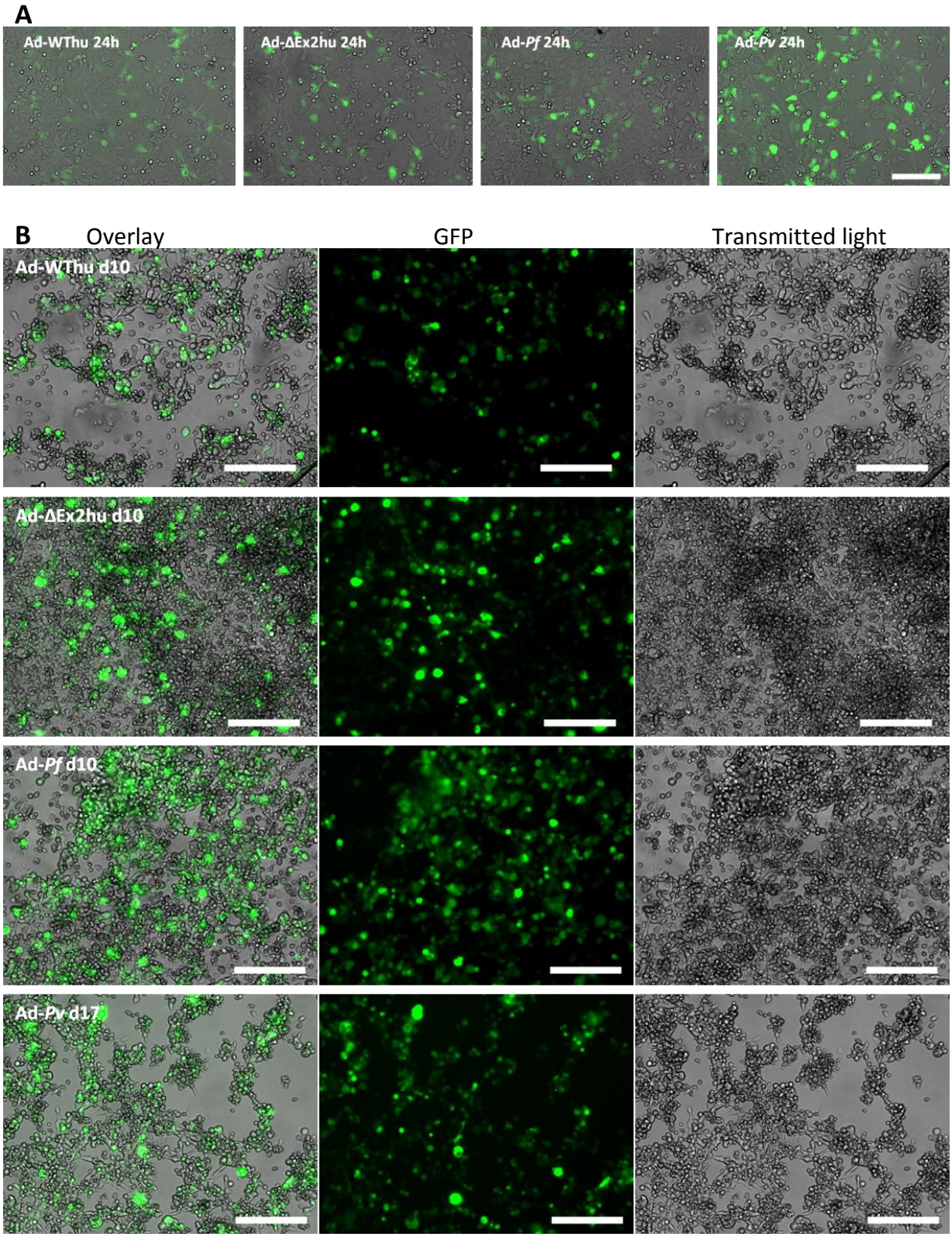

FIGURE 4.3 | **GFP expression after cotransfection of 293AD cells with the shuttle and backbone vector, after 24 hours (A) and after 10 to 17 days (B).** The images on day 10-17 show cell morphology and GFP expression on day of Ad harvest. Cell rounding and loss of cell attachment indicated that adenovirus had formed. Ad-WThu: adenoviral vector containing the WThuHGPRT cDNA sequence. Ad-ΔExhu: adenoviral vector containing ΔExhuHGPRT. Ad-*Pf*: adenoviral vector containing *Pf*HGPRT. Ad-*Pv*: adenoviral vector containing *Pv*HGPRT. The scale bar represents 200 µm.

To verify that the Ad vector was functional and contained the cloned HGPRT transgenes, A549 cells were transduced and monitored by fluorescence microscopy. After 72 h, GFP expression was obvious (Figure 4.4 A), indicating that the vectors were able of entering the cells and inducing transcription of the GFP gene. After DNA extraction on the infected A549 cells and amplification by HF-PCR using outer primers 39 and 40 (Table 3.2), we confirmed that the HGPRT transgenes were successfully cloned (Figure 4.4 B). Sequencing of the amplified HGPRT fragments assured that no accidental mutations had occurred during the homologous recombination event (result not shown).

The virus titers in the stocks were assessed by a plaque assay on 293AD cells (Figure 4.4 C). Plaques were counted manually in wells containing 5-50 plaques. In combination with the dilution factor added to that well, the number of plaque forming units per sample unit volume (PFU/mL) was calculated. The average titer produced was 1.02 x 10^8 PFU/ml. An A549 plaque assay indicated that our recombinant Ad stocks were free of detectable contamination by replication-competent Ad (Figure 4.4 C). Since A549 do not express E1 genes, the Ad vector is unable to replicate within these cells, unless replication-competent Ad particles would be present in our stocks. Neither of the wells containing serial dilutions of the Ad stocks, showed any sign of plaque formation after neutral red and crystal violet staining. Thus, with the RAPAd® System, we were able to generate four distinct Ad vectors, containing either the *Pf*HGPRT (Ad-*Pf*), *Pv*HGPRT (Ad-*Pv*), WThuHGPRT (Ad-WThu) or ΔEx2huHGPRT (Ad-ΔEx2hu) cDNA sequence, and the stocks that we produced were free of replication-competent Ad contaminants.

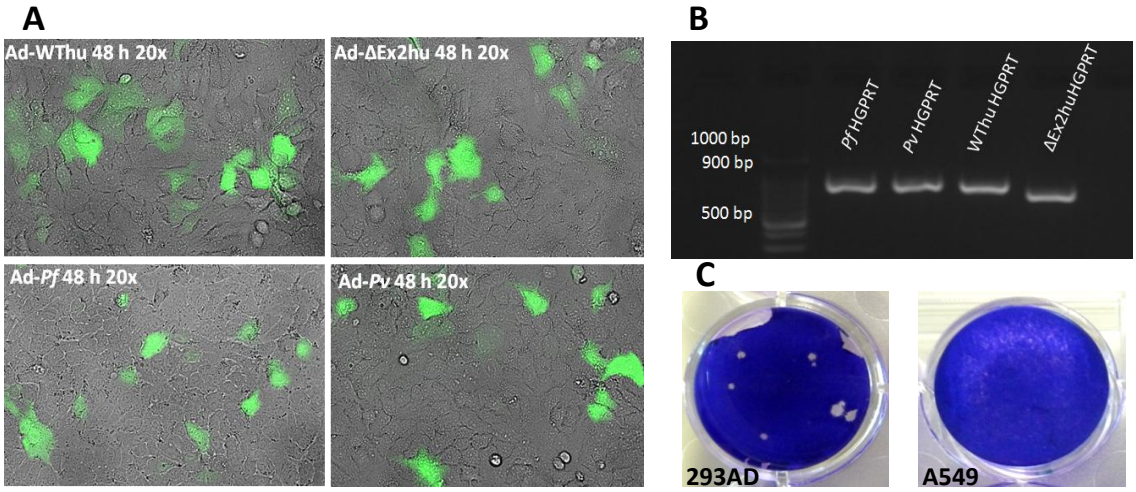

FIGURE 4.4 | **The Ad vectors are functional, contain the cloned transgenes and are replication incompetent.** (A) A549 cells were infected with the four recombinant Ad vectors. At 3 days post-infection, GFP expression was monitored by fluorescence microscopy. (B) After DNA extraction on the infected A549 cells, HF-PCR and separation on a 2% agarose gel, we confirmed the presence of the cloned transgenes within the four recombinant Ad vectors. (C) In E1-expressing 293AD cells, plaques were formed after infection (a representative example is shown on the left). In A549 cells, no plaques were formed (i.e. all wells looked like the picture on the right).

4.2 Adenoviral Transduction Efficiency of Different Cell Types

4.2.1 Adenovirus infection of diverse cell types

In the next step, we determined which cell types were efficiently transduced by our constructed Ad vectors. Our primary aim was to use the Ad vectors to induce HGPRT enzymatic activity in transduced cells. Hence, these experiments could only be performed in HGPRT-deficient cell lines that lack intrinsic HGPRT activity. HGPRT-deficient mutant cell lines are typically obtained by selection for 6-thioguanine (6-TG) resistance. Cells with a mutation in the HGPRT gene, resulting in a defective or absent HGPRT protein, cannot convert 6-TG to the toxic metabolite 6-thioguanine monophosphate (6-TGMP) and are thus able to survive in the presence of 6-TG, while wild type cells are killed by 6-TG (Johnson, 2012). In a pilot study, we investigated the transduction efficiency of several cell types by monitoring the expression of the GFP marker gene using fluorescence microscopy at different time points after Ad transduction (Table 4.1). The 1306, C32TG and HeLaTG are HGPRT-deficient cell lines. Since our laboratory also possesses HGPRT-deficient MDCK cells (Naesens et al. 2013), the transduction efficiency of this cell line was also tested. All cells were infected with an equal volume of S_2 stock (corresponding to a multiplicity of infection (MOI) of 65 PFU/cell and GFP expression was monitored after 24, 48 or 72 h by fluorescence microscopy. If no GFP expression (i.e. < 1% of GFP positive cells) was seen after 72 h, cells were considered to be "not transducable".

TABLE 4.1 | **Ad transduction efficiency of different cell types.**

Cell name[a]	**Species**	**Cell line description**	**Transducable with RAPAd® Ad vector?**
A549	*Homo sapiens*	Lung carcinoma epithelial cell line.	Yes
MDCK	*Canis familiaris*	Epithelial kidney cells.	No
HeLa	*Homo sapiens*	Cell line derived from cervical carcinoma cells. Contains genes of human papilloma virus.	Yes
HeLaTG	*Homo sapiens*	Cell line derived from cervical carcinoma cells and selected for 6-TG resistance. They are deficient in HGPRT.	No
C32TG	*Homo sapiens*	Cell line derived by the selection of the human melanoma cell line C32 for 6-TG resistance. They are deficient in HGPRT.	Yes
1306	*Homo sapiens*	Cell line derived by selection of the SV40-transformed human skin fibroblast line GM0637 for 6-TG resistance. They are deficient in HGPRT.	Yes

[a]Cells were seeded in 12-well plates. When confluency was reached, the cells were infected with 400 µl S_2 stocks (~MOI= 65). Successful transduction was monitored by fluorescence microscopy at 24, 48 or 72 h after transduction. If no GFP expression was observed at 72 h post-transduction, cells were considered to be not transducable.

The most efficient transduction was seen in cells known to have high CAR expression: A549 (Sharma et al. 2012) and HeLa cells (Carson et al. 2007), since both showed clear GFP expression after 24 h (results not shown). In contrast, the transduction rate of MDCK and HeLaTG was found to be significantly lower with almost no GFP positive cells after 72 h.

4.2.2 Ad transduction efficiency of HGPRT-deficient cells

The Ad transduction efficiency of three HGPRT-deficient cell lines, i.e. HeLaTG, C32TG and 1306, was determined more quantitatively by means of three different methods: (i) quantification of the percentage of GFP-positive cells by flow cytometry; (ii) determination of transgene HGPRT protein expression by Western blot analysis; and (iii) measurement of HGPRT enzymatic activity by the tritium release assay.

(i) Determination of GFP expression by flow cytometry

The GFP expression in Ad-transduced 1306, C32TG and HeLaTG was compared by analyzing cell suspensions with a FACSscan flow cytometer, at 48 h post Ad transduction. Table 4.2 shows the percentage of GFP-positive cells and the mean fluorescence value of Ad transduced cells after applying an MOI of 32. The three cell types exhibit different GFP expression levels. The highest percentage of successfully transduced cells was obtained in 1306 cells, with an average of 55% GFP-positive cells. The average amount of GFP-positive cells in C32TG is slightly lower, i.e. 43%. In line with our observations by fluorescence microscopy, HeLaTG cells appeared to be virtually non-permissive for Ad vector transduction. However, the mean fluorescence in HeLaTG is significantly higher compared to that seen in 1306 cells. Presumably, the HeLaTG cells that do become transduced, express the GFP gene at very high levels, and thus a high mean fluorescence is obtained. In contrast, in 1306 and C32TG cells, more cells are transduced but the GFP gene is expressed at lower levels. Since the expression of GFP is driven by the same CMV promoter as the transgene (Figure 4.1), monitoring GFP expression gives an indirect assessment of transgene expression. Since the percentage of GFP-positive cells is similar for the four Ad vectors, this implies that also the HGPRT transgenes are expressed at similar levels.

Table 4.2 | **GFP expression in Ad-transduced 1306, C32TG and HeLaTG cells.**

	Ad-*Pf*		**Ad-*Pv***		**Ad-WThu**		**Ad-ΔEx2hu**	
Cell name[a]	% GFP positive cells	Mean fluorescence	% GFP positive cells	Mean fluorescence	% GFP positive cells	Mean fluorescence	% GFP positive cells	Mean fluorescence
1306	47.2	28.9	62.5	66.6	54.9	34.3	56.3	32.6
C32TG	38.0	51.8	52.9	63.5	40.1	48.2	42.0	50.9
HeLaTG	2.1	61.6	9.5	75.5	1.5	72.4	1.7	56.0

[a] Cells were transduced with GFP expressing Ad vectors at an MOI of 32 PFU/cell and GFP expression was determined at 48 h post-transduction by flow cytometric analysis.

(ii) Assessment of HGPRT protein expression by Western blot analysis

Subsequently, we examined HGPRT protein expression in Ad-transduced and non-transduced HGPRT-deficient cells by Western blot analysis (Figure 4.5). The anti- HGPRT antibody (Ab10479, Abcam) recognizes an epitope in the C-terminal part of huHGPRT: RDLNHVCISETGKAKYKA (Figure 4.5 B).

Our laboratory previously reported on the genetic basis for the HGPRT deficiency in C32TG cells (Keough, Špaček, et al. 2013). Namely, cDNA sequencing revealed that these cells contain a deletion of exon 2 within the HGPRT mRNA sequence, causing a frame shift and

the formation of an unrelated protein. The mutations that cause the HGPRT deficiency in 1306 and HeLaTG cells are, to our knowledge, not known. To verify the absence of HGPRT protein within these cells, cell extracts were made and analyzed by Western blotting (Figure 4.5 A). The 24 kDa protein band, seen in A549 cells, corresponds to monomeric HGPRT. No HGPRT protein band was detected in all three HGPRT-deficient cell lines. This indicates that each of these cells either produces no HGPRT protein at all, or expresses a truncated form that lacks the C-terminal part. Equal protein loading was verified by detection of β-actin (47 kDa). Smearing of β-actin bands means that the lanes with HeLaTG, 1306 and C32TG protein extracts were slightly overloaded.

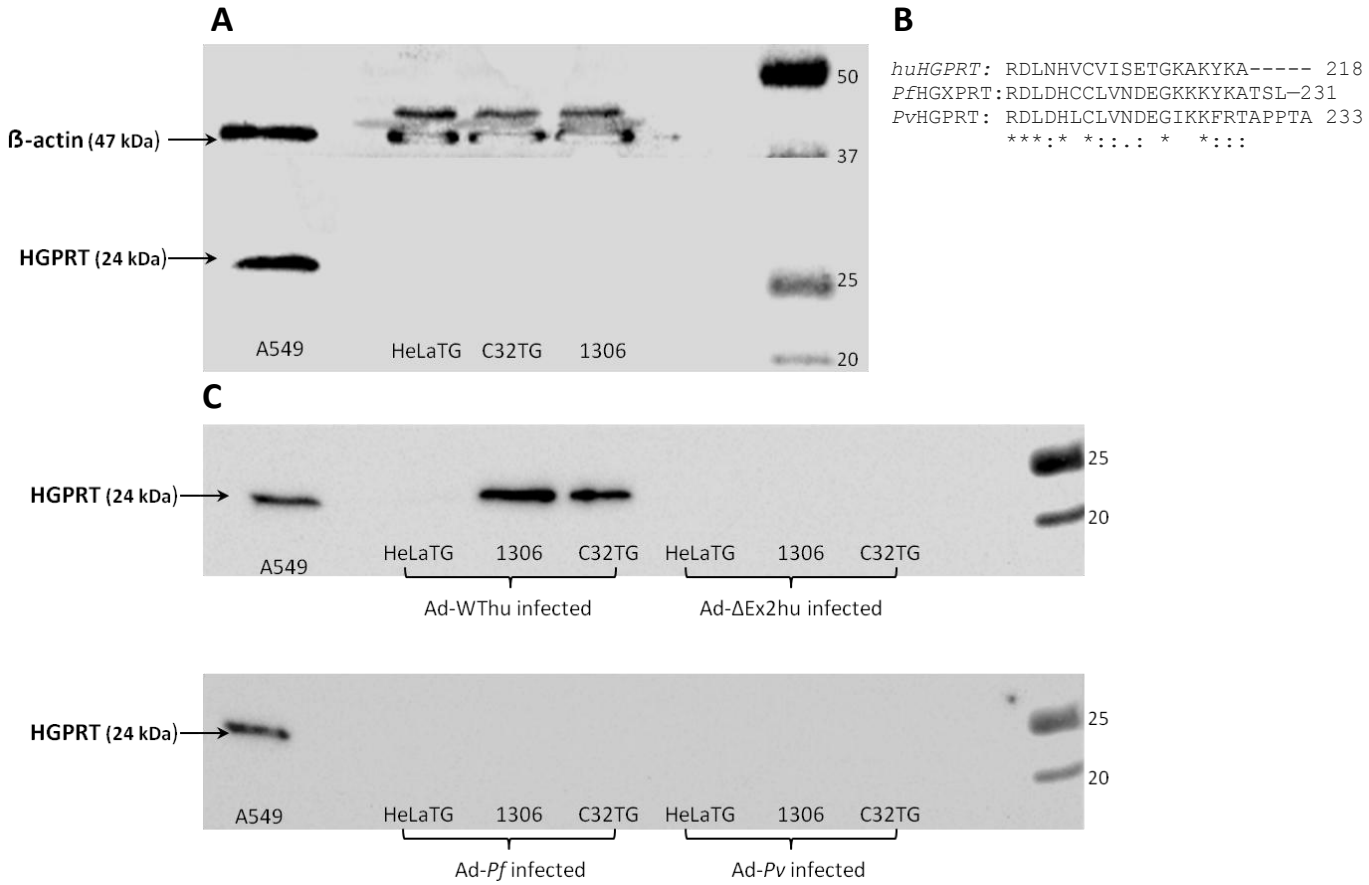

FIGURE 4.5 | **Western blot analysis of non-transduced and Ad-transduced HGPRT deficient cells.** (A) Western blot analysis to verify the absence of the HGPRT protein in the 6-TG resistant cell lines: HeLaTG, 1306 and C32TG. In positive control A549 cells, a strong HGPRT protein band was detected of 24 kDa. Equal protein loading (15µg total protein loaded per lane) was verified by detection of β-actin (47 kDa). (B) The anti-HGPRT antibody recognizes the C-terminal part of huHGPRT. Alignment of the C-terminal regions of *Pf* and *Pv*HGPRT shows sequence similarities and dissimilarities within these regions. "*" indicates identical residues, ":" indicates conserved substitutions and "." indicates semi-conserved substitution. (C) Western blot analysis of Ad vector transduced cells. HGPRT-deficient cells were transduced with Ad-WThu (MOI 16), AdΔEx2hu (MOI 16), Ad-*Pf* (MOI 50) or Ad-*Pv* (MOI 50). At 48 h after Ad transduction, cell extracts were made and analyzed by Western blot to examine whether succesfull transgene expression and translation led to the presence of a positive HGPRT band.

To verify successful Ad-transduction and HGPRT protein expression, protein extracts were made at 48 h after Ad transduction and analyzed with the same HGPRT antibody. 1306 and C32TG cells, infected with Ad-WThu, show a protein band at the expected height of 24 kDa

(Figure 4.5 C). Thus, the cloned huHGPRT transgene is successfully transcribed and translated into a full-length protein after Ad transduction of 1306 and C32TG cells. The band observed in Ad-WThu tranduced 1306 cells is slightly larger than in Ad-WThu transduced C32TG cells. Thus, the transgene (Figure 4.5 C) as well as the GFP marker gene (Table 4.2) are apparently more successfully expressed in the 1306 cell line. Consistent with the very low percentage of GFP positive cells, no HGPRT protein could be detected for Ad-WThu transduced HeLaTG cells byWestern blot analysis (Figure 4.5 C). Since we lacked established antibodies for *Pv*HGPRT and *Pf*HGPRT, we also tested the anti-huHGPRT antibody towards *Pf*HGPRT and *Pv*HGPRT, but no bands could be detected. Most likely, the epitope dissimilarity in the C-terminal region is too high for successful detection (Figure 4.5 B).

(iii) Assessment of HGPRT enzymatic activity by the tritium release assay

As evident from the flow cytometric data and Western blot analysis, HeLaTG cells appeared unfavorable target cells for Ad transduction. In a final step to determine which target cell type to choose for further experiments, we examined the obtained HGPRT enzymatic activity after Ad transduction of C32TG and 1306 cells. In Figure 4.6, cells were infected for 48 h with different MOIs. Then, cells were exposed to 0.8 µCi [2,8-^{3}H]Hx for 45 min (Ad-WThu) or 2 h (Ad-*Pv*, Ad-*Pf* and Ad-ΔEx2hu). Measurement of ^{3}H released in the culture medium by liquid scintillation counting allowed quantification of obtained HGPRT activity (Figure 3.1). Cells infected with Ad-WThu showed high dpm values and, thus, high HGPRT activity. With an MOI of 32, a 15-fold and 30-fold dpm increase was seen for 1306 and C32TG, respectively, compared to the non-Ad transduced cell control or Ad-ΔEx2hu infected cells. For C32TG cells, the dpm values showed a proportional increase with increasing MOI values. For 1306, this relationship was not seen, since dpm values were identical when cells were infected with different MOIs of Ad-WThu. The enzymatic activity obtained in cells infected with Ad-*Pf* and Ad-*Pv* was found to be markedly lower than in Ad-WThu infected cells, even when the cells were infected with higher MOIs. For Ad-*Pf* infected cells, the obtained signal-to-noise (S/N) ratio never exceeded a factor two. Infection with Ad-*Pv* resulted in higher dpm values in 1306 cells compared to C32TG.

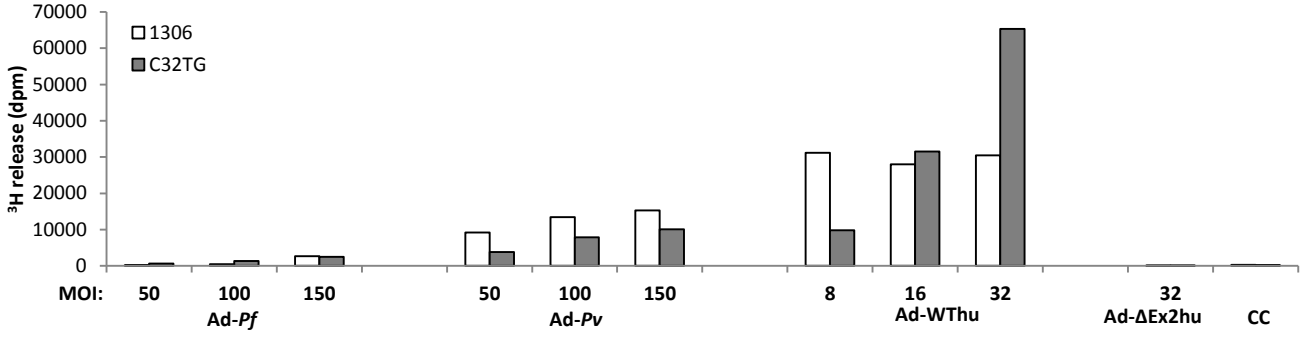

FIGURE 4.6 | **HGPRT enzymatic activity in Ad-transduced 1306 and C32TG cells.** Enzyme activity was measured at 48 h post-Ad transduction with different MOIs, by measurement of ^{3}H release after incubation with 0.8 µCi [2,8-^{3}H]Hx. CC= non-Ad transduced cell control.

4.2.3 Further optimization in Ad-transduced 1306 cells

After Ad-transduction, 1306 cells gave the highest percentage of GFP-positive cells (Table 4.2), the highest protein expression of huHGPRT (Figure 4.5) and clear dpm signals in the ^{3}H release test for both huHGPRT and *Pv*HGPRT (Figure 4.6). Based on these results, the 1306 human skin fibroblasts were chosen as the preferred cells for Ad transduction in all further experiments.

The progressing HGPRT reaction during incubation with [2,8-^{3}H]Hx was measured with the tritium release assay (Figure 4.7 A). This showed that product formation increases with incubation time. The relation is linear for up to 180 min and then levels off due to exhaustion of the radiolabeled Hx substrate. Figure 4.7 A also shows that, compared to the huHGPRT condition, the enzymatic activity is clearly lower in the *Pv*HGPRT-expressing cells and dramatically lower in the *Pf*HGPRT condition. For the Ad-*Pf* condition, we therefore measured ^{3}H release after 24 h incubation with [2,8-^{3}H]Hx (data not shown). However, dpm values in the non-infected cell control were markedly increased, probably due to basal xanthine oxidase activity that converts [2,8-^{3}H]Hx into [8-^{3}H]xanthine and [8-^{3}H]xanthine into [8-^{3}H]uric acid, resulting in the release of the tritium label at position 2. On the other hand, incorporation into nucleic acids at 24 h is not biased by xanthine oxidase activity since the purine base xanthine is not a constituent of DNA or RNA. Measurement of radioactivity incorporated into nucleic acids after 24 h incubation with [2,8-^{3}H]Hx showed that dpm values were 4-fold and 20-fold lower for Ad-*Pv* and Ad-*Pf* compared to Ad-WThu infected cells (Figure 4.7 B). Uninfected 1306 cells, exposed to [2,8-^{3}H]Hx did not metabolize the purine base further into nucleotides, due to their HGPRT deficiency (Figure 4.7 B). By contrast, in Ad-transduced cells, hypoxanthine is metabolized into the mono-, di- and triphosphates of adenosine and guanosine, via the common intermediate IMP (Figure 4.7 B). Radioactivity is mainly incorporated into ATP. Again, Ad-WThu transduced cells show the most efficient incorporation of the ^{3}H label in their purine pools, resulting in the highest incorporation into nucleic acids. Incorporation of [8-^{3}H]Ade into purine nucleotides and nucleic acids did not differ between the uninfected and infected cells (Figure 4.7 C). Also, inspection of the UV absorption chromatograms demonstrated that the purine and pyrimidine metabolism of the 1306 cells was not significantly disturbed after Ad infection (results not shown).

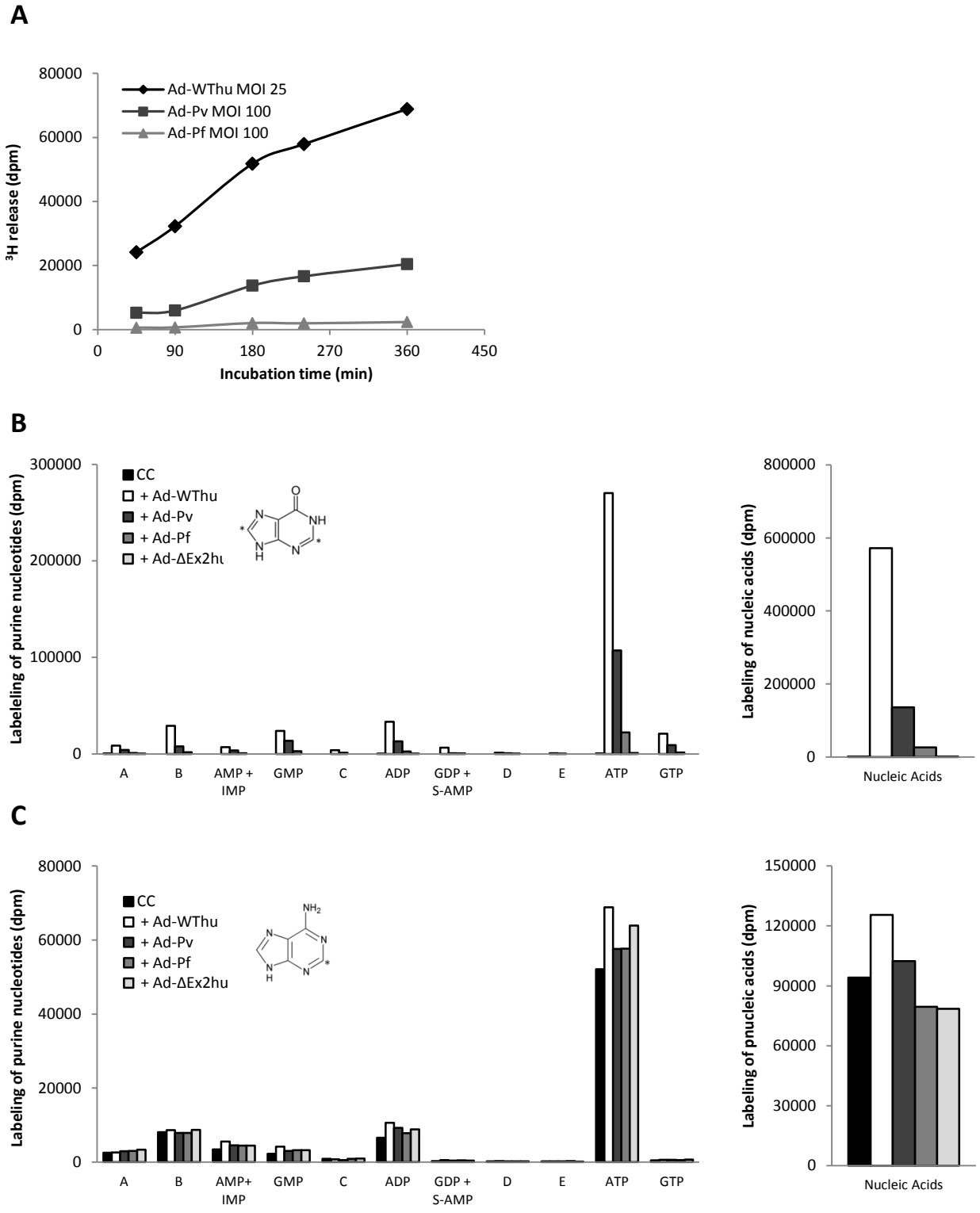

FIGURE 4.7 | **HGPRT enzymatic activity in Ad-transduced 1306 cells.** (A) Time-course experiment showing the progressing human, *Pv* and *Pf*HGPRT reaction during incubation with [2,8-^{3}H]Hx. (B) Incorporation of [2,8-^{3}H]Hx into purine nucleotides and nucleic acids of uninfected and Ad-transduced cells. (C) Incorporation of [8-^{3}H]Ade into purine nucleotide pools and nucleic acids of uninfected and Ad-transduced cells. Cells were infected with an MOI of 100 (Ad-*Pv*, Ad-*Pf* and Ad-ΔEx2hu) or 25 (Ad-WThu) PFU/ cell. Two days post infection, cells, maintained in medium containing 4.4 µM hypoxanthine, were incubated for 24 h with 0.0133 µM radiolabeled hypoxanthine (B) or adenine (C). Radioactive counts of G metabolites derived from [2,8-^{3}H]Hx were multiplied by a factor two since the ^{3}H label at position 2 is lost when [2,8-^{3}H]IMP is oxidized to [8-^{3}H]XMP. CC= non-Ad transduced cell control. The data shown are from one experiment.

4.3 HGPRT Inhibitor Studies

The final assay that we developed takes four days to complete. On the first day, 1306 skin fibroblast cells are seeded in gelatin-coated 12-well plates. One day later, cells are transduced with Ad-WThu (MOI= 25 PFU/cell) or Ad-*Pv* (MOI= 100 PFU/cell) and incubated for 48 h. On day 4, the medium containing 2% FCS is replaced by medium containing 10% FCS and serial dilutions of test compounds. To ensure cell membrane passage and intracellular conversion to the active metabolites, cells are pre-incubated for 4 h with the test compounds before the addition of 0.8 µCi [2,8-³H]Hx (final hypoxanthine concentration: 4.4 µM). Ad-WThu infected cells are incubated during 90 min and Ad-*Pv* during 180 min with [2,8-^{3}H]Hx, since product formation was maximal at that time (Figure 4.7 B). Then, the amount of released tritium is measured in the presence and absence of inhibitors as described in materials and methods. Due to the low S/N ratio, inhibition studies with *Pf*HGPRT were not possible thus far.

4.3.1 Effect of IMPDH inhibitors and purine base analogues in the ^{3}H release assay

The ^{3}H release test detects both HGPRT and IMPDH inhibition (Figure 3.1) (Balzarini and De Clercq 1992). Therefore, the validity of our assay was first assessed by evaluating IMPDH inhibition by the well known IMPDH inhibitors ribavirin (RBV) and mycophenolic acid (MPA). Unfortunately, no reference huHGPRT inhibitor could be included for this validitation experiment, since no proven huHGPRT inhibitor is available at this time.
A strong inhibition of ^{3}H release was seen when Ad-WThu and Ad-*Pv* transduced cells were exposed to these IMPDH inhibitors (Table 4.3). RBV is a broad-spectrum antiviral drug with different proposed mechanisms of antiviral action, including interference with RNA capping, viral polymerase inhibition and lethal virus mutagenesis (Graci and Cameron, 2005). It also acts as a potent competitive inhibitor of cellular IMPDH after phosphorylation, by adenosine kinase, to ribavirin 5'-monophosphate. RBV inhibited Ad-WThuHGPRT and Ad-*Pv*HGPRT with an IC_{50} of 2.4 µM and 7.0 µM, respectively. MPA, a substance derived from the fungus *Penicillium stoloniferum*, is a non-nucleoside compound that does not need further metabolism and acts as a selective and uncompetitive inhibitor of IMPDH. Like RBV, MPA was able to inhibit ^{3}H release at concentrations in the lower micromolar range (Table 4.3).

Subsequently, a range of purine base analogues and one pyrimidine analogue (6-azauridine) was tested for their potential to inhibit hypoxanthine metabolism. Their structures are given in Supplemental Figure 4. The purine base analogues represent an alternative approach for exploiting the HGPRT enzyme when designing new chemotherapeutic drugs. Instead of acting as direct HGPRT inhibitors, purine base analogues may act as HGPRT substrates, leading to their conversion into toxic nucleotides that become incorporated into the parasites' nucleic acids, resulting in cessation of cell replication (Keough et al. 2006). This strategy requires that these analogues are good substrates for the parasite enzyme but poor substrates

for huHGPRT (Keough et al. 2006). Some of these compounds have already been shown to inhibit the growth of *Pf* in *in vitro* erythrocyte cultures, e.g. 6-mercaptopurine (IC_{50} of 2 µM) (Keough et al., 2006). If these compounds indeed act as alternative HGPRT substrates, inhibition of ^{3}H release was expected due to competitive inhibition between the natural substrate [2,8-^{3}H]Hx and the purine base analogue.

TABLE 4.3 | **Inhibitory effect of various cytostatic agents on the metabolism of [2,8-^{3}H]Hx in human lung carcinoma A549 cells and Ad-transduced 1306 skin fibroblast cells.**

Compound	IC_{50} (µM)[a]		
	A549	Ad-WThuHGPRT	Ad-*Pv*HGPRT
Mycophenolic acid	5.1 ± 0.3	<0.4	5.2 ± 4.0
Ribavirine	7.6 ± 1.6	2.4 ± 0.5	7.0 ± 2.9
6-Azauridine	1.5 ± 0.4	0.8 ± 0.1	1.1 ± 0.5
6-Thioguanine	26 ± 77	11 ± 1	>500
6-Thioxanthine	>500	>500	>500
6-Mercaptopurine	111 ± 21	30 ± 88	242 ± 14
2-Aminopurine	>500	>500	>500
2,6-Diaminopurine	206 ± 49	164 ± 30	165 ± 26
6-Methyl mercaptopurine	>500	>500	>500
2-amino-6-chloropurine	111 ± 20	91 ± 9	>500

[a] The IC_{50} is the inhibitor concentration, expressed in µM, to reduce enzymatic conversion of [2,8-^{3}H]Hx (assessed by ^{3}H release assay) by 50%. Results are the mean ± S.E.M. of at least two independent experiments.

6-Thioguanine (6-TG) is a thio-analogue of guanine that is used in cancer treatment, especially for the treatment of leukemia. HGPRT converts this agent into the active metabolite 6-thioguanine 5'-monophosphate (6-TGMP). Accumulation of 6-TGMP hinders the synthesis of guanine nucleotides by competitive inhibition of IMPDH and pseudo-feedback inhibition of PRPP amidotransferase, the first enzyme of the de novo purine synthesis pathway (Aubrecht et al.1997; Karran and Attard 2008; Nelson et al. 1975; Pan and Nelson 1990). As shown in Table 4.3, 6-TG inhibited ^{3}H release when huHGPRT was the activating enzyme, but no inhibition was seen in Ad-*Pv* transduced cells. This is a remarkable observation since 6-TG has been shown to be a substrate of both huHGPRT and *Pv*HGPRT in enzymatic assays. Kinetic studies showed that 6-TG is a very efficient substrate for huHGPRT with a k_{cat}/K_M value of 5.1 $s^{-1}\mu M^{-1}$ (Keough et al. 2006) and a weaker, but still good substrate for *Pv*HGPRT having a k_{cat}/K_M of 1.4 $s^{-1}\mu M^{-1}$ (Keough et al. 2010). This appears to indicate that the cellular environment can significantly influence the inhibitory activity towards the enzyme. A second striking observation is the strong inhibitory effect on ^{3}H release of the pyrimidine nucleoside analogue 6-azauridine, with IC_{50} values ~1 µM. The primary effect of this compound, which occurs after its phosphorylation to 6-azauridine 5'-phosphate, is assumed to be inhibition of the de novo pyrimidine synthesis enzyme orotidylate decarboxylase. This results in decreased pools of pyrimidine nucleotides, cytidine triphosphate (CTP) and uridine triphosphate (UTP) (Handschumacher and Haven 1960).

Besides, some effects of 6-azauridine on purine metabolism have been reported, including accumulation of hypoxanthine, increased ATP levels, and decreased GTP levels (Janeway and Cha 1977; Hunting et al. 1980). Some observations provided evidence that the observed effect on purine pools is due to IMPDH inhibition (Hunting et al. 1980). Our results strongly support this hypothesis. Whether this effect is direct or indirect and is exerted by 6-azauridine itself or its metabolites is unknown (Hunting et al. 1980).
Three analogues (6-mercaptopurine, 2-amino-6-chloropurine and 2,6-diaminopurine) were able to inhibit ^{3}H release in Ad-WThu infected cells, while only two of them (i.e. 6-mercaptopurine and 2,6-diaminopurine) also inhibited ^{3}H release in Ad-*Pv* infected cells. The effect of 2,6-diaminopurine (2,6-DAP) on HGPRT or IMPDH activity must be an indirect effect since this is an adenine analogue that is activated by APRT (Weckbecker and Cory, 1989) and HGPRT is not able to bind adenine within its active site (Craig and Eakin 2000). Several compounds had no marked effect on ^{3}H release, even when tested at high concentration (up to 500 µM).
The compound IC_{50} values obtained in Ad-WThu transduced 1306 were compared with values obtained in A549 cells, which contain endogenous huHGPRT activity. Overall, comparable values were obtained, although the inhibition seen in Ad-transduced cells was slightly stronger, possibly due to higher huHGPRT enzyme expression levels.

4.3.2 Effect of ANP prodrugs in the ^{3}H release assay

Finally, prodrugs of the putative HGPRT bisphosphonate inhibitors were examined for their capacity to inhibit metabolic conversion of [2,8-^{3}H]Hx. As described in the introduction, these bisphosphonates are rationally designed compounds that contain a second phosphonate group attached to the ANP scaffold to increase their affinity for HGPRT. To mask the highly polar and negatively charged bisphosphonate groups, tetraphosphorodiamidate type prodrugs were synthesized. In compounds **18** and **19**, the bisphosphonate acyclic moiety is symmetrical, while in **9** and **10**, the linkers connecting the two phosphonate groups are different (Table 4.4).

As displayed in Table 4.4, three bisphosposhonate produgs were able to inhibit ^{3}H release in the micromolar range (IC_{50}~ 50 µM), and thus prove to be true HGPRT inhibitors. Interestingly, compound **19** with a guanine base attached is not active (IC_{50}> 200 µM), while compound **18** with a hypoxanthine base is able to inhibit both enzymes (Table 4.4). Compound **9**, with a hypoxanthine base, and compound **10** with a guanine base attached are both active. **9** has slightly lower IC_{50} values for both human and *Pv*HGPRT. Overall, the compounds with a hypoxanthine base attached seem to be more active than the analogous compounds with a guanine attached. The lipophilic prodrug of PEEG, compound **23**, was not able to inhibit HGPRT activity (IC_{50}> 200 µM).

TABLE 4.4 | **Inhibitory effect of ANP prodrugs in the ^{3}H release assay.** The chemical structures are shown below (Figures from Keough, Špaček, et al. 2013).

				IC_{50} (µM)[a]	
Compound	**Purine base**	**Prodrug of**	**Prodrug strategy**	**Ad-WThuHGPRT**	**Ad-*Pv*HGPRT**
9 (PP-P417)	Hx	**7**	Ethyl L-phenylalanine tetraphosphorodiamidate (3-4 C atoms in branch)	47± 10	42 ± 2.0
10 (PP-P364)	G	**8**		57 ± 22	63 ± 0.4
18 (PP-P343)	Hx	**16**	Ethyl L-phenylalanine tetraphosphorodiamidate (3-3 C atoms in branch)	46 ± 8.8	54 ± 2.8
19 (PP-P351)	G	**17**		>200	>200
23 (TT-T120310)	G	**PEEG**	One hexadecyloxypropyl chain	>200	>200

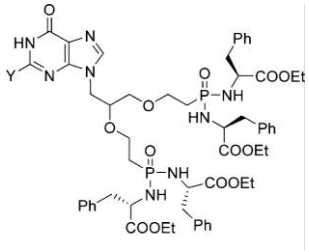

9 (Y= H)
10 (Y= NH_2)

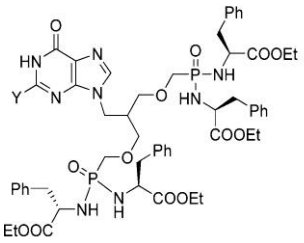

18 (Y= H)
19 (Y= NH_2)

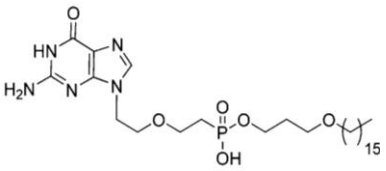

23

[a] The IC_{50} is the inhibitor concentration, expressed in µM, needed to reduce conversion of [2,8-^{3}H]Hx by 50%. Results are the mean ± S.E.M. of three independent experiments.

The inhibition is concentration-dependent (Figure 4.8) and human and *Pv*HGPRT are inhibited similarly. At a concentration of 100 µM cpd **9**, **10** or **18**, enzymatic conversion of [2,8-^{3}H]Hx was reduced by more than 75% (Figure 4.8).

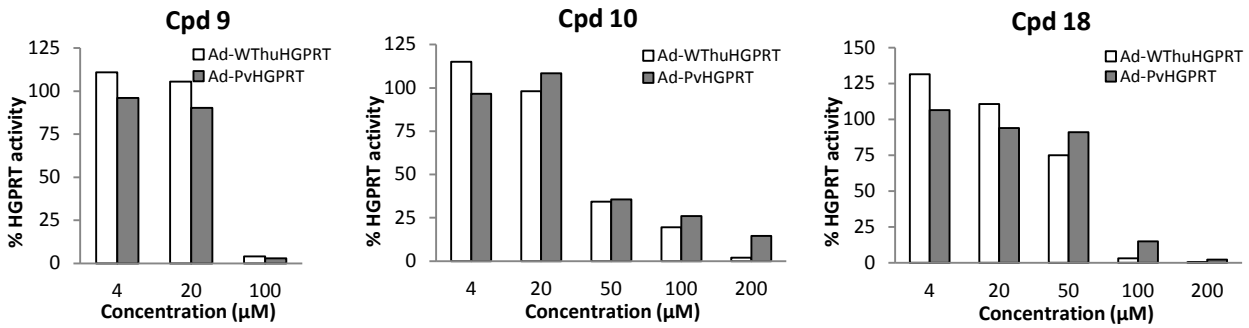

FIGURE 4.8 | **Inhibition of ^{3}H release from [2,8-^{3}H]Hx by three bisphosphonate prodrugs.** HGPRT enzymatic activity is expressed as the percentage activity compared to the non-Ad transduced cell control.

4.4 Characterization of Purine Metabolism in CHOK1 and AdeI cells

To investigate whether AdeI cells may be useful in cytotoxicity assays with the ANP analogues, we compared the purine metabolism in wild-type Chinese hamster (*Cricetulus griseus)* ovary cells (CHOK1) and a derived adenylosuccinate lyase (ADSL)-deficient mutant cell line AdeI. Since AdeI cells cannot synthesize purines de novo, we hypothesized that the activity of the salvage enzymes APRT and HGPRT should be heavily upregulated to meet purine demands. Hence, inhibitors of purine biosynthetic enzymes were expected to achieve higher cytotoxicity in AdeI compared to WT CHOK1 cells.
First, we characterized the purine metabolism of CHOK1 and AdeI using the radiolabeled purine nucleobases [2,8-^{3}H]Hx and [8-^{3}H]Ade. These nucleobases are salvaged through HGPRT and APRT to their respective monophosphate forms, IMP and AMP. IMP and AMP are then converted to all other purine nucleotides, with the triphosphate forms eventually ending up in DNA (dGTP and dATP) and RNA (GTP and ATP). By submitting cell extracts to high performance liquid chromatography (HPLC), the nucleotides formed were separated and incorporation of the ^{3}H label in the different purine metabolites was measured by liquid scintillation counting. The radioactivity incorporated into nucleic acids was determined by direct measurement of the methanol-insoluble fraction. This comparative study was aimed at understanding the differences in purine salvage metabolism between AdeI and CHOK1 cells. Second, we analyzed how different inhibitors interfere with purine nucleotide synthesis and how it differs in both cell types. Finally, a small cytotoxicity study was performed to investigate differences in sensitivity towards a number of cytostatic agents.
Paragraph 4.4.1 provides background information on the ADSL-deficient AdeI cells.

4.4.1 Background information on ADSL-deficient AdeI cells

AdeI cells are adenine requiring mutant Chinese hamster ovary (CHOK1) cells that are deficient in the enzyme adenylosuccinate lyase (ADSL) (Patterson 1976; Tu and Patterson 1977). ADSL catalyzes two non-sequential reactions in the de novo purine biosynthetic pathway: the conversion of succinylaminoimidazole carboxamide ribotide (SAICAR) to aminoimidazolecarboxamide ribotide (AICAR) and the conversion of S-AMP to AMP (Figure 4.9). Due to the deficient ADSL enzyme, AdeI cells accumulate the respective substrates of the enzyme: SAICAR and S-AMP (Patterson 1976; Tu and Patterson 1977). To obtain all purine nucleotides, AdeI cell survival and growth strictly depends on the availability of adenine in the growth medium (Patterson 1976; Tu and Patterson 1977). Without adenine, AdeI cells are not able to synthesize adenine nucleotides since synthesis of AMP from IMP is blocked at the S-AMP to AMP conversion step (Figure 4.9). In humans, congenital mutations in ADSL cause clinical disease that is characterized by developmental delay, often with autistic features. The exact cause is not known but is thought to be related to accumulation of SAICAR and S-AMP to toxic levels and insufficient purine nucleotide synthesis and recycling (Spiegel et al. 2006).

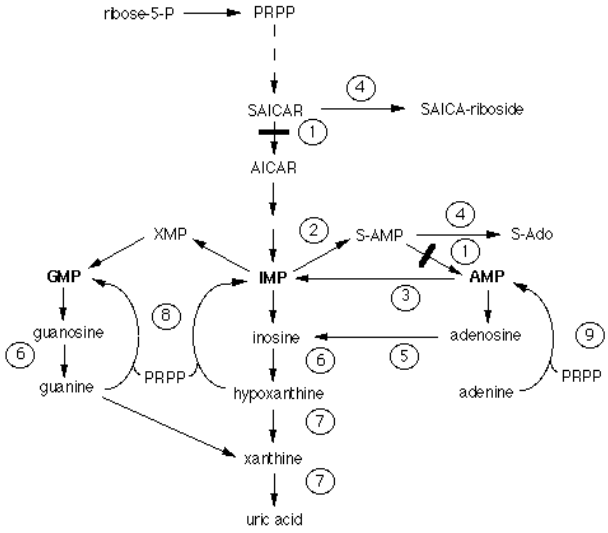

FIGURE 4.9 | **Schematic representation of purine metabolism.** The de novo purine synthesis pathway is represented by the broken line. The solid bars indicate reactions catalyzed by ADSL that are blocked in AdeI cells.Abbreviations: PRPP: phosphoribosyl pyrophosphate; SAICAR: succinylaminoimidazolecarboxamide ribotide; AICAR: aminoimidazolecarboxamide ribotide; IMP: inosine monophosphate; S-AMP: succinyl-AMP; S-Ado: succinyl-adenosine; XMP: xanthosine monophosphate. Enzymes: 1: adenylosuccinate lyase (ADSL); 2: adenylosuccinate synthetase; 3: AMP deaminase; 4: cytosolic 5'-nucleotidase; 5: adenosine deaminase; 6: purine nucleoside phosphorylase; 7: xanthine oxidase; 8: hypoxanthine-guanine phosphoribosyltransferase; 9: adenine phosphoribosyltransferase (http://www.icp.ucl.ac.be/adsldb/adsl.html).

Sequence analysis of the cDNA of AdeI cells revealed a C872T mutation resulting in an Ala291Val amino acid substitution in the ADSL enzyme. Genomic sequencing however revealed two genomic copies of the ADSL gene with heterozygosity for C-T at nucleotide 872. Since no expression of WT ADSL was observed at the mRNA level, it was hypothesized that the WT allele is silenced or its transcript is lost and that only the mutant ADSL allele is expressed (Vliet et al. 2011). It was also shown that this substitution inactives human ADSL (Vliet et al. 2011). The Ala291 residue of ADSL lies within a highly conserved signature sequence loop region. Figure 4.10 shows the relevant ADSL amino acid sequences from eight distinct species. Despite the relatively low overall sequence identity between two species (e.g. only 12% between human ADSL and *E. coli* ADSL), the loop region containing Ala291 is highly conserved.

```
Homo sapiens              EKQQIGSSAMPYKRNPMRSERCCSLARHLMALIMDPLQTASVQWFERTLD 332
Cricetulus griseus(CHOK1) EKQQIGSSAMPYKRNPMRSERCCSLARHLMALTMDPLQTASVQWFERTLD 332
Cricetulus griseus(AdeI)  EKQQIGSSVMPYKRNPMRSERCCSLARHLMALIMDPLQTASVQWFERTLD 332
Mus musculus              EKQQIGSSAMPYKRNPMRSERCCSLARHLMTLVMDPLQTASVQWFERTLD 332
Sea urchin                EKEQIGSSAMPYKRNPMRAERCCSLARHLMALVSNPLQTAAVQWLERTLD 330
Danio rerio               EKDQIGSSAMPYKRNPMRSERCCSLARHLTTLVMDPLQTLSVQWFERTLD 341
Drosophila melanogaster   ESTQIGSSAMPYKRNPMRSERCCALARHLITLFSSAANTHATQWLERTLD 327
Saccharomyces cerevisiae  AKGQKGSSAMPHKRNPIGSENITGISRVIRGYITTAYENVP-LWHERDIS 304
Escherichia coli          IAGEIGSSTMPHKVNPIDFENSEGNLGLSNAVLQHLASKLPVSRWQRDLT 338
                             : ***:**:* **:  *.  .             .. .    :* :
```

FIGURE 4.10 | **Amino acid sequence alignment of adenylosuccinate lyases from diverse species.** "*" indicates identical residues, ":" indicates conserved substitutions and "." indicates semi-conserved substitution. Alanine291 (which is mutated in AdeI cells) lies in the highly conserved flexible loop region that is marked with the box. The alignment was made with Clustal Omega.

This highly conserved loop region is thought to be very flexible. Thus far, no human ADSL crystal structure is available to reveal the protein structure of this region. Crystallographic analysis of two mutant *E.coli* ADSL enzymes in the presence of substrate (S-AMP) or products (AMP and fumarate) have demonstrated that the flexible loop closes over the active site upon substrate binding (Tsai et al. 2007). Since the loop is close to the substrate in the crystal structure of *E. coli* ADSL, it was proposed that this loop region is essential for catalysis. Indeed, mutagenesis of the two serine residues in the loop region of human ADSL shows that these amino acids are essential for catalysis, but not for substrate binding (Sivendran and Colman 2008). In AdeI cells, it may be that substitution of alanine with the more bulky valine at position 291 inhibits the mobility of the flexible loop, restricts the ability of the substrate to fit into the active site, or inhibits the contact of the active site serines with the substrate. Any of these alterations may also result in unstable ADSL protein (Vliet et al. 2011). An additional hypothesis proposes that the mutant ADSL enzyme may disrupt the formation of the purinosome, a transient multienzyme complex that contains all the enzymes of de novo purine synthesis (Vliet et al. 2011).

4.4.2 Metabolic characterization of AdeI and CHOK1 cells

We assessed the growth of AdeI cells in media supplemented with different concentrations of adenine and hypoxanthine (Figure 4.11). As mentioned above, AdeI cells are strictly dependent on adenine for growth. In this experiment, we added hypoxanthine to investigate whether this HGPRT substrate could partially substitute the adenine supply. The black curve with the black dots (0 µM Hx-30 µM Ade) represents the growth of AdeI cells in the medium used for subcultivation. The indicated hypoxanthine concentration represents the concentration added to the medium. We determined the concentration of hypoxanthine in fetal calf serum (Gibco) by reverse-phase HPLC which showed that FCS contains 44 µM hypoxanthine. Since the experiments in Figure 4.11 were done in culture medium with 10% FCS, the effective concentration of hypoxanthine is always 4.4 µM higher than the concentration indicated. When culture medium was supplemented with hypoxanthine, growth was increased, and this proliferation was highest in medium supplemented with both 30 µM adenine and 30 µM hypoxanthine. This seems logical since the AdeI cells can now use both purine bases as starting points for purine nucleotide synthesis via either APRT or HGPRT salvage. When the adenine concentration was reduced, growth was, as expected, severely diminished. Hypoxanthine could not complement for adenine. Hypoxanthine can be converted, by HGPRT, to the central branch point nucleotide IMP, which leads to the formation of guanine nucleotides via the action of IMPDH (Figure 4.9). However, the production of adenine nucleotides is impossible due to the ADSL deficiency. As a result, S-AMP accumulates in AdeI cells undergoing adenine starvation conditions (Supplemental Figure 5).

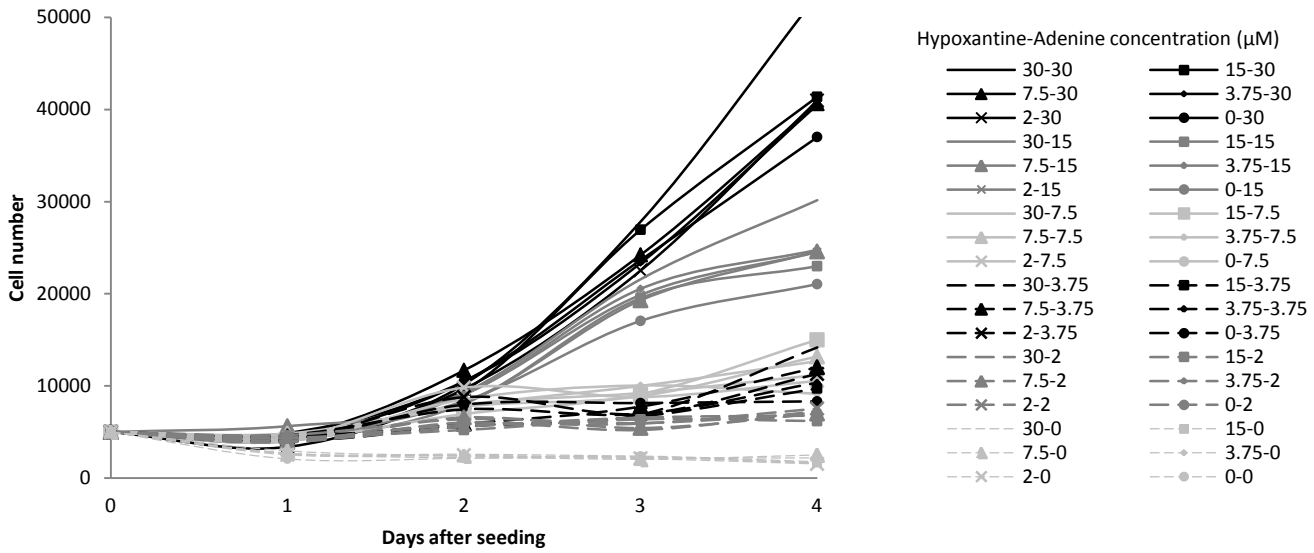

FIGURE 4.11 | **Growth curves of AdeI cells in the presence of different adenine and hypoxanthine concentrations.** AdeI cells grow best in media supplemented with both adenine and hypoxanthine. Note that the given hypoxanthine concentration is the concentration *added* to the growth medium which already contains 4.4 µM Hx originating from 10% added FCS.

To compare HGPRT and APRT enzymatic activity in CHOK1 and AdeI, cells were incubated with either [2,8-^{3}H]Hx or [8-^{3}H]Ade for 24 hours. Then, cell extracts were analyzed by HPLC to determine the radioactivity incorporated into purine nucleotide pools (Figure 4.12). By analyzing in parallel the methanol-insoluble fraction, the incorporation of [2,8-^{3}H]Hx or [8-^{3}H]Ade into nucleic acids was measured, which represents the final result of HGPRT or APRT salvage. Separation was not optimal for a few nucleotides, i.e. AMP and IMP co-eluted in the same radioactive fraction, and so did GDP and S-AMP. Since IMP is readily converted to other nucleotides and was not detectable on the UV-chromatogram, it can be assumed that the radioactivity in the third fraction originates exclusively from AMP. Fraction four, corresponding to S-AMP and GMP, is probably more biased in AdeI cells, since S-AMP accumulates in AdeI cells.

Incubation of AdeI cells with [8-^{3}H]Ade resulted in active incorporation of the labeled purine base in all nucleotides, which leads to marked incorporation of radiolabel in nucleic acids, with the incorporated radioactivity being 4.3-fold higher compared to CHOK1 (Figure 4.12 B). The difference is less pronounced (i.e only 2-fold higher in AdeI compared to CHOK1) when looking at incorporation of [2,8-^{3}H]Hx derived radioactivity into cellular nucleic acids (Figure 4.12 A). This result indicates that the purine salvage pathway, especially the APRT reaction, is indeed markedly upregulated AdeI cells. In AdeI receiving [2,8-^{3}H]Hx as the added precursor, radioactivity mainly ends up in G-nucleotides since ~ 80% of [2,8-^{3}H]Hx is converted to GMP, GDP and GTP, their labeling being 2.1-, 6.8- and 5.5-fold higher in AdeI than CHOK1 cells. This is a logical consequence of their ADSL deficiency. [2,8-^{3}H]Hx can be converted to the central nucleotide IMP, which is further metabolized towards GMP, GDP and GTP. However, the conversion towards A-nucleotides is halted at the S-AMP → AMP conversion step due to the ADSL deficiency.

A. *Incorporation of [2,8-^{3}H]Hx into purine nucleotide pools and nucleic acids.*

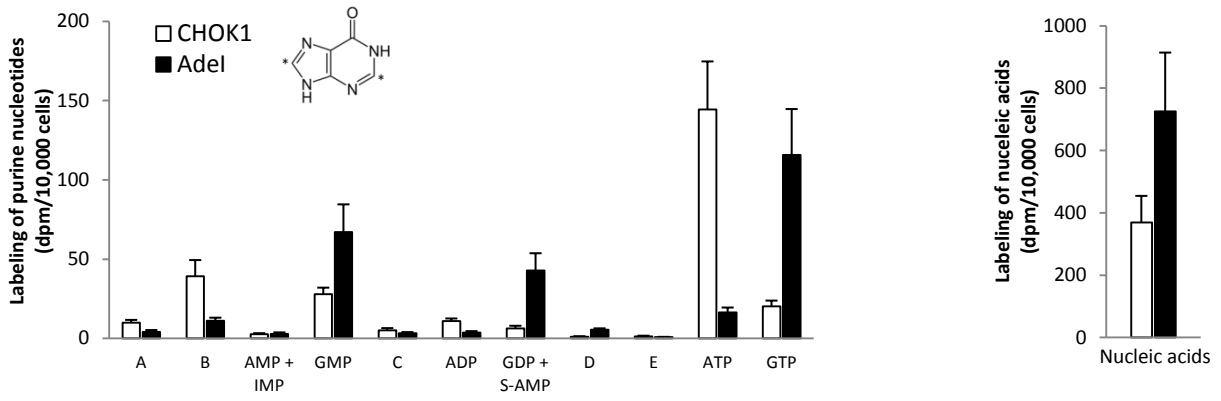

Metabolite:	A	B	AMP + IMP	GMP	C	ADP	GDP + S-AMP	D	E	ATP	GTP
Retention time (min)			7.9 8.7	9.9		15.1	17.6 17.2			24.8	30.1
% of total radioactivity in CHOK1:	3.8	14.0	1.0	11.1	1.9	4.2	2.2	0.4	0.5	53.3	7.6
% of total radioactivity in A*deI*:	1.5	4.9	1.0	23.6	1.4	1.4	15.0	2.0	0.4	6.9	42.0
Ratio AdeI/ CHOK1:	0.4	0.4	0.9	2.1	0.7	0.3	6.8	4.5	0.8	0.1	5.5

B. Incorporation of [8-³H]Ade into purine nucleotide pools and nucleic acids.

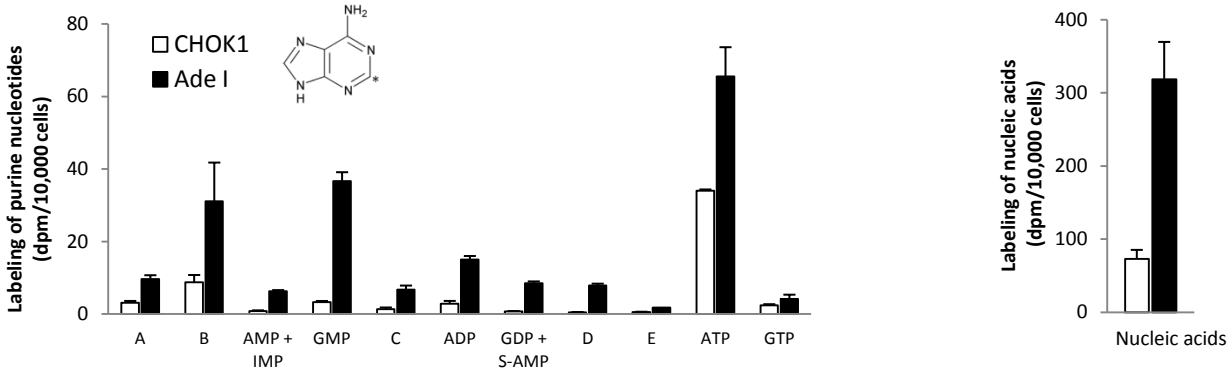

Metabolite:	A	B	AMP + IMP	GMP	C	ADP	GDP + S-AMP	D	E	ATP	GTP
Retention time (min)			7.9 8.7	9.9		15.1	17.6 17.2			24.8	30.1
% of total radioactivity in CHOK1:	5.3	15.0	1.4	5.6	2.3	4.9	1.2	0.8	1.0	58.4	4.2
% of total radioactivity in A*deI*:	5.0	16.0	3.3	19.0	3.5	7.8	4.4	4.1	1.0	34.2	2.2
Ratio AdeI/ CHOK1:	1.0	1.1	2.3	3.4	1.5	1.6	3.7	5.4	0.9	0.6	0.5

FIGURE 4.12 | **Comparison of the metabolism of [2,8-^{3}H]Hx and [8-^{3}H]Ade in CHOK1-WT cells and adenylosuccinate lyase-deficient AdeI cells.** Cells were maintained in medium containing 4.4 µM hypoxanthine (plus 30 µM adenine for AdeI) and incubated for 24 h with 0.0133 µM radiolabeled compound. The incorporation of [2,8-^{3}H]Hypoxanthine and [8-^{3}H]Adenine into purine nucleotides and nucleic acids, corrected for the number of cells, is shown in the column diagrams of panels A and B, respectively. Data are the mean ± S.E.M. of four (CHOK1) or five (AdeI) experiments. The relative contribution of the different metabolites to the total radioactivity is shown in the tables. When [2,8-^{3}H]IMP is oxidized to [8-^{3}H]XMP, the ^{3}H label at position 2 is lost. To correct for this loss, radioactive counts of G metabolites were multiplied by a factor two.

Surprisingly, a slight incorporation of [2,8-^{3}H]Hx into AMP, ADP and ATP is seen in AdeI cells (Figure 4.12 A). Since there is no alternative pathway to form A-nucleotides from hypoxanthine besides via IMP →S-AMP → AMP, this result suggests that the ADSL enzyme with the A291V substitution is not completely inactive.

The predominant nucleotide formed in CHOK1, both starting from [2,8-^{3}H]Hx and [8-^{3}H]Ade, is ATP, representing 53 and 58% of the total radioactivity. In AdeI cells, ATP only represents 7% (from [2,8-^{3}H]Hx) and 34% (from [8-^{3}H]Ade) of total labeling. The former is the result of the absent (or low) ADSL activity. The latter is probably due to the fact that adenine is the main starting point for the formation of all purine nucleotides. Probably, much AMP is converted to IMP to form sufficient G nucleotides. This results in less AMP available for ATP production. This is also reflected in the total ATP content which is 2-fold lower in AdeI compared to CHOK1 cells (Table 4.5). Conversely, AdeI cells contain a 3-fold higher GTP pool than CHOK1 cells. The lower ATP and higher GTP pools seen in ADSL-deficient AdeI cells are analogous to what has been reported for another enzyme deficiency in the purine de novo synthetic pathway, namely in the bifunctional enzyme AICAR transformylase/IMP cyclohydrolase (ATIC) (Marie et al. 2004).

TABLE 4.5 | **Peak area of A and G nucleotides calculated for 10,000 cells.**

	Purine nucleotides[a]			
	ADP	**ATP**	**GDP**	**GTP**
CHOK1	361	5093	105	1064
AdeI	585	2624	707	2725
Ratio AdeI/CHOK1	1.6	0.5	6.7	2.6

[a]Data shown are the peak areas (per 10,000 cells) in the UV_{249nm}-HPLC chromatograms. For the CHOK1 cells, the medium contained 4.4 µM Hx (i.e. 10% FCS) and 0 µM Ade; the AdeI cells were cultured in 4.4 µM Hx and 30 µM Ade.

4.4.3 Effect of IMPDH and HGPRT inhibitors on hypoxanthine metabolism

Subsequently, the effect of the above described IMPDH inhibitors RBV and MPA on the metabolism of [2,8-^{3}H]Hx was examined (Figure 4.13). The inhibitors were added to confluent AdeI or CHOK1 cells and pre-incubated for 4 h at 37°C before metabolic labeling with [2,8-^{3}H]Hx. In the presence of the IMPDH inhibitors, incorporation of radiolabel into nucleic acids were markedly (1.7-fold in CHOK1 and 3-fold in AdeI) reduced. We also studied the effect of the two acyclic nucleoside phosphonates, PEEG and PEEHx, which contain a guanine or hypoxanthine base, respectively (Figure 4.14). Biochemical studies have shown that PEEG and PEEHx inhibit the human HGPRT enzyme in enzymatic assays (Keough et al. 2009). When added to AdeI cells, neither PEEG nor PEEHx had an effect on hypoxanthine metabolism, suggesting that neither of the two acts as a true HGPRT inhibitor in a cellular context.

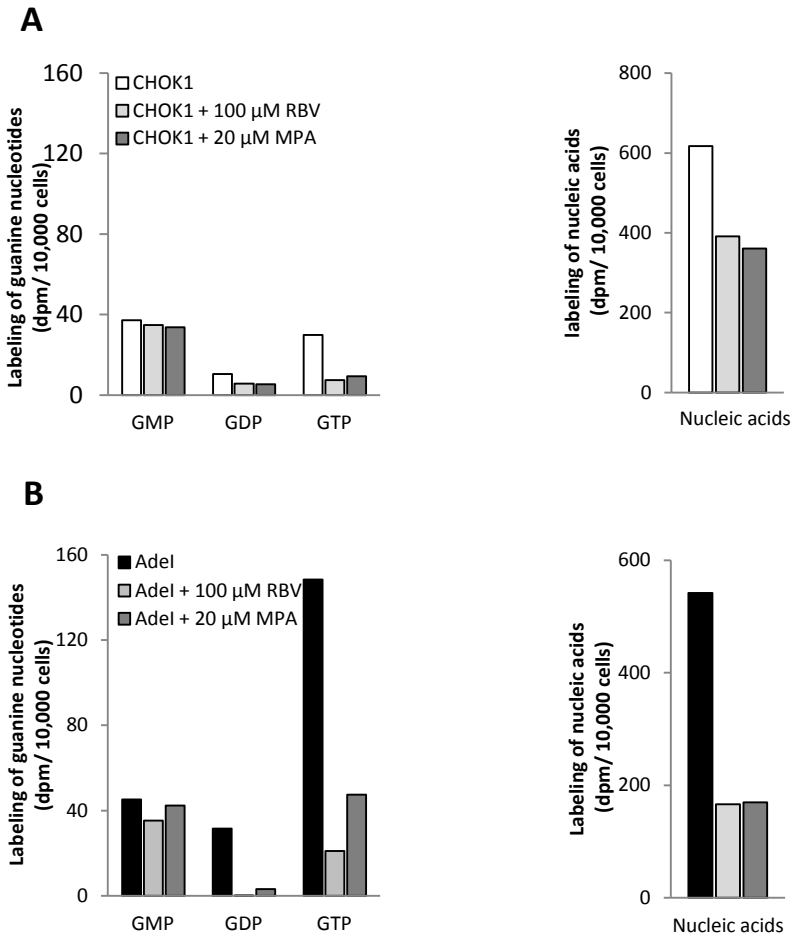

FIGURE 4.13 | **The effect of IMPDH inhibitors on hypoxanthine metabolism in CHOK1 (A) and AdeI (B).** Cells were pre-incubated for 4 h with mycophenolic acid (MPA) or ribavirin (RBV) before metabolic labeling of G pools and nucleic acids with [2,8-^{3}H]Hx for 24 h. The data shown are from one experiment.

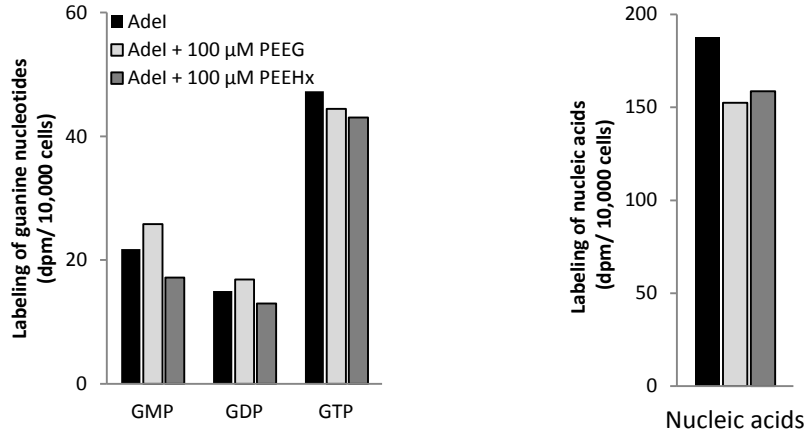

FIGURE 4.14 | **The effect of two potential HGPRT inhibitors on AdeI hypoxanthine metabolism.** Cells were pre-incubated for 4 h with PEEG or PEEHx before metabolic labeling of G pools and nucleic acids of AdeI cells with [2,8-^{3}H]Hx for 24 h. The data shown are from one experiment.

4.4.4 Cytotoxicity assay with several cytostatic agents

Next, we compared the sensitivity of CHOK1 cells and AdeI cells to a variety of cytostatic nucleoside analogues that interfere with de novo and salvage purine biosynthetic enzymes. Since AdeI have an aberrant purine synthesis pathway, we expected to see lower IC_{50} values (i.e. higher cytotoxicity) when these cells were exposed to compounds that block normal purine synthesis. Also, since HGPRT and APRT are upregulated in the AdeI cells, we expected that compounds that are activated by these purine salvage enzymes would be generally more cytotoxic for the AdeI cells compared to the WT CHOK1 cells. The IC_{50} values, i.e. product concentrations causing 50% reduction of cell proliferation, are given in Table 4.6.

TABLE 4.6 | **Sensitivity of CHOK1 and AdeI mutant cells to diverse cytostatic agents.**

		IC_{50} (µM)[a]			
		CHOK1		**AdeI**	
Compound	**Mode of action**	**-Ade[b]**	**+Ade**	**+Ade**	**+Ade/Hx**
6-Thioguanine	HGPRT substrate	0.5 ± 0.1	>20	>20	>20
PMEG	HGPRT inhibitor?	0.3 ± 0.1	0.2	0.6 ± 0.1	0.5
Mycophenolic acid	IMPDH inhibitor	0.9 ± 0.2	1.1	0.8 ± 0.4	0.5
2,6-Diaminopurine	APRT substrate	36 ± 18	>100	>100	>100
Ribavirin	IMPDH inhibitor	34 ± 6.0	28	7 ± 1	2.0
Cell proliferation number[c]:		*15*	*16*	*11*	*10*

[a] The IC_{50} is the compound concentration, expressed in µM, required to inhibit cell proliferation by 50%, as determined after 3 days of incubation. Data are the the result of one experiment or the mean ± S.E.M. of two independent experiments.
[b] Cells were maintained in medium without adenine (-Ade), with 30 µM adenine (+Ade) or containing both 30 µM adenine and 30 µM hypoxanthine (+ Ade/Hx).
[c] The cell proliferation number is defined as the fold increase in cell number of the untreated cell control between day 0 and day 3.

As described above, 6-Thioguanine (6-TG) is a thio-analogue of guanine that is converted to 6-thioguanine 5'-monophosphate (6-TGMP) by the action of HGPRT. 6-TGMP is a competitive competitive inhibitor of IMPDH and is after further phosphorylation to 6-thioguanine 5'-triphosphate, incorporated into DNA and RNA, which leads to single strand DNA breaks during DNA elongation (Aubrecht et al. 1997; Karran and Attard 2008; Nelson et al. 1975; Pan and Nelson 1990). Since our HPLC metabolism studies indicated that AdeI cells have higher HGPRT activity than WT CHOK1 cells, we expected a low IC_{50} value for 6-TG in AdeI cells. Surprisingly, AdeI cells proved to be resistant to 6-TG (IC_{50} > 20 µM), whereas CHOK1 showed high sensitivity (IC_{50} is 0.5 µM). When CHOK1 cells were supplemented with 30 µM adenine, they also became resistant to 6-TG (Table 4.6). As shown in Figure 4.9, cells can use adenine as the starting point for all purine nucleotides. Possibly, HGPRT activity is shut down when exogenous adenine is abundantly present.

2,6-Diaminopurine (2,6-DAP) is an adenine analogue that is activated by APRT (Weckbecker and Cory 1989). Despite the high APRT activity of AdeI, 2,6-DAP proved to be non-toxic in these cells (IC_{50} > 100 µM). Also here, it is the addition of adenine which leads to decreased sensitivity. The IC_{50} value of 2,6-DAP in CHOK1 was 36 µM when measured without adenine supplementation; in the presence of 30 µM adenine, the IC_{50} value rose above 100 µM. This effect is most likely explained by competitive inhibition. When adenine occupies the active site of APRT, it prevents binding of 2,6-DAP and thus its metabolic conversion is inhibited.

The growth inhibitory effect of MPA on cell proliferation was similar in CHOK1 and AdeI cells and independent of adenine supplementation. RBV was more cytostatic in AdeI cells than in CHOK1 cells. The data for MPA suggest that IMPDH activity is similar in AdeI and CHOK1 cells. Regarding the higher sensitivity of AdeI cells to RBV, this might be related to a higher activity of the RBV-activating adenosine kinase, which is another purine salvaging enzyme that phosphorylates adenosine into AMP.

9-(2-Phosphonylmethoxyethyl)guanine (PMEG) is a cytotoxic agent that demonstrates anticancer activity in murine and human leukemic cells (Pisarev et al. 1997). To become active, PMEG needs to be phosphorylated to its diphosphate derivative, PMEGpp. PMEGpp is a potent inhibitor of human DNA polymerase α and δ, two essential enzymes for DNA replication (Pisarev et al. 1997). PMEG has also been described to be an HGPRT inhibitor of human and *Pf*HGPRT with K_i values of 1.6 µM and 29 µM respectively (Keough et al. 2009). Its growth inhibitory effect was slightly lower in AdeI compared to CHOK1 cells (i.e. IC_{50} values: 0.6 and 0.3 µM, respectively). This contradicts the hypothesis that the cytotoxic effect of PMEG is related to HGPRT inhibition, since HGPRT activity is slightly increased in AdeI cells, as shown above. On the other hand, the 3-fold increased GTP pool in AdeI cells (Table 4.5) may result in higher competition of this polymerase substrate versus PMEGpp.

5 DISCUSSION

New and improved antimalarial drugs are urgently needed to support combination therapy approaches promoted by the World Health Organization. Emerging drug resistance of the *Plasmodium* parasite threatens the global efforts to control or eliminate malaria, and could wipe out decades of investment (Horn and Duraisingh 2014; White et al. 2014). To achieve the goal of malaria eradication, the search for new drugs with novel mechanisms of action must continue since no therapeutic alternative is available if artemisinin resistance spreads from South-East Asia to other regions.

An important route for finding new, effective and safe antimalarial chemotherapeutics is by rational drug design that exploits metabolic differences between the parasite and human host. A prominent example is related to the different routes that both organisms use to synthesize purine (adenine and guanine) nucleotides. Mammalian cells are able to synthesize the purine ring de novo. On the other hand, malaria parasites are purine auxotrophs and depend on salvage of host cell purines for the synthesis of A and G nucleotides. Therefore, since many years, the purine salvage pathway has been considered as a promising target for malaria therapy (Walsh and Sherman, 1968; Ullman and Carter, 1995). Within this purine salvage process, a critical role is played by the hypoxanthine guanine phosphoribosyltranferase (HGPRT) enzyme.

The collaborative network between the Rega Institute, the University of Queensland (Australia) and the IOCB Institute in Prague was created to rationally design HGPRT inhibitors that specifically target the malarial enzyme over the human counterpart by exploiting enzymatic structural differences between both enzymes. Since only one enzyme is targeted, toxicity and adverse effects should be significantly reduced, making HGPRT inhibitors superior to some currently used antimalarials. Acyclic nucleoside phosphonates (ANPs) with a guanine or hypoxanthine base are structural analogues of the nucleoside-5'-monophosphates HGPRT reaction products, GMP and IMP, repectively. They are excellent drug lead candidates since they selectively inhibit *Pf* and *Pv*HGPRT over huHGPRT in enzymatic assays; arrest the growth of *Pf* in erythrocyte cell culture and have low cytotoxicity towards human cell lines (Keough et al., 2009, 2010). Structure-based inhibitor design resulted in ANP inhibitors with a second phosphonate group attached, that are particularly strong HGPRT inhibitors, with K_i values as low as 30 nM (Keough, Špaček, et al. 2013).

Thus far, the inhibitory effect of ANPs on huHGPRT, *Pf*HGPRT and *Pv*HGPRT has only been proven in cell-free assays using isolated enzymes. It is assumed that the observed antiparasitic effect in *Pf*-infected erythrocyte cultures is due to the inhibition of the malarial HGPRT enzyme, leading to shortage of purine nucleobases and thus to inhibition of parasite

growth and survival. However, it cannot be excluded that the observed antiparasitic effect may be related to other effects than HGPRT inhibition. *Plasmodium* is a Eukaryote and possesses many enzymes that could serve as putative targets, either directly or after metabolic conversion of the ANP to other metabolites by intracellular kinases. For example, for PMEG, it is described that its diphosphorylated metabolite (PMEGpp) is a strong inhibitor of DNA polymerase α and δ in human cells (Pisarev et al. 1997). Thus, it is not unlikely that the growth inhibition of the malaria parasite is due to inhibition of another target. Clearly, there is a missing link between the enzymatic studies that assess HGPRT inhibition in an artificial cell-free environment, and the *Pf* erythrocyte assay that studies growth inhibition of the whole parasite. To unequivocally demonstrate that the inhibitors indeed act as HGPRT inhibitors, we here aimed at developing a new and complementary assay to validate HGPRT as the target of the ANP prodrugs.

For this purpose, we needed to obtain high levels of HGPRT enzyme activity in a HGPRT-deficient cell line. Ad vectors are known to be effective gene delivery tools for human cell lines and are able to express recombinant protein at high levels (Anderson et al. 2000). We were able to construct four distinct replication-incompetent Ad vectors that express either the human (WThuHGPRT and ΔEx2huHGPRT), *Pf* or *Pv* HGPRT gene followed by a GFP sequence. Adenovirus-mediated gene delivery requires the presence of specific virus entry receptors [coxsackievirus and adenovirus receptor (CAR) and integrins, Figure 4.1]. Investigation of the transduction efficiency of different cell lines revealed that MDCK and HeLaTG are impermissive for RAPAd® Ad infection (Table 4.1). The inefficient transduction of MDCK is explained by the absence of CAR from the apical surface of polarized epithelial cells. CAR is sequestered to the basolateral surface in tight junctions, where it is inaccessible for virus infection (Sharma et al. 2012). The inefficient transduction of HeLaTG cells was absolutely unexpected since normal HeLa cells were very permissive, corresponding with reports in literature (Cantwell et al 1996, Carson et al. 2007). Several explanations can be given. In the HeLaTG cells, the CAR receptor may be lacking or inaccessible due to its sequestration on the basolateral surface, as in MDCK cells. Also, a low abundance or absence of αv-integrins, required for Ad internalization, may hinder infection (Nemerow and Stewart 1999). Cells with low CAR expression and low Ad transduction efficiency typically need high quantities of virus to achieve sufficient infection levels. Possibly, HeLaTG can be infected if high quantities of virus are used, but this was not tested.

Flow cytometric analysis, Western blot analysis and measurement of obtained HGPRT activity indicated that human HGPRT-deficient 1306 skin fibroblast cells showed the best transduction efficiency for the Ad vectors that we generated. Assessment of HGPRT activity by measuring ^{3}H release from [2,8-^{3}H]Hx in Ad-transduced 1306 cells, revealed marked

differences in the catalytic activities of the three enzymes. Human HGPRT was found to be the best catalyst, while the activities of *Pv*HGPRT and especially *Pf*HGPRT were significantly lower (Figure 4.6 and 4.7). This is consistent with the lower hypoxanthine turnover number for *Pv*HGPRT (k_{cat}: 0.74 s^{-1}) and *Pf*HGPRT (k_{cat}: 0.33 s^{-1}) compared to huHGPRT (k_{cat}: 5.2 s^{-1}) (Table 1.3). This low turnover number is surprising when considering that the parasite critically depends on HGPRT for its survival. To explain this apparent contradiction, it was proposed that HGPRT expression levels are possibly much higher in the *Plasmodium* parasite compared to human cells and thus, turnover numbers do not have to be as high. However, even when we infected the 1306 cells with an MOI of 150, we barely detected *Pf*HGPRT activity. For *Pv*HGPRT, an MOI of 100 gave an average signal-to-noise ratio of 8, suitable for inhibitor testing.

The low catalytic activity of recombinant *Pf*HGPRT expressed in *Escherichia coli* has long been a major hurdle to purify the protein in sufficient quantities for enzymatic studies (Keough et al. 1999). One problem is related to codon usage, since *Pf* has the most A+T rich genome sequenced to date (Gardner et al. 2002). However, this cannot explain our observation in Ad-transduced 1306 cells, since our *Pf*HGPRT Ad construct contained a codon-optimized cDNA sequence suitable for expression in human cells. Development of a *Pf*HGPRT antibody and detection of protein expression by Western blot analysis could answer this question.

Another and more likely explanation could be that the *Pf*HGPRT protein is successfully expressed but is present in an inactive state. Several studies report the problem that purified recombinant *Pf*HGPRT has negligible enzyme activity, while human HGPRT is highly active upon purification (Keough et al. 1999; Raman et al. 2005; Sujay Subbayya and Balaram 2000). Keough et al. showed that incubation of the purified *Pf*HGPRT with its substrates, hypoxanthine and PRPP, significantly increased enzyme activity (Keough et al. 1999). Raman et al. showed that *Pf*HGPRT is activated by its reaction product, IMP (Raman et al. 2005). Binding of IMP triggers a conformational change to a high activity state that enables the enzyme to bind its substrates, hypoxanthine and PRPP. These observations suggest that *Pf*HGPRT requires very specific conditions for optimal activity. Presumably, the optimal requirements of protein levels, substrate and ligand concentrations are only found within the *Pf* parasitic cell. Apparently, *Pv*HGPRT does not have such precise requirements for activity and seems to be more similar to the human enzyme.

Due to the low enzymatic activity obtained for *Pf*HGPRT, our inhibitor studies in Ad-transduced 1306 cells were only performed with huHGPRT and *Pv*HGPRT. Studies with purine base analogues revealed marked differences in their ability to function as substrates for both enzymes (Table 4.3). This indicates that, although the active sites of both enzymes are largely conserved (Figure 1.6), differences in substrate binding exist which may be exploited in drug design. One region where the human and *Pv* enzyme significantly differ (59%

sequence identity) is in the flexible loop region (residues 100-117, human numbering system) (Figure 1.6). Crystallographic studies of free and huHGPRT in complex with substrates or inhibitors showed that this loop closes over the active site during catalysis, shielding it from the solvent (Keough et al. 2005). Amino acid differences in this loop may influence its movement over the active site and its interactions with the purine base analogue substrate. Hence, these loop residues may contribute to differences in binding affinity and selectivity towards compounds bound in the active site (Keough et al. 2009).

The main purpose of our project was to investigate whether the *in silico* designed bisphosphonate ANPs indeed act as HGPRT inhibitors in a cellular context (Figure 2.1). Three prodrug compounds (**9**, **10** and **18**) were able to inhibit ^{3}H release with IC_{50} values around 50 µM and thus indeed prove to be HGPRT inhitors in a cellular context (Table 4.4). The sister compounds, **9** (hypoxanthine base) and **10** (guanine base), are both active. For the other pair, **18** and **19**, only **18** (with hypoxanthine base) is active. The lack of activity of **19** (with guanine base) is unexpected, since its active metabolite, **17**, is the most potent ANP inhibitor in enzyme assays, with a K_i value of 30 nM for huHGPRT, 70 nM for *Pf*HGPRT and 600 nM for *Pv*HGPRT (Table 1.5). Its prodrug **19** was also effective in *Pf* growth inhibition with an IC_{50} value of 9.7 µM (Table 1.5). The corresponding guanine-analogue, **18**, has the best antimalarial activity in *Pf* erythrocyte culture (IC_{50} of 3.8 µM), although the affinity of its active metabolite, **16**, is markedly lower compared to **17**, with K_i values being 33-fold higher for huHGPRT and 3-fold higher for *Pv*HGPRT. In our cell assay, **18** inhibited ^{3}H release in both Ad-WThuHGPRT and Ad-*Pv*HGPRT tranduced cells (IC_{50} of 46 µM and 54 µM respectively), but we did not see inhibition of huHGPRT or *Pv*HGPRT (IC_{50}> 200 µM) when cells were exposed to **19**. This suggests that the observed antiparasitic effect in *Pf* erythrocyte culture may be due to inhibition of (an)other target enzyme(s). This hypothesis awaits confirmation until suitable conditions are found to increase *Pf*HGPRT activity. Since **18** and **19** only differ in the attached base, the inactivity of **19** cannot be attributed to difficulties in membrane passage or intracellular cleavage of their prodrug branches.
Compound **9**, **10** and **18** inhibit huHGPRT and *Pv*HGPRT to the same extent. This is logical since their affinities for the two enzymes are similar (Table 1.5). To improve selectivity towards the malarial enzymes, crystal structures of *Pf* and *Pv*HGPRT in complex with these compounds are needed. Selective inhibitors will avoid potential host toxicity problems associated with inhibition of huHGPRT.
The lipophilic prodrug of PEEG, compound **23**, was not able to inhibit HGPRT activity (IC_{50} > 200 µM) (Table 4.4). It has been demonstrated that intracellular removal of the hexadecyloxypropyl chain is performed by phospholipase C (Hostetler 2009). Possibly, inefficient intracellular conversion may result in low concentrations of the active product PEEG. Alternatively, PEEG may not act as an HGPRT inhibitor in a cellular context. This may be due to its rapid conversion to other metabolites (e.g. phosphorylation by kinases) with

other mechanisms of action. These findings clearly demonstrates that enzyme inhibition *in vitro* cannot be readily extrapolated to assume that inhibition in a cellular context will occur and thus that a cellular assay is indispensable to validate HGPRT as the target enzyme of the ANPs.

Still, some limitations have to be kept in mind. The first point to note is that we cannot definitely exclude that HGPRT is the only enzyme targeted by the ANP bisphosphonate compounds. It remains possible that also other proteins, either direct or indirect, are targeted by the ANPs. Secondly, the malarial enzymes are expressed in a human host cell and the intracellular conditions may be very different inside the malarial parasite. As explained above, specific cellular conditions may be required to induce *Pf*HGPRT activity. Performing the tritium release test in *Pf*-infected red blood cells could provide a solution. Analogous as in our test, *Pf*-infected erythrocytes can be exposed to [2,8-^{3}H]Hx in the presence or absence of the ANP prodrugs, after which ^{3}H release can be measured by liquid scintillation. Additionally, incorporation of radiolabeled hypoxanthine into purine nucleotides and nucleic acids of the parasite can be measured by HPLC analysis. Similar tests were performed by Hazleton et al. (2012). However, uptake and metabolism of hypoxanthine by the parasite is a general marker for parasite growth and replication, and inhibition of hypoxanthine incorporation is used as an indicator of antimalarial drug activity (Desjardins et al. 1979). For instance, chloroquine, that blocks haemozoin biocrystallization, also inhibits [2,8-^{3}H]Hx incorporation with an IC_{50} of 0.017 µM (Keough, Špaček, et al. 2013). Thus, inhibition of hypoxanthine incorporation into parasite nucleotide pools does not necesseraly implicate direct inhibition of HGPRT. In addition, these metabolic investigations can only be done with *P. falciparum,* since it is the only malaria parasite that can be grown in cell culture. Drug discovery for *P.vivax* is seriously impeded by the difficulties of maintaining them in continuous *in vitro* cell culture. This parasite requires reticulocytes (immature red blood cells) that are difficult to obtain. These obstacles have limited the research of *P. vivax* biology at both the cellular and molecular levels (Udomsangpetch et al. 2008). Our assay provides an easy and alternative way to identify inhibitors that target the HGPRT enzyme of *P. vivax* in a cellular context.

The assay that we developed has some other interesting features that can further broaden its scope. A major strength is that the Ad transduction system also enables to evaluate inhibitors towards HGPRT enzymes from other parasites, provided that Ad vectors are constructed that carry the cDNA coding for these enzymes. As described in the introduction, all parasitic protozoan parasites studied to date are purine auxotrophs and, thus, the enzymes compromising the purine salvage pathway are promising drug targets. Furthermore, since the active site residues are highly conserved (Figure 1.6), inhibitors of *Pf* and *Pv*HGPRT can be used as lead compounds for the development of other antiparasitic chemotherapeutics. Although single enzyme inhibition is not expected to result in killing of *Leishamania* or *T.*

cruzi, inhibition of multiple enzymes, including HGPRT, can provide a good alternative (Berg et al. 2010). Thus, our assay based on Ad transduction of 1306 cells is not limited to identify new antimalarials but provides opportunities for the development of related drugs against parasites that cause a series of neglected tropical diseases.

Besides the master project discussed above, we also conducted a metabolic study in CHOK1 and AdeI cells to reveal differences in their purine metabolism and to investigate if these cells could be useful in ANP cytotoxicity assays. Since AdeI cells are deficient in adenylosuccinate lyase, an enzyme catalyzing two non sequential reactions in de novo purine synthesis, we hypothesized that the salvage enzymes, APRT and HGPRT, should be heavily upregulated in these cells. Indeed, the purine salvage pathway, especially the APRT reaction, was considerably upregulated in AdeI compared to CHOK1 cells (Figure 4.12). The results of the cytotoxicity experiments were different than expected (Table 4.6). We assumed that AdeI cells would generally be more sensitive to cytostatic agents compared to CHOK1, since AdeI cells already have an aberrant purine synthesis pathway and have higher activities of compound activating enzymes APRT (2,6-DAP) and HGPRT (6-TG). However, the strict dependence of these cells on exogenous adenine interfered with our aim to estimate their sensitivity to the cytostatic agents and showed to obscure the cytotoxicity evaluations. Therefore, we did not proceed with our original plan to carry out such experiments with the ANPs.

6 CONCLUSION

We reached our principal objective, i.e. the development of a novel target validation assay to assess the inhibitory effect of the bisphosphonate ANP inhibitors towards HGPRT in a cellular environment. It is a rapid and convenient method which takes only four days to complete. With this new cellular assay, we proved that three rationally designed ANP compounds indeed act as inhibitors of human and *Pv*HGPRT, making them interesting lead compounds for further drug development. The activity of *Pf*HGPRT was surprisingly low. Further optimization of the experimental conditions is required before inhibitor testing will be possible. Compound **17** (evaluated under its prodrug form **19**), the most potent inhibitor in enzyme assays, did not inhibit ^{3}H release in our cellular assay, and thus its antiparasitic effect may be associated with inhibition of another target. This demonstrates that a combination of enzymatic, cellular and whole parasite assays is needed to reach the final goal of this project, i.e. the development of clinically relevant ANP inhibitors that inhibit *Pv* and *Pf*HGPRT while having minimal effect on human HGPRT. In the future, this class of HGPRT inhibitors could represent an entirely new class of antiparasitic drugs, particularly for the treatment and control of malaria. The new assay that we developed will be very instrumental to guide this antimalarial drug development process.

7 REFERENCES

Journal articles

Agnandji, S.T. et al. 2011. "First Results of Phase 3 Trial of RTS,S/AS01 Malaria Vaccine in African Children." *The New England journal of medicine* 365(20):1863–75.

Agnandji, S.T. et al. 2012. "A Phase 3 Trial of RTS,S/AS01 Malaria Vaccine in African Infants." *The New England journal of medicine* 367(24):2284–95.

Anderson, R.D., R.E. Haskell, H. Xia, B.J. Roessler, and B.L. Davidson. 2000. "A Simple Method for the Rapid Generation of Recombinant Adenovirus Vectors." *Gene therapy* 7(12):1034–38.

Ariey, F. et al. 2014. "A Molecular Marker of Artemisinin-Resistant Plasmodium Falciparum Malaria." *Nature* 505(7481):50–55.

Aubrecht, J., M.E. Goad, and R.H. Schiestl. 1997. "Tissue Specific Toxicities of the Anticancer Drug 6-Thioguanine Is Dependent on the Hprt Status in Transgenic Mice." *The Journal of pharmacology and experimental therapeutics* 282(2):1102–8.

Baird, J.K. 2005. "Drug Therapy: Effectiveness of Antimalarial Drugs." *New England Journal of Medicine* 352(15):1565–77.

Balzarini, J., and E. De Clercq. 1992. "Assay Method for Monitoring the Inhibitory Effects of Antimetabolites on the Activity of Inosinate Dehydrogenase in Intact Human CEM Lymphocytes." *The Biochemical journal* 287 (3):785–90.

Bell, A.S., J.E. Mills, G.P. Williams, J.A. Brannigan, A.J. Wilkinson, T. Parkinson, R.J. Leatherbarrow, E.W. Tate, A.A. Holder and D.F. Smith. 2012. "Selective Inhibitors of Protozoan Protein N-Myristoyltransferases as Starting Points for Tropical Disease Medicinal Chemistry Programs." *PLoS neglected tropical diseases* 6(4):e1625.

Berg, M., P. Van der Veken, A. Goeminne, A. Haemers, and K. Augustyns. 2010. "Inhibitors of the Purine Salvage Pathway: A Valuable Approach for Antiprotozoal Chemotherapy?" *Current medicinal chemistry* 17(23):2456–81.

Boitz, J. M., and B. Ullman. 2006. "A Conditional Mutant Deficient in Hypoxanthine-Guanine Phosphoribosyltransferase and Xanthine Phosphoribosyltransferase Validates the Purine Salvage Pathway of Leishmania Donovani." *The Journal of biological chemistry* 281(23):16084–89.

Boitz, J. M., and B. Ullman. 2010. "Amplification of Adenine Phosphoribosyltransferase Suppresses the Conditionally Lethal Growth and Virulence Phenotype of Leishmania Donovani Mutants Lacking Both Hypoxanthine-Guanine and Xanthine Phosphoribosyltransferases." *The Journal of biological chemistry* 285(24):18555–64.

Bousema, T., and C. Drakeley. 2011. "Epidemiology and Infectivity of Plasmodium Falciparum and Plasmodium Vivax Gametocytes in Relation to Malaria Control and Elimination." *Clinical microbiology reviews* 24(2):377–410.

Cantwell M.J., S. Sharma, T. Friedmann and T.J. Kipps. 1996. Adenovirus vector infection of chronic lymphocytic leukemia B cells. *Blood* 88(12):4676-83 .

Carlton, J. 2003."The Plasmodium Vivax Genome Sequencing Project."*Trends in parasitology* 19(5):227–31.

Carson, S.D., K.S. Kim, S.J. Pirruccello, S. Tracy, and N.M. Chapman. 2007. "Endogenous Low-Level Expression of the Coxsackievirus and Adenovirus Receptor Enables Coxsackievirus B3 Infection of RD Cells." *The Journal of general virology* 88(Pt 11):3031–38.

Cassera, M.B., Y. Zhang, K.Z. Hazleton, and V.L. Schramm. 2011. "Purine and Pyrimidine Pathways as Targets in Plasmodium Falciparum." *Current topics in medicinal chemistry* 11(16):2103–15.

De Clercq, E. 2007. “Acyclic Nucleoside Phosphonates: Past, Present and Future. Bridging Chemistry to HIV, HBV, HCV, HPV, Adeno-, Herpes-, and Poxvirus Infections: The Phosphonate Bridge.” *Biochemical pharmacology* 73(7):911–22.

De Clercq, E., and A. Holý. 2005. “Acyclic Nucleoside Phosphonates: A Key Class of Antiviral Drugs.” *Nature reviews. Drug discovery* 4(11):928–40.

Clinch, K., D.R. Crump, G.B.Evans, K.Z. Hazleton, J.M. Mason, V.L. Schramm and P.C. Tyler. 2013. “Acyclic Phosph(on)ate Inhibitors of Plasmodium Falciparum Hypoxanthine-Guanine-Xanthine Phosphoribosyltransferase.” *Bioorganic & medicinal chemistry* 21(17):5629–46.

Craig, S.P., and E. Eakin. 2000. “Purine Phosphoribosyltransferases.” *The Journal of biological chemistry* 275(27):20231–34.

Dawson, P.A., R.B. Gordon, D.T. Keough, and B.T. Emmerson. 2005. “Normal HPRT Coding Region in a Male with Gout due to HPRT Deficiency.” *Molecular Genetics and Metabolism* 85(1):78–80.

Desjardins, R.E., C.J. Canfield, J.D. Haynes, and J.D. Chulay. 1979. “Quantitative Assessment of Antimalarial Activity in Vitro by a Semiautomated Microdilution Technique.” *Antimicrobial agents and chemotherapy* 16(6):710–18.

Dondorp, A.M., F.Nosten, P. Yi, D. Das, A.P. Phyo, J. Tarning, K. M. Lwin, F. Ariey, W. Hanpithakpong, S.J. Lee, P. Ringwald, K. Silamut, M. Imwong, K. Chotivanich, P. Lim, T. Herdman, S. S. An, S. Yeung, P. Singhasivanon, N.P.J. Day, N. Lindegardh, D.Socheat, and N.J. White, et al. 2009. “Artemisinin Resistance in Plasmodium Falciparum Malaria.” *The New England journal of medicine* 361(5):455–67.

Downie, M.J., K. Kirk, and C.B. Mamoun. 2008. “Purine Salvage Pathways in the Intraerythrocytic Malaria Parasite Plasmodium Falciparum.” *Eukaryotic cell* 7(8):1231–37.

Fernández, D., M.A. Wenck, S.P. Craig, and J.M. Delfino. 2004. “The Purine Transferase from Trypanosoma Cruzi as a Potential Target for Bisphosphonate-Based Chemotherapeutic Compounds.” *Bioorganic & medicinal chemistry letters* 14(17):4501–4.

Garçon N., P. Chomez, and M. Van Mechelen. 2007. “GlaxoSmithKline Adjuvant Systems in vaccines: concepts, achievements and perspectives.” *Expert Review of Vaccines* 6(5):723-739.

Gardner, M.J., N. Hall, E. Fung, O.White, M. Berriman, R.W. Hyman, J.M Carlton, A. Pain, K.E. Nelson, S. Bowman, I.T. Paulsen, K. James, J.A. Eisen, K. Rutherford, S.L. Salzberg, A. Craig, S. Kyes, M.S. Chan , V. Nene, S.J. Shallom, B. Suh, J. Peterson, S. Angiuoli, M. Pertea, J. Allen, J. Selengut, D. Haft, M.W.Mather, A.B. Vaidya, D.M. Martin, A.H. Fairlamb, M.J. Fraunholz, D.S. Roos, S.A. Ralph,G.I. McFadden, L.M. Cummings, G.M. Subramanian, C. Mungall, J.C. Venter, D.J. Carucci, S.L. Hoffman, C. Newbold, R.W. Davis, C.M. Fraser and B. Barrelll. 2002. “Genome Sequence of the Human Malaria Parasite Plasmodium Falciparum.” *Nature* 419(6906):498–511.

Ginsberg, H.S., U. Lundholm-Beauchamp, R.L. Horswood, B. Pernis, W.S. Wold, R.M. Chanock and G.A. Prince. 1989. “Role of Early Region 3 (E3) in Pathogenesis of Adenovirus Disease.” *Proceedings of the National Academy of Sciences of the United States of America* 86(10):3823–27.

Guerra, C.A.R., E. Howes, A.P. Patil, P. W. Gething, T. P. Van Boeckel, W.H. Temperley, C. W. Kabaria, A.J. Tatem, B.H. Manh, I.R. F. Elyazar, J. K. Baird, R. W. Snow and S. I. Hay. 2010. “The International Limits and Population at Risk of Plasmodium Vivax Transmission in 2009.” *PLoS neglected tropical diseases* 4(8):e774.

Handschumacher, R.E., and N. Haven. 1960. “Orotidylic Acid Decarboxylase: Inhibition Studies with Azauridine 5’-Phosphate.” *Journal of Biological Chemistry* 235(10).

Hatse, S., E. De Clercq, and J. Balzarini. 1999. “Role of Antimetabolites of Purine and Pyrimidine Nucleotide Metabolism in Tumor Cell Differentiation.” *Biochemical pharmacology* 58(4):539–55.

Hazleton, K.Z., M.C. Ho, M.B. Cassera, K. Clinch, D.R. Crump, I.J.Rosario, E.F. Merino, S.C. Almo, P.C. Tyler and V.L. Schramm. 2012. “Acyclic Immucillin Phosphonates: Second-Generation Inhibitors of Plasmodium Falciparum Hypoxanthine-Guanine-Xanthine Phosphoribosyltransferase.” *Chemistry and Biology* 19(6):721–30.

Horn, D., and M.T. Duraisingh. 2014. “Antiparasitic Chemotherapy: From Genomes to Mechanisms.” *Annual review of pharmacology and toxicology* 54:71–94.

Hostetler, K.Y. 2009. “Alkoxyalkyl Prodrugs of Acyclic Nucleoside Phosphonates Enhance Oral Antiviral Activity and Reduce Toxicity: Current State of the Art.” *Antiviral Research* 82(2): A84-98.

Hotez, P.J., D.H. Molyneux, A.Fenwick, J. Kumaresan, S.E. Sachs, J.D. Sachs, and L. Savioli. 2007. “Control of Neglected Tropical Diseases.” *New England Journal of Medicine* 357:1018–27.

Hyde, J.E. 2007. “Targeting Purine and Pyrimidine Metabolism in Human Apicomplexan Parasites.” *Current drug targets* 8(1):31–47.

Janeway, C.M., and S. Cha. 1977. “Effects of 6-Azauridine on Nucleotides , Orotic Acid , and Orotidine in L5178Y Mouse Lymphoma Cells in Vitro .” *Cancer Research* (37): 4382–88.

Johnson, G.E. 2012. “Mammalian cell HPRT gene mutation assay: test methods.” *Methods of Molecular Biology* 817: 55-67.

de Jersey, J., A. Holý, D. Hocková, L. Naesens, D.T. Keough and L.W. Guddat. 2011. “6-Oxopurine Phosphoribosyltransferase: A Target for the Development of Antimalarial Drugs.” *Current topics in medicinal chemistry* 11(16):2085–2102.

Kantele, A., and T.S. Jokiranta. 2011. “Review of Cases with the Emerging Fifth Human Malaria Parasite, Plasmodium Knowlesi.” *Clinical infectious diseases : an official publication of the Infectious Diseases Society of America* 52(11):1356–62.

Karran, P., and N. Attard. 2008. “Thiopurines in Current Medical Practice: Molecular Mechanisms and Contributions to Therapy-Related Cancer.” *Nature reviews. Cancer* 8(1):24–36.

Keough, D.T., A.L. Ng, D.J. Winzor, B.T. Emmerson, and J. de Jersey. 1999. “Purification and Characterization of Plasmodium Falciparum Hypoxanthine-Guanine-Xanthine Phosphoribosyltransferase and Comparison with the Human Enzyme.” *Molecular and biochemical parasitology* 98(1):29–41.

Keough, D.T., I.M. Brereton, J. de Jersey, and L.W. Guddat. 2005. “The Crystal Structure of Free Human Hypoxanthine-Guanine Phosphoribosyltransferase Reveals Extensive Conformational Plasticity throughout the Catalytic Cycle.” *Journal of Molecular Biology* 351(1):170–81.

Keough, D.T., T. Skinner-Adams, M.K. Jones, A.L. Ng, I.M. Brereton, L.W. Guddat and J. de Jersey. 2006. “Lead Compounds for Antimalarial Chemotherapy: Purine Base Analogs Discriminate between Human and P. Falciparum 6-Oxopurine Phosphoribosyltransferases.” *Journal of medicinal chemistry* 49(25):7479–86.

Keough, D. T., D. Hocková, A. Holý, L. Naesens, T. Skinner-Adams,J. de Jersey and L.W. Guddat. 2009. “Inhibition of Hypoxanthine-Guanine Phosphoribosyltransferase by Acyclic Nucleoside Phosphonates: A New Class of Antimalarial Therapeutics.” *Journal of medicinal chemistry* 52(14):4391–99.

Keough, D.T., D. Hocková, M. Krecmerová, M. Cesnek, A. Holý, L. Naesens, I.M. Brereton, D.J. Winzor, J. de Jersey J and L.W. Guddat. 2010. “Plasmodium Vivax Hypoxanthine-Guanine Phosphoribosyltransferase: A Target for Anti-Malarial Chemotherapy.” *Molecular and biochemical parasitology* 173(2):165–69.

Keough, D.T., P. Špaček, D. Hocková, T. Tichý, S. Vrbková, L. Slavětínská , Z. Janeba, L. Naesens, M.D. Edstein, M. Chavchich , T.-H. Wang, J. de Jersey, and L. W. Guddat .2013. “Acyclic Nucleoside Phosphonates Containing a Second Phosphonate Group Are Potent Inhibitors of 6-Oxopurine Phosphoribosyltransferases and Have Antimalarial Activity.” *Journal of medicinal chemistry* 56(6):2513–26.

Keough, D.T., D. Hocková, D. Rejman, P. Špaček, S. Vrbková, M. Krečmerová, W. S. Eng, H. Jans, N.P. West, L.M.J. Naesens, J. de Jersey and L. W. Guddat. 2013. “Inhibition of the Escherichia Coli 6-Oxopurine Phosphoribosyltransferases by Nucleoside Phosphonates: Potential for New Antibacterial Agents.” *Journal of medicinal chemistry* 56(17):6967–84.

Kicska, G., P.C. Tyler, G.B. Evans, R.H. Furneaux, V. L. Schramm and K. Kim. 2002. "Purine-Less Death in Plasmodium Falciparum Induced by Immucillin-H, a Transition State Analogue of Purine Nucleoside Phosphorylase." *The Journal of biological chemistry* 277(5):3226–31.

Köhler, S., C.F. Delwiche, P.W. Denny, L.G. Tilney, P. Webster, R.J. Wilson, J.D. Palmer and D.S. Roos. 1997. "A Plastid of Probable Green Algal Origin in Apicomplexan Parasites." *Science (New York, N.Y.)* 275(5305):1485–89.

Lesch, M., and W.L. Nyhan. (1964). "A familial disorder of uric acid metabolism and central nervous system function." *American Journal of Medicine* 36: 561-70.

Li, C.M., P.C. Tyler, R.H. Furneaux, G. Kicska, Y. Xu, C. Grubmeyer, M.E. Girvin and V.L. Schramm. 1999. "Transition-State Analogs as Inhibitors of Human and Malarial Hypoxanthine-Guanine Phosphoribosyltransferases." *Nature structural biology* 6(6):582–87.

Lüscher, A., P. Onal, A.M.Schweingruber, and P. Mäser. 2007. "Adenosine Kinase of Trypanosoma Brucei and Its Role in Susceptibility to Adenosine Antimetabolites." *Antimicrobial agents and chemotherapy* 51(11):3895–3901.

Marie, S., B. Heron, P. Bitoun, T. Timmerman, G. Van Den Berghe and M.F. Vincent. 2004. "AICA-Ribosiduria: A Novel, Neurologically Devastating Inborn Error of Purine Biosynthesis Caused by Mutation of ATIC*." American journal of human genetics* 74(6): 1276-81

Mehellou, Y., J. Balzarini, and C. McGuigan. 2009. "Aryloxy Phosphoramidate Triesters: A Technology for Delivering Monophosphorylated Nucleosides and Sugars into Cells." *ChemMedChem* 4(11):1779–91.

Meshnick, S.R., T.E. Taylor, and S. Kamchonwongpaisan. 1996. "Artemisinin and the Antimalarial Endoperoxides: From Herbal Remedy to Targeted Chemotherapy." *Microbiological reviews* 60(2):301–15.

Miles, R.W., P.C. Tyler, R.H. Furneaux, C.K. Bagdassarian, and V.L. Schramm. 1998. "One-Third-the-Sites Transition-State Inhibitors for Purine Nucleoside." *American Chemical Society* 37(24): 8615-21

Moorthy, V.S., and W.R. Ballou. 2009. "Immunological Mechanisms Underlying Protection Mediated by RTS,S: A Review of the Available Data." *Malaria journal* 8:312.

Morrissette, N. S., and L. D. Sibley. 2002. "Cytoskeleton of Apicomplexan Parasites." *Microbiology and molecular biology reviews* 66(1):21–38; table of contents.

Naesens, L., R. Snoeck, G. Andrei, J. Balzarini, J. Neyts, and E. De Clercq. 1996. "HPMPC (cidofovir), PMEA (adefovir) and related acyclic nucleoside phosphonate analogues: a review of their pharmacology and clinical potential in the treatment of viral infections." *Antiviral Chemistry & Chemotherapy* 8 (1):1-23

Naesens, L, L. Guddat, D. Keough, A. van Kuilenburg, J. Meijer, J. Vande Voorde and J. Balzarini. 2013. "Role of Human Hypoxanthine Guanine Phosphoribosyltransferase in Activation of the Antiviral Agent T-705 (favipiravir)." *Molecular pharmacology* 84(4):615–29.

Nelson, J.A., J.W. Carpenter, L.M. Rose, and D.J. Adamson. 1975. "Mechanisms of Action of 6-Thioguanine, 6-Mercaptopurine, and 8-Azaguanine." *Cancer research* 35(10):2872–78.

Nemerow, G.R., and P.L. Stewart. 1999. "Role of Av Integrins in Adenovirus Cell Entry and Gene Delivery." *Microbiology and Molecular Biology Reviews* 63(3):725–34.

Nyhan, W.L., P.J. O' Neill, H.A. Jinnah and J.C. Harris. 2000 (initial posting), 2014 (last updated). "Lesch-Nyhan syndrome." *GeneReviews.* Bookshelf ID: NBK1149

Overbosch, D., H. Schilthuis, U. Bienzle, R.H. Behrens, K.C. Kain, P.D. Clarke, S. Toovey, J. Knobloch, H.D. Nothdurft, D. Shaw, N.S. Roskell and J.D. Chulay. 2001. "Atovaquone-Proguanil versus Mefloquine for Malaria Prophylaxis in Nonimmune Travelers: Results from a Randomized, Double-Blind Study. " *Clinical infectious diseases* 33(7): 1015-1021

Pan, B.F., and J.A. Nelson. 1990. "Characterization of the DNA Damage in 6-Thioguanine-Treated Cells." *Biochemical pharmacology* 40(5):1063–69.

Pasvol, G. 2010. “Protective Hemoglobinopathies and Plasmodium Falciparum Transmission.” *Nature genetics* 42(4):284–85.

Patterson, D. 1976. “Biochemical Genetics of Chinese Hamster Cell Mutants with Deviant Purine Metabolism. IV. Isolation of a Mutant Which Accumulates Adenylosuccinic Acid and Succinylaminoimidazole Carboxamide Ribotide.” *Somatic cell genetics* 2(3):189–203.

Pisarev, V.M., S.H. Lee, M.C. Connelly, and A. Fridland. 1997. “Intracellular Metabolism and Action of Acyclic Nucleoside Phosphonates on DNA Replication.” *Molecular pharmacology* 52(1):63–68.

Pollack, Y., R. Shemer, S. Metzger, D.T. Spira, and J. Golenser. 1985. “Plasmodium Falciparum: Expression of the Adenine Phosphoribosyltransferase Gene in Mouse L Cells.” *Experimental parasitology* 60(3):270–75.

Queen, S.A., D.L. Vander Jagt, and P. Reyes. 1989. “Characterization of Adenine Phosphoribosyltransferase from the Human Malaria Parasite, Plasmodium Falciparum.” *Biochimica Biophysica Acta* 996(3):160–65.

Ramakrishnan S., M.D. Docampo, J.I. MacRae, F.M. Pujol, C.F. Brooks, G.G. van Dooren, J.K.Hiltunen, A.J. Kastaniotis, M.J. McConville, and B. Striepen 2012. “Apicoplast and Endoplasmic Reticulum Cooperate in Fatty Acid Biosynthesis in Apicomplexan Parasite Toxoplasma Gondii.” *Journal of Biological Chemistry* 287(7):4957–71.

Raman, J., C.S. Ashok, S.I. Subbayya, R.P. Anand, S.T. Selvi and H. Balaram. 2005. “Plasmodium Falciparum Hypoxanthine Guanine Phosphoribosyltransferase. Stability Studies on the Product-Activated Enzyme.” *The FEBS journal* 272(8):1900–1911.

Ridley, R. G. 2002. “Medical Need, Scientific Opportunity and the Drive for Antimalarial Drugs.” *Nature* 415(6872):686–93.

Sarkar, D., I. Ghosh, and S. Datta. 2004. “Biochemical Characterization of Plasmodium Falciparum Hypoxanthine-Guanine-Xanthine Phosphorybosyltransferase: Role of Histidine Residue in Substrate Selectivity.” *Molecular and biochemical parasitology* 137(2):267–76.

Sauerwein, R.W., M. Roestenberg, and V.S. Moorthy. 2011. “Experimental Human Challenge Infections Can Accelerate Clinical Malaria Vaccine Development.” *Nature reviews. Immunology* 11(1):57–64.

Seegmiller, J.E., F.M. Rosenbloom, and W.N. Kelley. 1967. “Enzyme Defect Associated with a Sex-Linked Human Neurological Disorder and Excessive Purine Synthesis.” *Science (New York, N.Y.)* 155(770):1682–84.

Sharma, P., A.O. Kolawole, S.M. Wiltshire, K. Frondorf, and K.J.D.A. Excoffon. 2012. “Accessibility of the Coxsackievirus and Adenovirus Receptor and Its Importance in Adenovirus Gene Transduction Efficiency.” *Journal of General Virology* 93(1):155–58.

Sivendran, S., and R.F. Colman. 2008. “Effect of a New Non-Cleavable Substrate Analog on Wild-Type and Serine Mutants in the Signature Sequence of Adenylosuccinate Lyase of Bacillus Subtilis and Homo Sapiens.” *Protein science : a publication of the Protein Society* 17(7):1162–74.

Spiegel, E.K., R.F. Colman, and D. Patterson. 2006. “Adenylosuccinate Lyase Deficiency.” *Molecular Genetics and Metabolism* 89(1-2):19–31.

Stewart, M.J., and J.P. Vanderberg. 1988. “Malaria Sporozoites Leave behind Trails of Circumsporozoite Protein during Gliding Motility.” *The Journal of protozoology* 35(3):389–93.

Sujay Subbayya, I.N., and H. Balaram. 2000. “Evidence for Multiple Active States of Plasmodium Falciparum Hypoxanthine-Guanine-Xanthine Phosphoribosyltransferase.” *Biochemical and biophysical research communications* 279(2):433–37.

Torres, R.J., and J.G. Puig. 2007. “Hypoxanthine-Guanine Phosophoribosyltransferase (HPRT) Deficiency: Lesch-Nyhan Syndrome.” *Orphanet journal of rare diseases* 2:48.

Traut, T.W. 1994. “Physiological Concentrations of Purines and Pyrimidines.” *Molecular and cellular biochemistry* 140(1):1–22.

Tsai, M., J. Koo, P. Yip, R.F. Colman, M.L. Segall and P.L. Howell. 2007. "Substrate and Product Complexes of Escherichia Coli Adenylosuccinate Lyase Provide New Insights into the Enzymatic Mechanism." *Journal of Molecular Biology* 370(3):541–54.

Tu, A.S., and D. Patterson. 1977. "Biochemical Genetics of Chinese Hamster Cell Mutants with Deviant Purine Metabolism. VI. Enzymatic Studies of Two Mutants Unable to Convert Inosinic Acid to Adenylic Acid." *Biochemical genetics* 15(1-2):195–210.

Udomsangpetch, R., O. Kaneko, K. Chotivanich, and J. Sattabongkot. 2008. "Cultivation of Plasmodium Vivax." *Trends in Parasitology* 24(2):85–88.

Ullman, B., and D. Carter. 1995. "Hypoxanthine-Guanine Phosphoribosyltransferase as a Therapeutic Target in Protozoal Infections." *Infectious agents and disease* 4(1):29–40.

Vliet, L.K., T.G. Wilkinson, N. Duval, G. Vacano, C. Graham, M. Zikánová, V. Skopova, V. Baresova, A. Hnízda, S. Kmoch and D. Patterson. 2011. "Molecular Characterization of the AdeI Mutant of Chinese Hamster Ovary Cells: A Cellular Model of Adenylosuccinate Lyase Deficiency." *Molecular Genetics and Metabolism* 102(1):61–68.

Walsh, C.J. and I.W. Sherman. 1968. Purine and pyrimidine synthesis by the avian malaria parasite, Plasmodium lophurae. *Journal of Protozooly* 15: 763-70.

Weckbecker, G., and J.G. Cory. 1989. "Metabolic Activation of 2,6-Diaminopurine and 2,6-Diaminopurine-2'-Deoxyriboside to Antitumor Agents." *Advances in enzyme regulation* 28:125–44.

Wells, T.N.C., P.L. Alonso, and W.E. Gutteridge. 2009. "New Medicines to Improve Control and Contribute to the Eradication of Malaria." *Nature reviews. Drug discovery* 8(11):879–91.

White, N.J., S. Pukrittayakamee, T.T. Hien, M.A. Faiz, O.A. Mokuolu and A.M. Dondorp. 2014. "Malaria." *Lancet* 383(9918):723–35.

Book

Pankajakshan, D. and D.K. Agrawal.2013. "Clinical and Translational Challenges in Gene Therapy of Cardiovascular Diseases." *Gene Therapy - Tools and Potential Applications*, book edited by Francisco Martin Molina, ISBN 978-953-51-1014-9.

Websites

Q&A on artemisinin resistance. 2014.
(http://www.who.int/malaria/media/artemisinin_resistance_qa/en/index.html)

Malaria Fact sheet N° 94. 2014.
(http://www.who.int/mediacentre/factsheets/fs094/en/)

RTS,S/AS01 Candidate Malaria vaccine Summary for the SAGE meeting. 2009.
(http://www.who.int/immunization/sage/1_SAGE_RTSS_summary_final_Malaria.pdf)

Malaria vaccine initiative. Press release. 2013.
(http://www.malariavaccine.org/files/RTSS_18_months_followup_RELEASE_EMBARGOED_UNTIL_0001_BST_08_Oct_2013_.pdf)

Trypanosomiasis, human African (sleeping sickness) Fact sheet N°259. 2014.
(http://www.who.int/mediacentre/factsheets/fs259/en/)

Leishmaniasis Fact sheet N°375. 2014.
(http://www.who.int/mediacentre/factsheets/fs375/en/)

Chagas disease (American trypanosomiasis) Fact sheet N°340. 2014.
(http://www.who.int/mediacentre/factsheets/fs340/en/)

Vector Biolabs. Adenovirus and Recombinant Adenovirus.
(http://www.vectorbiolabs.com/vbs/page.html?m=61)

Classical Gene Therapy. 2012.
(http://www.biotechspace.site90.com/?p=116)

ADDENDUM-SUPPLEMENTARY FIGURES

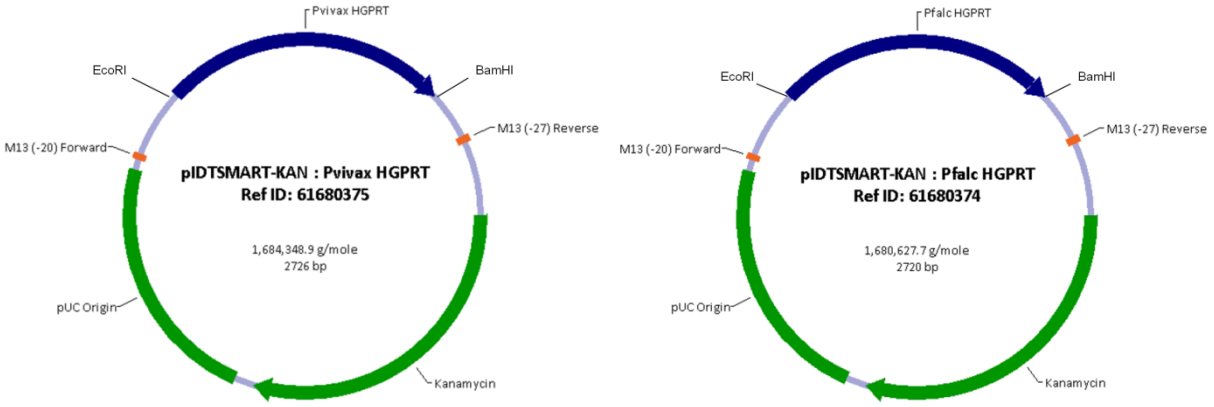

SUPPLEMENTAL FIGURE 1 | **pIDTSmart-KAN plamids.** They contain the codon optimized *Pv* and *Pf*HGPRT sequences flanked by EcoRI (5') and BamHI (3') restriction sites.

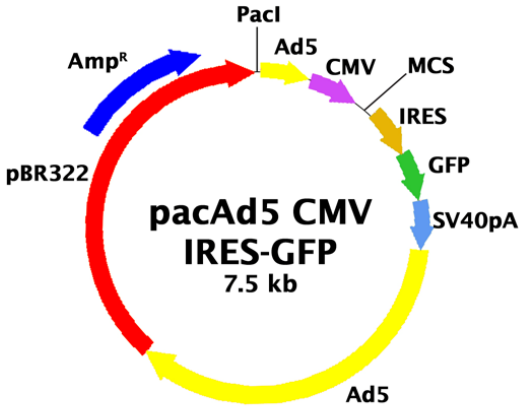

pacAd5 CMV-IRES-GFP vector features:
3-10: PacI
16-368: 1-353 of Ad5 (contains the left hand ITR and packaging signal)
382-912 CMV Promotor
919-964: MCS
983-1596: IRES
1597-2316: GFP
2317-2764: SV40 pA
2759-5223: 3328-5792 of Ad5 (contains the 9.2-16.1 kb adenoviral gene region)
6471-7331: β Lactamase

Multiple cloning site:

Pme I EcoR I
TTGGTACCGTTTAAACTCGAGGTCGACGGTATCGATAAGCTTGATATCGAATTCCTGCAGCCCGGGGGATCCACTAGT
Cla I EcoR V BamH I

SUPPLEMENTAL FIGURE 2 | **PacAd5 CMV-IRES-GFP shuttle Vector.** 7539 bp, Ampicillin-resistant (Product manual, cell biolabs VPK-254).

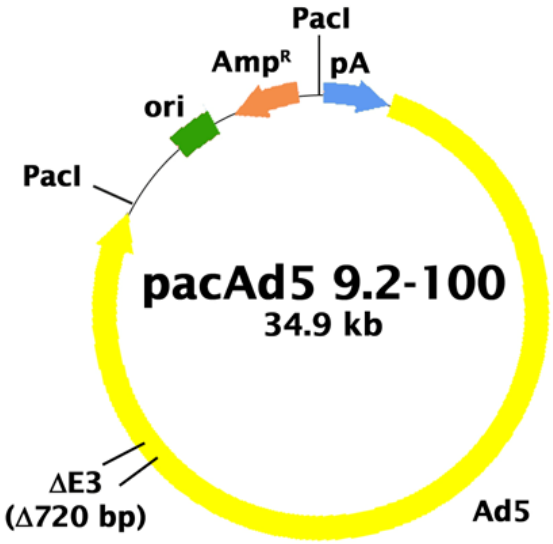

SUPPLEMENTAL FIGURE 3 | **PacAd5 9.2-100 Ad backbone vector.** 34947 bp, Ampicillin-resistant, devoid of the left-hand ITR, the packaging signal and E1/E3 sequences (Product manual, cell biolabs VPK-254).

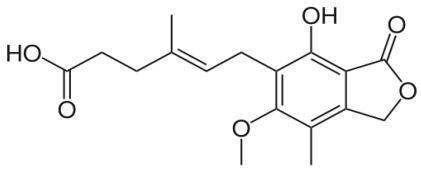

Mycophenolic acid

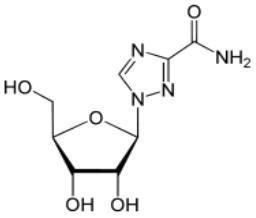

Ribavirin

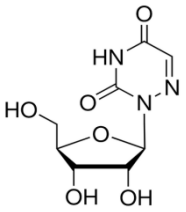

6-Azauridine

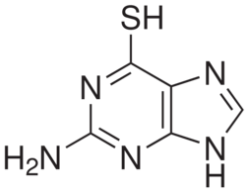

6-Thioguanine

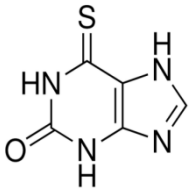

6-Thioxanthine

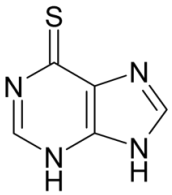

6-Mercaptopurine

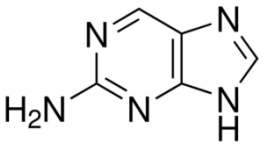

2-Aminopurine

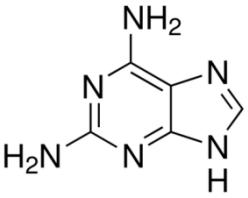

2,6-Diaminopurine

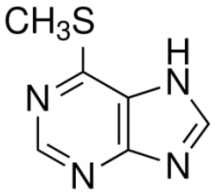

6-Methylmercaptopurine

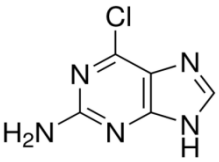

2-Amino-6-chloropurine

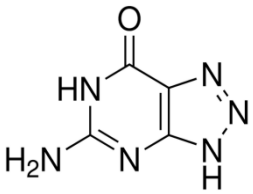

8-azaguanine

SUPPLEMENTAL FIGURE 4 | **Chemical structures of mycophenolic acid and purine and pyrimidine (6-azauridine) analogues** (Wikipedia and http://www.sigmaaldrich.com/).

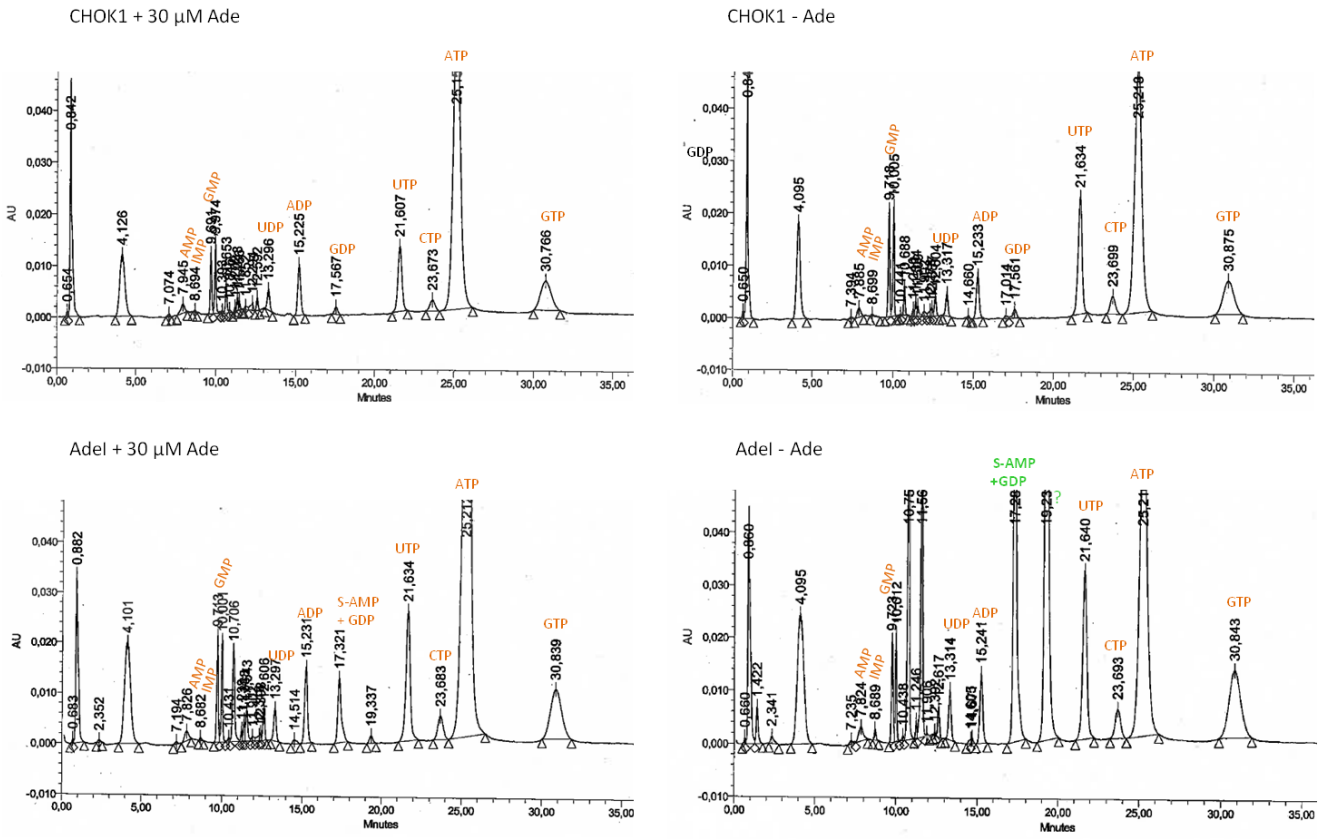

SUPPLEMENTAL FIGURE 5 | **$UV_{(249\ nm)}$ HPLC- chromatograms showing purine and pyrimidine peaks.** Cells were maintained in medium containing 4.4 µM Hx (i.e. 10% FCS) with 30 µM adenine (+Ade) or without adenine (-Ade). Adenine starved AdeI cells (6 h) accumulate two metabolites, one is S-AMP (Retention time is 17.2 min). The identity of the peak of 19.2 min is unknown.

ADDENDUM-RISK ASSESSMENT

TABLE 1 | **Hazard identification, risk class, safety precautions and control measures for chemical compounds used.**

HAZARD IDENTIFICATION		RISK CLASS	SAFETY PRECAUTIONS ADAPTED FOR RISK MINIMISATION	WHAT TO DO IN CASE OF FAILURE/ ACCIDENT?
Acrylamide 	Hazardous in case of skin or eye contact, if ingested and if inhaled. Severe over-exposure can result in death. May cause cancer and genetic defects. Suspected of damaging fertility.	E4 (very dangerous)	Wear suitable protective clothing: lab coat and gloves. Wash hands after handling. Only open in a fume hood.	In case of eye or skin contact, flush eyes or skin with cold running water for at least 10 min. Remove contact lenses if easily possible. If inhaled, remove to fresh air. If ingested, do not induce vomiting unless directed to do so by medical personnel. In all cases seek medical advice immediately and show the container or the label.
Adenine (Ade) 	Harmful if swallowed.	E1 (little dangerous)	Wear suitable protective clothing: lab coat and gloves. Wash hands after handling.	If swallowed: Call a poison center or doctor/physician if person feels unwell.
Dimethylsulfoxide (DMSO)	Slightly irritating to eyes, respiratory tract and skin.	Not classified as dangerous according to the criteria of Regulation (EC) No 1272/2008	Wear suitable protective clothing: lab coat and gloves.	In case of eye or skin irritation, flush eyes or skin with cold running water for at least 10 min. Remove contact lenses if easily possible. If inhaled, remove to fresh air. If ingested, do not induce vomiting unless directed to do so by medical personnel. Get medical attention if irritation develops.
Ethanol 	1) Highly flammable 2) Causes irritation in case of skin or eye contact and when inhaled. Ingestion may cause gastritis, intoxication, blindness and in acute cases, death.	E3 (dangerous)	1) Keep container tightly closed and sealed and store in a well-ventilated place. Keep away from heat, sparks and flame. No smoking. 2) Wear suitable protective clothing: lab coat and gloves. Avoid generation of aerosols (pipette gently, no pouring out,…). Do not inhale solvent vapor.	1) In case of fire: use suitable extinguishing medium for extinction. 2) In case of eye or skin irritation, flush eyes or skin with cold running water for at least 10 min. Remove contact lenses if easily possible. If inhaled, remove to fresh air. If ingested, do not induce vomiting unless directed to do so by medical personnel. In all cases seek medical advice immediately and show the container or the label.
Ethidiumbromide (EtBr) 	1) Toxic in case of ingestion. Irritating to skin, eyes and respiratory tract. 2) Suspected of causing genetic defects.	E4 (very dangerous)	Wear suitable protective clothing: lab coat and gloves. Do not breathe dust/fume/gas/mist/vapours/spray. Use separate pipettes, table, glasswork for potential EtBr contaminated material. This material is only handled when gloves are worn.	In case of accident or if person feels unwell, seek medical advice immediately and show the container or the label.

Formaldehyde 	1) Toxic if inhaled, in contact with skin and eyes and if swallowed. Causes severe skin burns and eye damage. 2) Suspected of causing cancer.	E4 (very dangerous)	Wear suitable protective clothing: lab coat and gloves. Do not breathe dust/fume/gas/mist/vapours/spray. Only open in a fume hood.	In case of eye or skin contact, flush eyes or skin with cold running water for at least 10 min. If inhaled, remove to fresh air. If ingested, do not induce vomiting unless directed to do so by medical personnel. In all cases seek medical advice immediately and show the container or the label.
Formamide 	1) Hazardous in case of skin or eye contact. 2) May damage the unborn child.	E4 (very dangerous)	Wear suitable protective clothing: lab coat and gloves.	In case of eye or skin contact, flush eyes or skin with cold running water for at least 10 min. Remove contact lenses if easily possible. If inhaled, remove to fresh air. If ingested, do not induce vomiting unless directed to do so by medical personnel. In all cases seek medical advice immediately and show the container or the label.
Liquid nitrogen 	1) Can cause tissue freezing (frostbite) and severe cryogenic burns of skin and eyes. 2) Liquid-to-gas expansion ratio of nitrogen is 1:694 at 20°C. Pressure in a container can build up due to heat and it may rupture if pressure relief devices should fail to function. 3) Liquid nitrogen, when spilled, will vaporize rapidly, thereby reducing the oxygen concentration in the air. This might cause suffocation, especially in confined spaces.	E1 (little dangerous)	1) Wear thermal insulated gloves, long sleeves and trousers. Safety glasses are recommended. 2) Cryogenic containers are equipped with pressure relief devices to control internal pressure. If containers aren't correctly closed, an alarm will go off. 3) Foresee adequate ventilation. Oxygen sensors are sometimes used as a safety precaution when working with liquid nitrogen to alert workers of gas spills into a confined space	1) Do not rub frozen parts as tissue damage may result. Place the affected area in a warm water bath (max. 40°C). Call a physician in case of a serious burn. 3) Evacuate the area if liquid nitrogen is spilled. Increase ventilation and monitor oxygen level. Persons suffering from lack of oxygen should be moved to fresh air. If victim is not breathing, administer artificial respiration. Call a physician.
Methanol 	1) Highly flammable 2) Toxic if inhaled, in contact with skin and eyes, and if swallowed.	E4 (very dangerous)	1) Store in a in a cool, well-ventilated area. Keep container tightly closed and sealed. Keep away from heat, sparks and flame. No smoking. 2) Wear suitable protective clothing: lab coat and gloves. Only open container in a fume hood. To avoid inhalation of solvent vapor.	In case of eye or skin contact, flush eyes or skin with cold running water for at least 10 min. Remove contact lenses if easily possible. If inhaled, remove to fresh air. If ingested, do not induce vomiting unless directed to do so by medical personnel. In all cases seek medical advice immediately and show the container or the label.
Mycophenolic acid (MPA) 	1) Harmful if swallowed 2) Suspected of causing genetic defects 3) May harm the unborn child.	E3 (dangerous)	Wear suitable protective clothing: lab coat and gloves. Wash hands thoroughly after handling.	In case of accident or if persons feels unwell, seek medical advice immediately (show the label where possible).

Purine base analogues (6-thioxanthine, 6-mercaptopurine, 2,6 DAP, 2-aminopurine, 6-thioguanine, ribavirin…) 	1) Harmful if swallowed, in contact with skin and eyes and if inhaled. 2) 2,6-DAP is suspected of causing cancer. 3) 6-TG and RBV may damage fertility and the unborn child.	E2 (moderately dangerous) – E4 (very dangerous)	Wear suitable protective clothing: lab coat and gloves. Wash hands thoroughly after handling. Avoid breathing dust/fume/gas/mist/vapours/spray (work is performed under laminar flow).	In case of eye or skin contact, flush eyes or skin with cold running water for at least 10 min. If inhaled, remove to fresh air. If ingested or if persons feels unwell, seek medical advice immediately (show the label where possible).
Sodium dodecyl sulfate (SDS) 	Irritating to skin, eyes, respiratory system and gastrointestinal tract.	E1 (little dangerous)	Wear suitable protective clothing: lab coat and gloves. Wash hands thoroughly after handling.	In case of eye or skin contact, flush eyes or skin with cold running water for at least 10 min. If inhaled, remove to fresh air. If ingested, rinse mouth. Do not induce vomiting. Call a physician if persons feels unwell or when irritation develops.
Solid carbon dioxide (dry ice)	1) Contact with solid Carbon Dioxide or cold gas can cause frostbite to skin, eyes, and other exposed tissue. 2) Large spills in enclosed spaces may cause oxygen deficiency.		1) Do not handle solid carbon dioxide with bare hands. Wear thermal insulated gloves and use a plastic or metal scoop. 2) Containers of solid carbon dioxide should be stored upright and be firmly secured to prevent falling or being knocked over. Carbon dioxide sublimates at -78.5°C, containers should be thermally insulated and kept at the lowest possible temperature to maintain the solid state and avoid generation of carbon dioxide gas.	1) Do not rub frozen parts as tissue damage may result. Place the frostbitten part in warm water (max. 40°C) or try to warm up the frozen tissues. Call a physician in case of a serious burn. 2) Provide adequate ventilation.
Trichloroacetic acid (TCA) 	1) Corrosive agent to the eyes, skin and respiratory tract. 2) Very toxic to aquatic organisms, may cause long-term adverse effects in the aquatic environment	E3 (dangerous)	1) Wear suitable protective clothing: lab coat and gloves. Only open container in a fume hood to avoid inhalation of solvent vapor. 2) This material and its container must be disposed of as hazardous waste. Avoid release to the environment.	In case of eye or skin contact, flush eyes or skin with cold running water for at least 10 min and remove contact lenses if easily possible. If inhaled, remove the victim to fresh air. If ingested, do not induce vomiting. Corrosive chemicals will destroy the membranes of the mouth, throat, and esophagus. In all cases seek medical advice immediately and show the container or the label.

TABLE 2 | **Hazard identification, safety precautions and control measures for <u>biological agents</u> used.**

HAZARD IDENTIFICATION		SAFETY PRECAUTIONS ADAPTED FOR RISK MINIMISATION	WHAT TO DO IN CASE OF FAILURE/ ACCIDENT?
Adenoviral vectors serotype 5	The recombinant Ad vectors are deleted in the essential E1 gene as well as the E3 gene and will not replicate in cells other than complementing 293 cells. Still, care should be taking when handling replication incompetent viral vectors. Some studies suggest that serial amplification of Ad vectors in 293 cells can result in the generation of wild-type adenovirus which can eventually overgrow the recombinant viruses. Replication competent adenoviruses can occur due to homologous recombination between the Ad genome and the E1 region of the 293 genome. However, with the RAPAd® system, no infectious wt particles could be observed by A549 plaque assay, even after 15 serial amplifications (Anderson et al. 2000). Wild type adenovirus serotype 5 primarily cause upper respiratory tract infections (infectious dose: > 150 pfu), but do not cause serious illness in healthy people. Transmission of adenoviruses can occur through ingestion, inhalation of aerosolized droplets, mucous membrane contact, and accidental injection (needlestick). There is no specific antiviral drug available. Adenovirus type 5 is very stable and can survive 3-8 weeks on environmental surfaces at room temperature.	Adenovirus and adenoviral vectors must be manipulated following Biosafety Level 2 practices and facilities. All manipulations must be conducted within a Biological Safety Cabinet Type II to avoid spread of infectious material by aerosol. No work on the open bench. Since the amount of replication competent adenovirus is expected to increase with the number of passages in 293 cells, low passage (maximal two) Ad viral stocks are used. Wear suitable protective clothing: lab coat and gloves. Wash hands thoroughly before and after handling the vector. Work surfaces are decontaminated before and after each procedure with 1% sodium hypochlorite, 2% glutaraldehyde or 0.25% sodium dodecyl sulfate. Note: Alcohol is not an effective disinfectant against adenovirus (non-enveloped). Viral wastes are decontaminated before disposal as biohazardous waste.	In case of eye or skin contact, flush eyes or skin with running water for at least 10 min. In case of spills inside a biological safety cabinet, cover the spill with paper towels and disinfectant the spill area. Let the disinfectant soak for 20 minutes before cleaning up the spill. After initial clean up, disinfect area a second time. For spills outside a biological safety cabinet: Allow aerosols to settle: wearing protective clothing gently cover the spill with absorbent paper towel and apply sodium hypochlorite to the spill, starting at the perimeter and working towards the center; allow sufficient contact time (30 min) before clean up.
JM109 *E.coli*	Nonpathogenic isolates. May cause irritation to skin, eyes, and respiratory tract, may affect kidneys.	Wear suitable protective clothing: lab coat and gloves. Wash hands thoroughly after handling. Desinfect work surfaces with ethanol.	In case of eye or skin contact, flush eyes or skin with running water for at least 10 min. If the material was swallowed, rinse the mouth with water. Call a physician.

Animal cell cultures (human and dog)	1) All cell lines used are established cell lines. The cell lines used are not known to cause disease in healthy adult humans. Contamination by viruses (e.g. Hepatitis B, HIV) or other adventitious agents (e.g. mycoplasma) cannot be excluded. HeLa cells contain the E6 and E7 genes of Human papillomavirus. However, no mature virus can be formed. 293AD cells contain the E1 genes of adenovirus and thus complement the E1 deletion of Ad vectors. Recombination between the E1 sequence of the cell line and the vector can result in the formation of replication competent adenovirus particles. 2) Cells are transported as frozen cultures which may contain a 5%-10% solution of Dimethyl sulfoxide as a cryoprotectant (see above). Frozen ampoules could explode on warming due to the expansion of trapped liquid N.	1) All cells can be handled as potentially biohazardous material under Biosafety Level 1. Ad vector infected 293AD cells are classified under Biolosafety Level 2. All manipulations must be conducted within a Biological Safety Cabinet Type II. 2) When ampoules with frozen cells are taken out of the liquid N vessel, transport them in a styrofoam box.	In case of eye or skin contact, flush eyes or skin with running water for at least 10 min. If the material was swallowed, rinse the mouth with water. Call a physician. In case of spills: allow aerosols to settle; wearing protective clothing, gently cover spill with paper towel and pour desinfecant over the spillage (e.g. 10% sodium hypochlorite). Start cleaning at perimeter and work towards the center; allow sufficient contact time before clean up (30 min).

TABLE 3 | **Hazard identification, safety precautions and control measures for radioactive compounds and UV transmitting machinery (radiation).**

HAZARD IDENTIFICATION		SAFETY PRECAUTIONS ADAPTED FOR RISK MINIMISATION	WHAT TO DO IN CASE OF FAILURE/ ACCIDENT?
Tritium labeled purine bases: [8-^{3}H]Ade (1µCi/ µl) and [2,8-^{3}H]Hx (1µCi/ µl)	Tritium decays into ^{3}He by β- decay. β-particles from tritium can penetrate only about 6.0 mm of air, and they are incapable of passing through the dead outermost layer of human skin, therefore they do not impose an external radiation hazard. However, tritium is potentially dangerous if inhaled or ingested.However,only very high doses have potentially a significant effect.	Maintain your occupational exposure to radiation As Low As Reasonably Achievable [ALARA]. Avoid skin contamination, ingestion and inhalation by wearing protective clothing. Clearly outline radioactive material and use areas with tape bearing the legend "radioactive". Cover lab bench tops where radioactive material will be handled with plastic-backed absorbent paper; change this covering periodically and whenever it's contaminated.	In case of spills: allow aerosols to settle; wearing protective clothing, gently cover spill with paper towel and pour isopropanol over the spillage. Start cleaning at perimeter and work towards the center. If ingested or inhaled is urinalysis the easiest bioassay method for determining exposure to tritium.
UV transilluminator	UV radiation can cause damage to the eyes (photokeratitis, photoconjunctivitis, cataract) and skin (erythema, elastosis).	Skin exposure should be avoided by wearing a lab coat with long sleeves and gloves. Eye exposure should be avoided by a shield that is fixed to the UV transilluminator.	Call a physician if concerned.

TABLE 4 | **Hazard identification, safety precautions and control measures for machinery used.**

HAZARD IDENTIFICATION		SAFETY PRECAUTIONS ADAPTED FOR RISK MINIMISATION	WHAT TO DO IN CASE OF FAILURE/ ACCIDENT?
Microwave	Risk of burning to boiling liquid (e.g. agar, agarose solution).	Never leave the microwave unattended when using it.Use pot holders to manipulate flasks containing hot liquid.	In case of burning, cool the burned area under cool running water for 15-20 minutes, do not use ice. Cover the burned area in gauze. Call a physician in the case of a major burn.
-80°C fridge	Risk of frostbite when touching the metal racks.	Wear a lab coat with long sleeves and thermal insulates gloves.	Do not rub frozen parts as tissue damage may result. Place the frostbitten part in warm water (max. 40°C) or try to warm up the frozen tissues. Call a physician in case of a major burn.
Bunser burner	1) Risk of burning. 2) Risk of a fire.	Tie-back long hair and loose clothing. Do not leave open flames unattended. Shut off gas when its use is complete. Place the Bunsen burner away from any overhead shelving. Remove combustible materials and excess chemicals from the area.	1) In case of burning, cool the burned area under cool running water for 15-20 minutes, do not use ice. Cover the burned area in gauze. Call a physician in the case of a major burn. 2) In case of a small fire, use the nearest fire extinguisher to control/ extinguish it. In case of a large fire, activate the nearest fire alarm pull station, notify all lab personnel, and evacuate the building. Call the emergency number of the KULeuven: 016/32.22.22

To ensure the health and safety of all workers and to prevent contamination of experiments, everybody works in accordance to the Safe Microbiological Techniques described in the VIB-Brochure “Bioveiligheid in het laboratorium” (p.26).

1. Doors and windows are closed when experiments are performed.
2. Always wear a labcoat. Labcoats worn in the P2 lab don’t leave this room. Wear suitable gloves when handling biohazardous materials.
3. Eating, drinking and smoking are prohibited. Food and beverages are not stored in laboratory areas.
4. Do not wear jewelry, cosmetics and watches.
5. Clean and sterilize spills immediately.
6. Minimize the formation of aerosols.
7. Pipetting by mouth is prohibited. Instead, use a pipetting aid. Used pipettes are collected in a disinfecting solution.
8. All used glassware and other equipment that has been in contact with cell culture, microbial and viral material is immersed in disinfectant, washed and autoclaved before reuse.
9. Biological waste is inactivated and disposed as biohazardous waste.
10. Wash hands with disinfecting soap and water after work. Bench surface areas have to be cleaned and desinfected with ethanol before and after performing an experiment. Keep area clean and organized.

In case of accident, this is reported to the supervisor.

In case of a serious accident: Call KU Leuven emergency: 016/32 22 22

REFERENCES RISK ASSESSMENT

Material Safety Data Sheets

MSDS acrylamide. Sciencelab. Last updated: 05/21/2013
(http://www.sciencelab.com/msds.php?msdsId=9927422)

MSDS Dimethylsulfoxide. Sciencelab. Last updated: 05/21/2013
(http://www.sciencelab.com/msds.php?msdsId=9927347)

MSDS Ethanol. Sciencelab. Last updated: 05/21/2013
(http://www.sciencelab.com/msds.php?msdsId=9923956)

MSDS Ethidiumbromide. Sciencelab. Last updated: 05/21/2013
(http://www.sciencelab.com/msds.php?msdsId=9927667)

MSDS Formaldehyde. Sciencelab. Last updated: 05/21/2013
(http://www.sciencelab.com/msds.php?msdsId=9924095)

MSDS Formamide. Sciencelab. Last updated: 05/21/2013
(http://www.sciencelab.com/msds.php?msdsId=9927348)

MSDS Liquid nitrogen. Air Products and Chemicals. Inc, Last updated: 03/14/2008
(http://www.jmfx.net/files/products/safety/Liquid_Nitrogen_Material_Safety_Data_Sheet_M SDS.pdf)

MSDS Methanol. Sciencelab. Last updated: 05/21/2013
(http://www.sciencelab.com/msds.php?msdsId=9927227)

MSDS Ribavirin. PhytoTechnology Laboratories. Last updated: 02/03/2005
(http://www.phytotechlab.com/MSDS/R795msds.pdf)

MSDS Sodium dodecyl sulfate. Last updated: 06/16/2011
(http://www.nwmissouri.edu/naturalsciences/sds/s/Sodium%20lauryl%20sulfate.pdf)

MSDS Solid carbon dioxide. Airgas. Last updated: 03/26/2013
(http://www.airgas.com/documents/pdf/001091.pdf)

MSDS Trichloroacetic acid. Sciencelab. Last updated: 05/21/2013
(http://www.sciencelab.com/msds.php?msdsId=9927303)

MSDS Trichloroacetic acid. Duke University Medical Center. Last updated: 05/03/2000
(http://www.safety.duke.edu/ohs/MSDS/TCA.pdf)

MSDS recombinant adenoviral vector. Cell Biolabs, Inc.
(http://www.cellbiolabs.com/sites/default/files/MSDS%20(ADV-xxx).pdf)

MSDS adenovirus and adenoviral vectors. NCI-Frederick Environment,Health&Safety. October 2011
(http://ncifrederick.cancer.gov/ehs/ibc/Media/Documents/Adenovirus_Adenoviral_Vectors.pdf)

MSDS adenovirus types 1, 2, 3, 4, 5 and 7. Public Health Agency of Canada. 2001.
(http://www.phac-aspc.gc.ca/lab-bio/res/psds-ftss/msds3e-eng.php)

MSDS *E.coli* JM109. New England Biolabs. Last updated: 01/05/2012
(https://www.neb.com/~/media/Catalog/All-Products/5DE0C89D1496402AA68D24C86EB2BE2D/MSDS/msdsE4107.pdf)

MSDS Animal cell cultures. American Type Culture Collection. Last updated: 07/2010
(http://ehs.uky.edu/docs/pdf/bio_msds_atcc.pdf)

NSDS (Nuclide Safety Data Sheet) Tritium. The North Carolina Chapter of the Health Physics Society.
(http://hpschapters.org/northcarolina/NSDS/3HPDF.pdf)

MSDS UV transilluminator. University College London. Last updated: 02/2010
(http://www.ucl.ac.uk/estates/safetynet/guidance/radiation/non-ionising/transilluminator_safety.pdf)

MSDS Bunsen burner. Worcester Polytechnic Institute.
(http://www.wpi.edu/offices/safety/bunsen.html)

Other resources

World Health Organization (2004). Laboratory biosafety manual 3rd edition.
(http://www.who.int/csr/resources/publications/biosafety/en/Biosafety7.pdf)

Vlaams Instituut voor Biotechnologie (2004). Bioveiligheid in het laboratorium, 3e herziene editie.
(http://www.vib.be/nl/educatie/Documents/Bioveiligheid%20in%20het%20laboratorium.pdf)

Databank voor gevaarlijke stoffen KU Leuven.
(http://www.kuleuven.ac.be/sapredir/gevaarlijkestoffen) (NL)
(http://www.kuleuven.ac.be/sapredir/hazardousproducts) (ENG)

DEPARTMENT OF
MICROBIOLOGY AND IMMUNOLOGY
Rega institute for Medical Research
Minderbroederstraat 10
3000 Leuven, BELGIË
tel. + 32 16 33 73 67
fax + 32 16 33 73 40
www.rega.kuleuven.be